ISSN 0042-3211

THE VELIGER

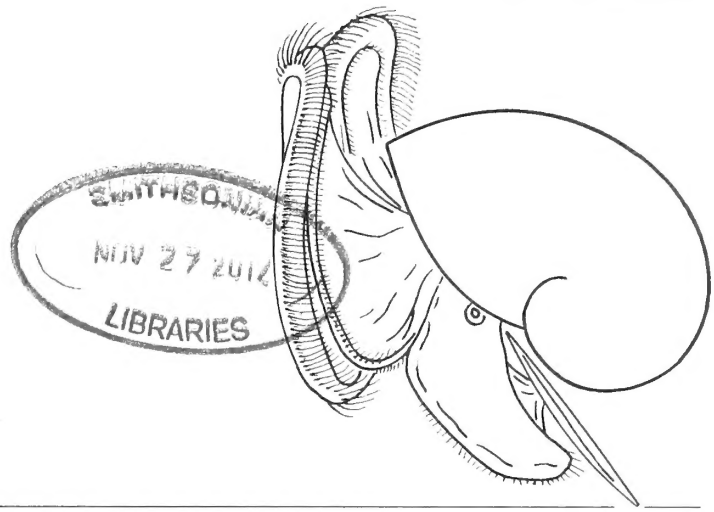

A Quarterly published by
CALIFORNIA MALACOZOOLOGICAL SOCIETY, INC.
Berkeley, California
R. Stohler (1901–2000), Founding Editor

Volume 51 November 16, 2012 Number 3

Contents

Contents — *Continued*

The Veliger (ISSN 0042-3211) is published quarterly by the California Malacozoological Society, Inc., % Santa Barbara Museum of Natural History, 2559 Puesta del Sol Road, Santa Barbara, CA 93105. Periodicals postage paid at Berkeley, CA and additional mailing offices. POSTMASTER: Send address changes to *The Veliger*, Santa Barbara Museum of Natural History, 2559 Puesta del Sol Road, Santa Barbara, CA 93105.

THE VELIGER

Scope of the Journal

The Veliger is an international, peer-reviewed scientific quarterly published by the California Malacozoological Society, a non-profit educational organization. *The Veliger* is open to original papers pertaining to any problem connected with mollusks. Manuscripts are considered on the understanding that their contents have not appeared, or will not appear, elsewhere in substantially the same or abbreviated form. Holotypes of new species must be deposited in a recognized public museum, with catalogue numbers provided. Even for non-taxonomic papers, placement of voucher specimens in a museum is strongly encouraged and may be required.

Membership and Subscription

Affiliate membership in the California Malacozoological Society is open to persons (not institutions) interested in any aspect of malacology. New members join the society by subscribing to *The Veliger*. Rates for Volume 51 are US $65.00 for affiliate members in North America (USA, Canada, and Mexico) and US $120.00 for libraries and other institutions. Rates to members outside of North America are US $75.00 and US $130.00 for libraries and other institutions. All rates include postage, by air to addresses outside of North America.

Memberships and subscriptions are by Volume only. Payment should be made in advance, in US Dollars, using checks drawn from US banks or by international postal order. No credit cards are accepted. Payment should be made to *The Veliger* or "CMS, Inc." and *not* the Santa Barbara Museum of Natural History. Single copies of an issue are US $30.00, postage included. A limited number of back issues are available.

Send all business correspondence, including subscription orders, membership applications, payments, and changes of address, to: The Veliger, Dr. Henry Chaney, Secretary, Santa Barbara Museum of Natural History, 2559 Puesta del Sol Road, Santa Barbara, CA 93105, USA.

Send manuscripts, proofs, books for review, and correspondence regarding editorial matters to: David R. Lindberg, Museum of Paleontology, 1101 VLSB MC# 4780, University of California, Berkeley, CA 94720-4780, USA.

The Veliger 51(3):97–101 (November 16, 2012)

THE VELIGER

Notes on the Veliger Larvae and Settlement in the Anaspidean *Akera bullata*

HELEN C. MARSHALL

Institute of Biological, Environmental and Rural Sciences, Edward Llwyd Building, Aberystwyth University, Ceredigion, SY23 3DA

Abstract. *Akera bullata* is the only member of the Anaspidea to produce lecithotrophic larvae that settle in response to a variety of different substrata.

INTRODUCTION

In recent years, a great deal of research has been conducted on members of the Anaspidea, primarily investigating settlement and metamorphosis of the "sea hares," the Aplysiidae (Switzer-Dunlap & Hadfield, 1977; Strenth & Blankenship, 1978; Switzer-Dunlap, 1978; Otsuka et al., 1981; Switzer-Dunlap & Hadfield, 1981; Paige, 1986; Pawlik, 1989; Plaut et al., 1995). *Akera bullata* (Müller, 1776), however, has been largely overlooked. Phylogenetic studies have often included *A. bullata* to investigate the evolution of the Anaspidea and Opisthobranchia (Medina & Walsh, 2000; Klussmann-Kolb, 2003; Vonnemann et al., 2005; Klussmann-Kolb et al., 2008); despite this, little is know about its ecology. Populations of *A. bullata* have been found throughout the British Isles, and further afield from the Baltic and North Sea, the Atlantic Ocean, and the Mediterranean Sea: France, Italy, Spain, and Greece (Thompson, 1976; Thompson & Seaward, 1989).

Members of the Anaspidea typically produce planktotrophic veligers that spend approximately 1 mo feeding and developing before metamorphosis (Kriegstein et al., 1974; Switzer-Dunlap & Hadfield, 1977; Strenth & Blankenship, 1978; Switzer-Dunlap, 1978; Otsuka et al., 1981; Paige, 1986, 1988; Pawlik, 1989; Plaut et al., 1995). Anspideans metamorphose in response to stimuli produced by several different species of red, green, brown, and blue-green algae; often, the species inducing metamorphosis is the preferred food of the adult (Kriegstein et al., 1974; Switzer-Dunlap & Hadfield, 1977; Strenth & Blankenship, 1978; Switzer-Dunlap, 1978; Otsuka et al., 1981; Paige, 1986, 1988; Pawlik, 1989; Plaut et al., 1995). *Phyllaplysia taylori* is the exception: this species is unusual in that it undergoes direct development; metamorphosis occurs within the egg capsules, thus juveniles emerge from the egg mass (Bridges, 1975). Metamorphosis is similar for all species studied (Kriegstein et al., 1974; Switzer-Dunlap & Hadfield, 1977; Switzer-Dunlap, 1978; Paige, 1988). Once committed to metamorphosis, the veligers stop crawling and retract partially or completely into their shell. They remain in this state for most of metamorphosis, which can last between 2 and 4 days (Switzer-Dunlap, 1978). The velar cilia are shed, and the velum is reabsorbed. The oral tentacles (if present) start to develop at the site of the velum. Crawling is often resumed 1–2 days after the commencement of metamorphosis. The adult heart then develops, taking over in function from the larval heart (Switzer-Dunlap & Hadfield, 1977). During metamorphosis, feeding ceases despite the ability of the juveniles to rotate the radula and buccal mass (Kriegstein et al., 1974). Approximately 3 days after metamorphosis, the juveniles are able to bite and swallow (Kriegstein et al., 1974; Switzer-Dunlap & Hadfield, 1977; Switzer-Dunlap, 1978). This process is quicker for *B. leachii plei*, in which feeding was observed 1 day after metamorphosis (Paige, 1988). See Switzer-Dunlap & Hadfield (1977) and Switzer-Dunlap (1978) for further details regarding settlement cues and the morphological changes that occur during metamorphosis.

During June 2004, spawn from *A. bullata* was gathered from Langton Hive Point (UK grid reference SY606814), the Fleet, United Kingdom. The Fleet is a shallow, saline tidal lagoon covering an area of approximately 480 ha. It spans 12.5 km and is boarded by Chesil Beach northwest of Portland Bill, Dorset. Langton Hive Point is situated 8 km from the mouth of the lagoon and is predominantly brackish. Each spawn mass was placed into a sterile 100-mL glass beaker containing 50 mL of 0.45-μm-filtered sea water. In accordance with Switzer-Dunlap & Hadfield (1981), penicillin G and streptomycin sulfate were added to each beaker after every water change to create a final concentration of 60 μg mL^{-1} and 50 μg mL^{-1}, respectively. A 0.41-μm nylon mesh was floated on the meniscus to prevent the larvae rafting. Parafilm was used to cover the beakers to prevent evaporation. The

Table 1

Combinations of substratum, phytoplankton, or both used to investigate veliger settlement.

Substratum/ phytoplankton provided	No. replicates	Metamorphic success (%)*	Minimum larval period	Maximum larval period (days)
Chondrus crispus (C)	2	25 and 45	48 hr	25
Ulva lactuca (U)	2	60 and 50	5 days	32
Nemalion helminthoides	2	65 and 40	72 hr	25
Rhinomonas (R)	2	90 and 35	10 days	38
Tetraselmis (T)	2	10 and 35	15 days	31
Isochrysis (I)	2	95 and 75	48 hr	43
Chaetoceros (Ch)	2	25 and 45	25 days	43
Biofilm (B)	2	56 and 90	24 hr	17
Control	2	35 and 25	20 days	32
R + C	1	100	24 hr	16
R + U	1	56	72 hr	19
R + B	1	73	48 hr	16
T + C	1	43	5 days	13
T + U	1	70	5 days	19
T + B	1	37	24 hr	17
I + C	1	63	48 hr	19
I + U	1	57	24 hr	20
I + B	1	70	72 hr	21
Ch + C	1	57	24 hr	17
Ch + U	1	80	24 hr	24
Ch + B	1	33	5 days	10

* The two numbers given for metamorphic success are from replicates A and B, respectively.

water was changed on alternate days. The beakers were kept in a constant temperature room (18–20°C), with a light/dark photoperiod of 12:12 hr. Once hatched, 30 healthy veligers were removed using a Pasteur pipette and transferred to sterile 60-mL plastic containers. Each vessel contained a different substratum to investigate settlement (Table 1). The juveniles were not reared to sexual maturity.

RESULTS AND DISCUSSION

Akera bullata veligers successfully hatched from spawn gathered from the Fleet. The embryonic period could not be accurately determined in this study, although Thorson (1946, cited by Thompson, 1976) stated it to be 30 days at 15°C or 20 days at 20°C. The uncleaved eggs measured 154.4 ± 4.0 μm (mean ± SD) in diameter, and there was only one egg per capsule. This corresponds with Thompson (1976) and Thompson & Seaward (1989) who both reported diameters between 156 and 170 μm. On hatching, *A. bullata* had a shell length of 255.1 ± 13.1 μm (mean ± SD), and they possessed eyes, a large yellow yolk store within the left digestive diverticulum (termed the liver by Thorson [1946]), a stomach, a hind gut terminating at the anus, a larval kidney, a metapodium, larval retractor muscles, velar lobes with cilia, statocysts, and an operculum. Other larval structures were difficult to identify due to the density of the yolk (Figure 1A, B). Based on the evidence presented here, we conclude that *A. bullata* exhibits lecithotrophic development (type 2 of Thompson, 1967) and possesses a shell-type 2 of Thompson (1961). This is in agreement with Thorson (1946) but is a contradiction to the record of *A. bullata* possessing a shell-type 1 (Thompson, 1976).

Despite being lecithotrophic, the veligers are fully competent plankton feeders (facultative planktotrophs). When provided with *Rhinomonas*, the veligers' stomachs became pigmented, and the newly settled juveniles were able to produce defensive purple ink when disturbed (indicating the assimilation of phycoerythrin as a result of *Rhinomonas* digestion). However, feeding on phytoplankton is not necessary for metamorphosis, as has been recorded for other species of opisthobranchs but not for any species of the Anaspidea.

In agreement with the findings of Thorson (1946), shell growth did not occur during the planktonic stage. Metamorphic competence was attained once the propodium had inflated, in some veligers this occurred within 24 hr of hatching. Settlement and consequently metamorphosis occurred within 43 days after hatching, depending on the substratum, phytoplankton provided, or both (Table 1). Metamorphosis followed a pattern similar to that of other anaspideans. Most individuals had made the transition from swimming veliger to crawling juvenile between 6 and 12 hr after initial settlement. Metamorphosis in *A. bullata* was never a stationary event, and crawling was frequently observed.

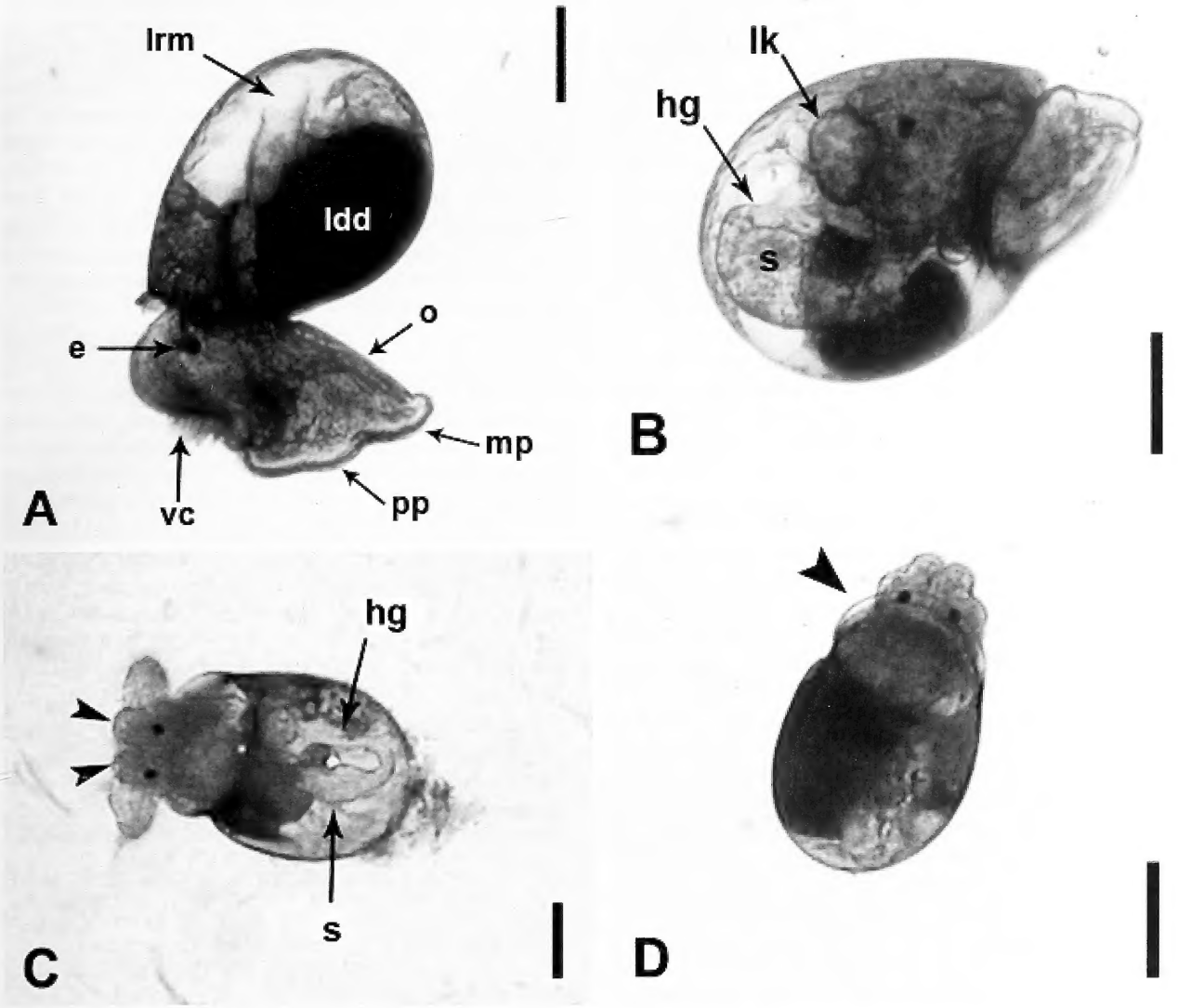

Figure 1. Newly hatched *Akera bullata* veligers (**A**, **B**) showing the type 2 shell; **C**, veliger undergoing metamorphosis; arrows point to the formation of the bilobed anterior region of the cephalic shield; **D**, metamorphosis is complete, although the operculum is still attached (arrow). Abbreviations: e, eye; hg, hind gut; lk, larval kidney; lrm, larval retractor muscle; mp, metapodium; o, operculum; pp, propodium; s, stomach; vc, velar cilia. Scale bars: A–D = 100 μm.

Initially, the velar cilia were absorbed, followed by the absorption of the velar lobes (Figure 1C). During the absorption of the velar lobes, the bilobed anterior end to the cephalic shield was formed (Figure 1D). This completed the veliger's transition into the benthic phase, after which it could no longer swim (until the parapodial lobes developed). The stage at which the operculum was lost (during metamorphosis) varied; after the loss of the operculum, the juvenile assumed the adult form. A larval heart was not visible at any time during the veliger stage. Statocysts were present but were difficult to distinguish due to the density of the tissues around the shell aperture. Movement of the buccal mass was observed within 48 hr of metamorphosis, although it is unknown whether food was swallowed during this time. After metamorphosis, the propodium formed a temporary pedal sole that then developed into the parapodial lobes that fold around the cephalic shield. Adult pigmentation appeared 7–18 days after metamorphosis. New shell growth initially formed as a collar extending from the original veliger shell. This progressively developed into whorls (Figure 1E). In some juveniles, a small finger-like projection was visible from the posterior end (Figure 1F). Although never reared

through to sexual maturity, the juvenile *A. bullata* were miniature replicas of the adults. The white pallial patterns of the juveniles as viewed through the shell were almost identical to those described by Thompson & Seaward (1989).

Members of the Anaspidea are generalist herbivores; however, in every species studied, successful postmetamorphic growth was restricted to only a few prey species. Switzer-Dunlap & Hadfield (1977) investigated the settlement preferences of several different species of aplysiids. The veligers of *Aplysia juliana* settled in response to the green algae *Ulva fasciata* and *Ulva reticulata*. *Aplysia dactylomela* veligers were not as specific and settled in response to *Laurencia*, *Chondrococcus*, *Gelidium*, *Martensia*, *Polysiphonia*, and *Spyridia* spp. However, *Laurencia* induced the greatest numbers of veligers to metamorphose. The larvae of *Dolabella auricularia* also metamorphosed in response to a variety of different algae: *Laurencia*, *Amansia*, *Spyridia*, *Sargassum*, and an unidentified mat-forming blue-green alga. Despite the range of metamorphic inducers, the juveniles of this species initially only consumed diatoms and blue-green algae. As they aged, their preferred diet changed to a mixture of *Spyridia*, *Acanthophora*, and *Laurencia*. *Stylocheilus longicauda* metamorphosed in response to *Lyngbya majuscula*, *Acanthophora*, and *Laurencia*, although only *L. majuscula* induced postlarval growth. The species that resulted in the greatest postmetamorphic survivorship in the study by Switzer-Dunlap & Hadfield (1977) were the species on which the adults were typically found. They did note however that for all species without a substrate no metamorphosis occurred. The veligers of *A. brasiliana* were induced to metamorphose by contact with *Callithamnion* and *Polysiphonia*; however, the greatest metamorphic success occurred on the latter species (Strenth & Blankenship, 1978). Pawlik (1989) discovered that *Aplysia californica* metamorphosed when exposed to any one of 18 different species of algae and in control dishes with no stimulus. Despite their indiscriminate settlement, they required a diet of either *Laurencia pacifica* or *Plocamium cartilagineum* for postlarval development (Pawlik, 1989). *Aplysia oculifera* metamorphosed in response to six of 12 macroalgal species tested by Plaut et al. (1995). None of the veligers metamorphosed under control conditions.

Akera bullata is known to be herbivorous. Thompson & Seaward (1989) documented *Enteromorpha* and possibly *Zostera* roots as prey. Morton & Holme (1955) found *A. bullata* grazing *Ulva* in Plymouth and also recorded it as a deposit feeder; in this study, adults also were found to graze a variety of different red and green algae and on the leaves of *Zostera* spp. It is not surprising therefore that *A. bullata* will settle on a variety of different substrata, including a bacterial biofilm, several species of phytoplankton, and algae. Similarly to the newly settled juveniles of *D. auricularia* (Switzer-Dunlap & Hadfield, 1977), all *A. bullata* juveniles were observed consuming biofilms. As they grew larger, the juveniles provided with *Ulva lactuca* were seen to consume the thin fronds, but never during this study were juveniles observed feeding upon *Chondrus crispus* or *Nemalion helminthoides*. It is likely that they had not reached a size that would have enabled them to consume the thick fronds. For the latter two conditions, the juveniles were only observed grazing on biofilms formed on the surface of the container and fronds.

The adoption of lecithotrophy may have profound implications on the ecology of *A. bullata*, particularly within an enclosed habitat such as the Fleet. Previous studies investigating British populations of the lecithotrophic nudibranch *Adalaria proxima*, which is able to undergo metamorphosis within 1–2 days after hatching (Thompson, 1958; Kempf & Todd, 1989; Lambert & Todd, 1994), were found to have significant differentiation over 100 km (Todd et al., 1998; Lambert et al., 2003). The short larval duration combined with a behavioral constraint were both implemented in its reduced dispersal (Todd et al., 1998; Lambert et al., 2003). A similar situation may be occurring between populations of *A. bullata* within the Fleet and elsewhere; however, further investigation is required to substantiate this claim.

Acknowledgments. I thank Dr. P. Dyrynda for collecting *Akera* from the Fleet and Dr. P. Hayward, Prof. M. Edmunds, and an anonymous referee for critically reading the manuscript. This work was financed by a Swansea University scholarship.

LITERATURE CITED

Bridges, C. B. 1975. Larval development of *Phyllaplysia taylori* Dall, with a discussion of the development in the Anaspidea (Opisthobranchiata: Anaspidea). Ophelia 14: 161–184.

Kempf, S. & C. Todd. 1989. Feeding potential in the lecithotrophic larvae of *Adalaria proxima* and *Tritonia hombergi*: an evolutionary perspective. Journal of the Marine Biological Association of the United Kingdom 69: 659–682.

Klussmann-Kolb, A. 2003. Phylogeny of the Aplysiidae (Gastropoda, Opisthobranchia) with new aspects of the evolution of seahares. Zoologica Scripta 33:439–462.

Klussmann-Kolb, A., A. Dinapoli, K. Kuhn, B. Streit & C. Albrecht. 2008. From sea to land and beyond—new insights into the evolution of euthyneuran Gastropoda (Mollusca). BMC Evolutionary Biology 8:1–16.

Kriegstein, A. R., V. Castellucci & E. R. Kandel. 1974. Metamorphosis of *Aplysia californica* in laboratory culture. Proceedings of the National Academy of Sciences USA 71:3654–3658.

Lambert, W., C. Todd & J. Thorpe. 2003. Genetic population structure of two intertidal nudibranch mol-

luscs with contrasting larval types: temporal variation and transplant experiments. Marine Biology 142:461–471.

LAMBERT, W. J. & C. D. TODD. 1994. Evidence for a waterborne cue inducing metamorphosis in the dorid nudibranch mollusc *Adalaria proxima* (Gastropoda: Nudibranchia). Marine Biology 120:265–271.

MEDINA, M. & P. J. WALSH. 2000. Molecular systematics of the order Anaspidea based on mitochondrial DNA sequence (12S, 16S, and CO1). Molecular Phylogenetics and Evolution 15:41–58.

MORTON, J. E. & N. A. HOLME. 1955. The occurrence at Plymouth of the opisthobranch *Akera bullata*, with notes on its habits and relationships. Journal of the Marine Biological Association of the United Kingdom 34:101–112.

OTSUKA, C., L. OLIVER, Y. ROUGER & E. TOBACH. 1981. *Aplysia punctata* added to the list of laboratory-cultured *Aplysi*a. Hydrobiologia 83:239–240.

PAIGE, J. A. 1986. The laboratory culture of two aplysiids, *Aplysia brasiliana* Rang, 1828, and *Bursatella leachii plei* (Rang, 1828) (Gastropoda: Opisthobranchia) in artificial seawater. The Veliger 29:64–69.

PAIGE, J. A. 1988. Biology, metamorphosis and postlarval development of *Bursatella leachii plei* Rang (Gastropoda: Opisthobranchia). Bulletin of Marine Science 42:65–75.

PAWLIK, J. R. 1989. Larvae of the sea hare *Aplysia californica* settle and metamorphose on an assortment of macroalgal species. Marine Ecology Progress Series 51:195–199.

PLAUT, I., A. BORUT & M. E. SPIRA. 1995. Growth and metamorphosis of *Aplysia oculifera* larvae in laboratory culture. Marine Biology 122:425–430.

STRENTH, N. E. & J. E. BLAKENSHIP. 1978. Laboratory culture, metamorphosis and development of *Aplysia brasiliana* Rang, 1828 (Gastropoda: Opisthobranchia). The Veliger 21:99–103.

SWITZER-DUNLAP, M. 1978. Larval biology and metamorphosis of aplysiid gastropods. Pp. 197–206 in F. S. Chia & M. E. Rice (eds.), Settlement and Metamorphosis of Marine Invertebrate Larvae. Elsevier: New York.

SWITZER-DUNLAP, M. & M. G. HADFIELD. 1977. Observations on development, larval growth and metamorphosis of four species of Aplysiidae (Gastropoda: Opisthobranchia) in laboratory culture. Journal of Experimental Marine Biology and Ecology 29:245–261.

SWITZER-DUNLAP, M. & M. G. HADFIELD. 1981. Laboratory culture of *Aplysia*. Pp. 199–216 in Laboratory Animal Management, Marine Invertebrates. Committee on Marine Invertebrates. National Academy Press: Washington, DC.

THOMPSON, T. E. 1958. The natural history, embryology, larval biology and post-larval development of *Adalaria proxima* (Alder and Hancock) (Gastropoda, Opisthobranchia). Philosophical Transactions of the Royal Society Series B 242:1–58.

THOMPSON, T. E. 1961. The importance of larval shell in the classification of the Sacoglossa and the Acoela (Gastropoda Opisthobranchia). Proceedings of the Malacological Society London 34:233–238.

THOMPSON, T. E. 1967. Direct development in the nudibranch *Cadlina laevis*, with a discussion of developmental processes in Opisthobranchia. Journal of the Marine Biological Association of the United Kingdom 47:1–22.

THOMPSON, T. E. 1976. Biology of Opisthobranch Molluscs. Vol. 1. Ray Society: London.

THOMPSON, T. E. & D. R. SEAWARD. 1989. Ecology and taxonomic status of the Aplysiomorph *Akera bullata* in the British Isles. Journal of Molluscan Studies 55:489–496.

THORSON, G. 1946. Reproduction and larval development of Danish marine bottom invertebrates, with special reference to the planktonic larvae in the sound (Øresund). C. A. Reitzels forlag: København. 523 pp.

TODD, C. D., W. LAMBERT & J. THORPE. 1998. The genetic structure of intertidal populations of two species of nudibranch molluscs with planktotrophic and pelagic lecithotrophic larval stages: are pelagic larvae "for" dispersal? Journal of Experimental Marine Biology and Ecology 228:1–28.

VONNEMANN, V., M. SCHRÖDL, A. KLUSSMANN-KOLB & H. WÄGELE. 2005. Reconstruction of the phylogeny of the Opisthobranchia (Mollusca: Gastropoda) by means of 18S and 28S rRNA gene sequences. Journal of Molluscan Studies 71:113–125.

The Veliger 51(3):102–108 (November 16, 2012)

THE VELIGER

The Genus *Amarophos* Woodring, 1964 (Gastropoda: Buccinoidea) in the Tropical American Neogene, with a Description of Two New Species

BERNARD LANDAU*

Departamento e Centro de Geologia da Faculdade de Ciências da Universidade de Lisboa, Campo Grande, 1749-016 Lisboa, Portugal and International Health Centres, Avenida Infante de Henrique 7, Areias São João, P-8200 Albufeira, Portugal
(e-mail: bernielandau@sapo.pt)

AND

CARLOS M. DA SILVA

Departamento e Centro de Geologia da Faculdade de Ciências da Universidade de Lisboa, Campo Grande, 1749-016 Lisboa, Portugal

Abstract. The presence of the extinçt buccinid genus *Amarophos* in the tropical American Caribbean Neogene is reviewed with the description of two new Lower Pliocene species: *Amarophos woodringi* nov. sp. from the Shark Hole Point Formation of the Bocas del Toro region, Panama; and *Amarophos arayaensis* nov. sp. from the Aramina Formation of the Araya Peninsula, Venezuela. These new records extend both the previously known geographical and geological distribution of the genus.

INTRODUCTION

The genus *Amarophos* was described by Woodring (1964) based on fossil material from the Lower Pliocene Chagres Formation of Panama (now considered Messinian, uppermost Miocene; Coates et al., 2005: fig. 9). In the generic description, Woodring (1964) argued that *Amarophos* was closely similar in outline to *Rhipophos* Woodring, 1964, described from the Upper Miocene Middle and Upper Gatun Formations of Panama, but with a wider and more channelled suture. In *Amarophos*, the ribs on the later teleoconch whorls are obsolete or almost so, and if present they are crowded and poorly delimited, so that the spiral sculpture is always predominant on the last whorl. In *Rhipophos*, the axial ribs also are crowded, but they persist on the last whorl and are more or less equal in strength to the spiral cords, giving the last whorl a finely cancellate appearance.

Woodring considered *Ptychosalpynx*? *dentalis* Olsson, 1922 from the then Lower Miocene Uscari Shale of Costa Rica the earliest member of the genus and stated that it is a very typical shell for the Upper Uscari Formation. The uppermost Uscari Formation is now considered to be Tortonian-Messinian in age by Coates et al. (2005: fig. 9). Woodring (1964) also reported that Olsson had collected *Amarophos dentalis* from the Lower Miocene Las Perdices Shale of Colombia (Olsson, personal communication in Woodring, 1964). These deposits are now considered upper Middle to Upper Miocene (Duque-Caro, 1990). Taking into account the recalibration of the age of the assemblages, until now *Amarophos* was known only from the Upper Miocene.

In this paper, two additional members for the genus are described, both from the Lower Pliocene: one species from the Shark Hole Point Formation of the Valiente Peninsula (Bocas del Toro region), Panama, and the other species from the Aramina Formation, Araya Peninsula (Sucre), Venezuela.

MATERIALS AND METHODS

This work includes previously known museum fossil material present in the Panama Palaeontological Project collections (Naturhistorisches Museum Basel [NMB], Switzerland) and newly collected specimens resulting from extensive fieldwork undertaken by us in the Caribbean Neogene Formations of Panama and Venezuela during the past 10 yr.

The material from the Shark Hole Point comes from the east coast of the Valiente Peninsula, Bocas del Toro region, Panama (Figure 1). Coates et al. (2005) review the stratigraphy of the Neogene rocks of the Bocas del Toro region, and they dated the Shark Hole Point Formation as Lower Pliocene (5.3–3.6 Ma). Benthic foraminifera indicate that the paleobathymetry ranged

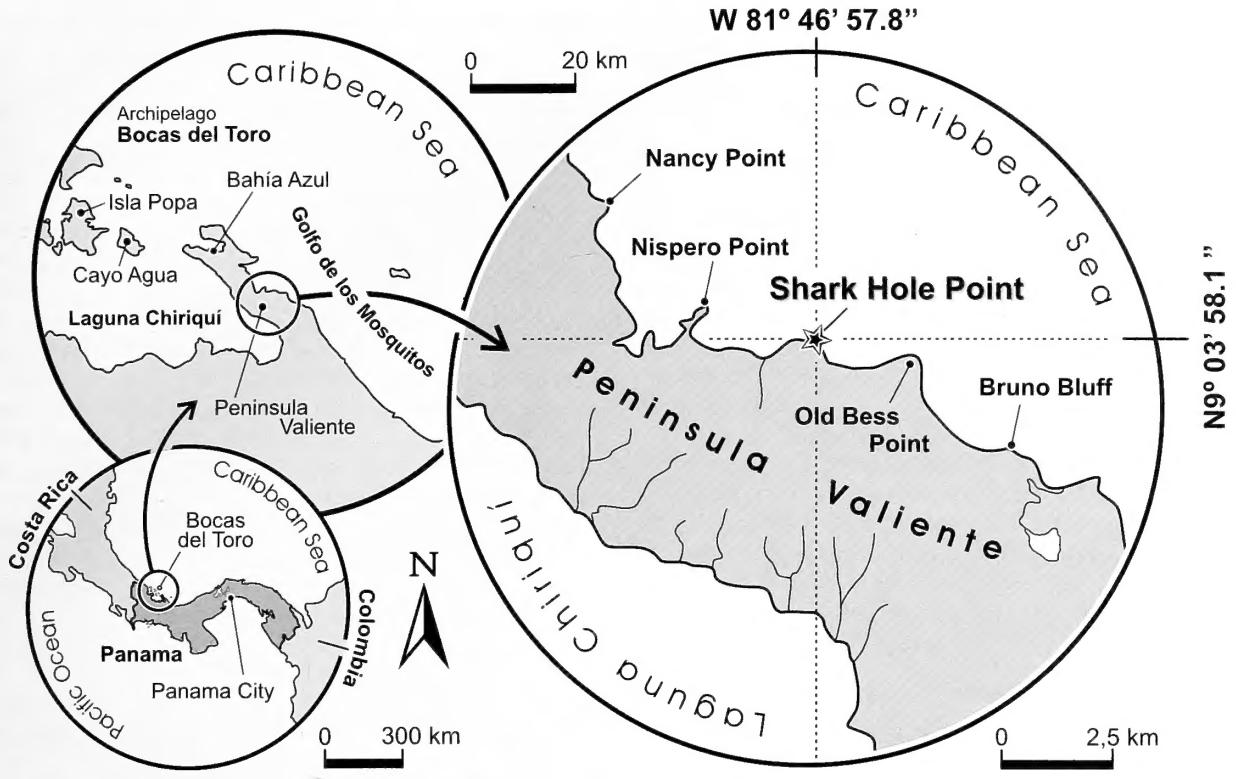

Figure 1. Geographical location of the Shark Hole Point outcrop in the Valiente Peninsula, Bocas del Toro region, Panama.

from −100 to −200 m (Collins, 1993). For further information, see Coates et al. (2005).

The material from Cerro Barrigón comes from the Araya Peninsula, Sucre, mainland Venezuela (Figure 2). Macsotay & Hernandez (2005) considered the sedimentary sequence at Cerro Barrigón to correspond to the Aramina Formation, Cubagua Group, Lower Pliocene. For further information, see Landau and Da Silva (2010).

The material described and discussed here is housed in the Naturhistorisches Museum Basel (NHB collection [coll.]), Switzerland, and in the Bernard Landau collection to be housed in the Naturhistorisches Museum Wien (NHMW coll.), Vienna, Austria. Type material is deposited in the Naturhistorisches Museum Wien (NHMW coll.), Vienna, Austria.

In the Systematic Palaeontology section, we have followed the classification proposed by Bouchet & Rocroi (2005).

SYSTEMATIC PALAEONTOLOGY

BUCCINOIDEA Rafinesque, 1815

BUCCINIDAE Rafinesque, 1815

Pisaniinae Gray, 1857

Traditionally, the sand-dwelling "*Phos*" group of taxa have been placed in the Photinae Gray 1857, synonymized with Pisaniinae Gray, 1857 by Bouchet & Rocroi (2005:255). This position was followed by Watters (2009) in his revision of several pisinine genera in the Recent western Atlantic. This may not be correct, and molecular data are needed to confirm this synonymy (Vermeij, personal communication).

Genus *Amarophos* Iredale, 1921

Type species: By original designation, *Amarophos bothrus* Woodring, 1964: 267. Fossil, Neogene Caribbean.

Amarophos woodringi nov. sp.

(Figures 3–11)

Dimensions and type material: Holotype NHMW 2010/0176/0001 (Figures 1–3), height 25.2 mm, maximum width 16.7 mm; paratype 1 NHMW 2010/0176/0002 (Figures 4–6), height 25.0 mm; paratype 2 NHMW 2010/0176/0003 (Figures 7–9), height 30.7 mm (NHMW coll., ex BL coll.).

Etymology: Named in honour of Wendell Phillips Woodring, in recognition of his enormous contribution to Caribbean Neogene malacology during his work with the U.S. Geological Survey (USGS).

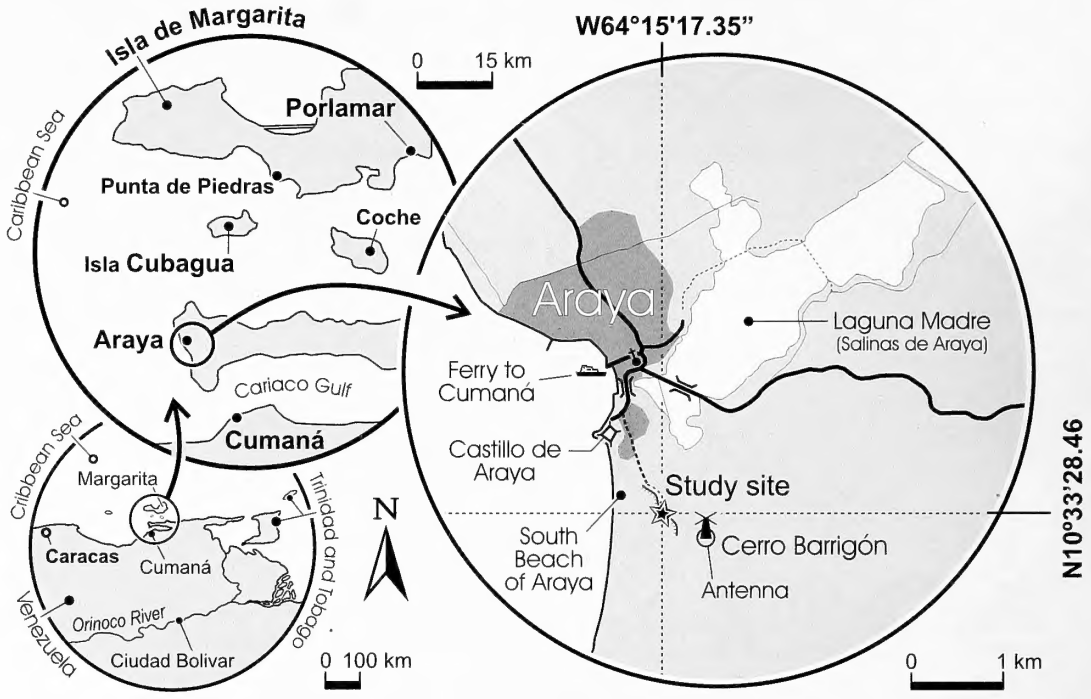

Figure 2. Geographical location of the Araya Peninsula outcrop in the Araya Peninsula, Sucre, Venezuela.

Type locality: Shark Hole Point, Valiente Peninsula, Bocas del Toro region, Panama.

Stratum typicum: Shark Hole Point Formation, Lower Pliocene.

Additional material: Fourteen specimens, Shark Hole Point Formation, Shark Hole Point, Valiente Peninsula, Bocas del Toro region, Panama. (BL coll./ NHMW coll.).

Locality PPP00386 (NMB17854), 10 specimens, unnumbered lot; PPP00388 (NMB17855), four specimens, unnumbered lot; PPP00390 (NMB17856), six specimens, unnumbered lot; locality PPP00392 (NMB17857), two specimens, unnumbered lot; locality PPP00391 (NMB17858), five specimens, unnumbered lot; locality PPP00396 (NMB17908), one specimen, unnumbered lot; locality PPP00397 (NMB17859), 47 specimens, unnumbered lot; locality PPP00400 (NMB17860), eight specimens, unnumbered lot; locality PPP01293 (NMB18545), seven specimens, unnumbered lot; locality PPP01714 (NMB18768), four specimens, unnumbered lot; locality PPP02189 (NMB18688), 35 specimens, unnumbered lot; locality PPP02191 (NMB18690), seven specimens, unnumbered lot; locality PPP02190 (NMB18689), one specimen, unnumbered lot; seven specimens, unnumbered lot; locality PPP02195 (NMB18694), 11 specimens, unnumbered lot; locality PPP02196 (NMB18695), seven specimens, unnumbered lot; locality PPP02197 (NMB18696), 18 specimens, unnumbered lot; locality PPP02198 (NMB18697), 21 specimens, unnumbered lot; locality PPP02199 (NMB18698), one specimen, unnumbered lot; locality PPP02200 (NMB18699), one specimen, unnumbered lot; locality PPP02201 (NMB18700), nine specimens, unnumbered lot; locality PPP02202 (NMB18701), 12 specimens, unnumbered lot; locality PPP02203 (NMB18702), one specimen, unnumbered lot; locality PPP02204 (NMB18703), 16 specimens, unnumbered lot; locality PPP02227 (NMB18724), five specimens, unnumbered lot; locality PPP02229 (NMB18726), 17 specimens, unnumbered lot.

Diagnosis: A small- to medium-sized *Amarophos* species, with a relatively narrow canaliculate suture, convex spire whorls, inflated-ovate last whorl, and a very fine reticulate sculpture on later teleoconch whorls, with the spiral component predominant, finely beaded.

Description: Shell small- to medium-sized for genus, relatively solid, ovate with a scalate spire. Protoconch and early teleoconch whorls decorticated in all specimens. Teleoconch consists of five to six convex whorls, with the periphery at the abapical suture. Suture deeply canaliculate, forming a narrow infrasutural gutter, widening slightly abapically. Third teleoconch whorl (first teleoconch whorl with surface ornament preserved) bears 11–13 narrow, elevated, widely spaced axial ribs and five or six narrow, close-set spiral cords. A secondary spiral thread or cord is

developed in the interspaces, variable in strength and onset. Abapically the axial ribs weaken, obsolete on the penultimate and last whorl, where the axial sculpture consists of sharp, close-set growth lines giving the surface a finely reticulate appearance. At the intersections where the spiral cords override the axial growth lines, the cords are lightly thickened, giving them a finely beaded appearance. Penultimate whorl with five to six spiral cords. Last whorl inflated, ovate, widely convex in profile, constricted at the base, bearing 16–19 narrow, elevated spiral cords. Aperture small- to medium-sized, ovate. Outer lip sinuous in profile, with a pronounced notch abapically; lip edge sharp, crenulated; lip callus absent; aperture strongly and deeply lirate within, 13–15 well-developed lirae that stop just short of the lip edge; anal canal poorly developed, marked by a shallow groove; siphonal canal open, relatively long, narrow, strongly posteriorly recurved. Columella deeply excavated in the mid-portion, with a strong columellar fold at its abapical edge bordering the siphonal canal and five or six weaker tubercles or folds above the terminal columellar fold, weakening adapically, developed to a variable degree. Columellar callus hardly developed, the spiral sculpture visible through the very fine callus wash. Siphonal fasciole somewhat swollen, sculptured by spiral cords.

Discussion: *Amarophos woodringi* nov. sp. is relatively common in the Pliocene clays of Shark Hole Point, Panama. The shells are fairly uniform in shape and height of spire, but they vary in size, measuring from 20.3 to 30.8 mm in height. The most variable shell feature is the strength of the secondary spiral cords and the position at which they first appear. In the holotype, the secondary threads only appear on the last whorl and remain very weak, whereas is other specimens they appear as early as the fourth teleoconch whorl and are only slightly weaker than the primary spiral cords. The strength and number of columellar folds or tubercles developed above the abapical columellar fold is also highly variable. Unfortunately, the protoconch and early teleoconch whorls are decorticated or missing in all the specimens available. Interestingly, Woodring (1964) made the same observation for his specimens of *Amarophos bothrus* Woodring, 1964 from the Chagres Formation of Panama.

Woodring (1964:267) mentioned the presence of an undescribed *Amarophos* species in "strata of late Miocene age in the Bocas del Toro area of northwestern Panamá (USGS 8322, Valiente Peninsula)." He was undoubtedly referring to this species, a common species at Shark Hole Point.

Amarophos bothrus Woodring, 1964 (Figures 12, 13, holotype; Figures 14–19, additional specimens) from the Chagres Formation of Panama was considered to be Lower Pliocene by Woodring (1964) but is now known to be Messinian, uppermost Miocene (Collins et al., 2005:fig. 9; 5.8–6.2 Ma). Woodring (1964) distinguished *A. bothrus* from the then undescribed Valiente Peninsula species as being smaller and more slender. Size may not be a reliable feature by which to separate the two taxa, because many shells of *A. woodringi* are smaller than the size given for *A. bothrus* (24.7 mm in height). *Amarophos woodringi* has a more ovate, slightly more inflated and squatter shell, the spire whorls are more convex, the last whorl more inflated, less elongate and slightly more strongly constricted at the base, and the primary spiral cords are sharper and narrower than in *A. bothrus*.

Amarophos dentalis (Olsson, 1922; Figures 20, 21) from the Tortonian-Messinian Miocene of Atlantic Costa Rica differs from *A. woodringi* in having a taller, more regularly conical spire; a narrower and less strongly developed sutural gutter; a more rounded last whorl adapically; and axial ribs that persist, albeit weakly, onto the last whorl, whereas there are no ribs on the last whorl of *A. dentalis*.

Amarophos arayaensis nov. sp.

(Figures 22–24)

Dimensions and type material: Holotype NHMW 2010/0176/0004 (Figures 22–24), height 41.2 mm, width 20.7 mm (NHMW coll., ex BL coll.).

Etymology: Named after the type locality, Araya Peninsula.

Type locality: Upper reddish coarse sandy bed, Cerro Barrigón, Araya Peninsula (of Landau & Silva, 2010), Venezuela.

Stratum typicum: Aramina Formation, Cubagua Group, Lower Pliocene.

Diagnosis: A large *Amarophos* species, with a very wide infrasutural gutter, barrel-shaped last whorl, relatively numerous axial ribs on the early teleoconch whorls, relatively numerous spiral cords on the penultimate whorl, elongated aperture, siphonal canal hardly posteriorly recurved, narrowly excavated columella and thick columellar callus for genus.

Description: Shell large for genus, relatively solid, barrel-shaped last whorl, scalate spire. Protoconch and early teleoconch whorls decorticated. Teleoconch consists of seven convex whorls, with the periphery at the abapical suture. Suture deeply canaliculate, forming a wide, slightly concave to flat-bottomed, infrasutural gutter. Fourth teleoconch whorl (first teleoconch whorl with surface ornament well pre-

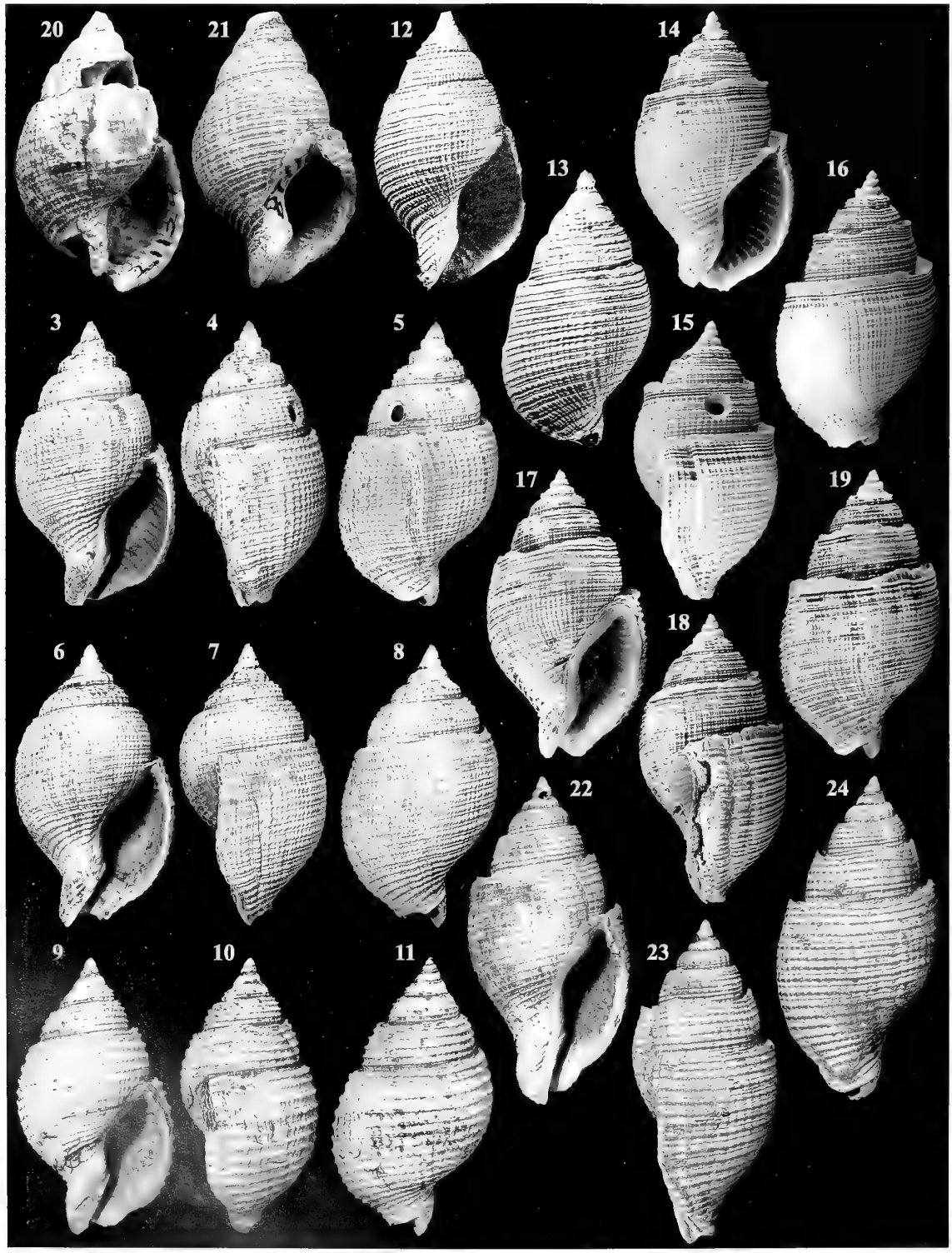

Figures 3–5. *Amarophos woodringi* nov. sp. Holotype NHMW 2010/0176/0001 (NHMW coll., ex BL coll.). Height 25.2 mm. Shark Hole Point Formation, Lower Pliocene, Shark Hole Point, Valiente Peninsula, Bocas del Toro region, Panama.
Figures 6–8. *Amarophos woodringi* nov. sp. Paratype 1 NHMW 2010/0176/0002 (NHMW coll., ex BL coll.). Height 25.0 mm. Shark Hole Point Formation, Lower Pliocene, Shark Hole Point, Valiente Peninsula, Bocas del Toro Region, Panama.

served) bears 16 rounded, prosocline axial ribs and eight narrow, close-set spiral cords. A secondary and sometimes tertiary spiral thread is developed in the interspaces on the penultimate and last whorls. Abapically the axial ribs weaken, subobsolete on second half of the fourth whorl. On the second half of the penultimate whorl and last whorl the axial sculpture reappears, consisting of narrow, poorly defined, very close-spaced, flattened ribs. The spiral cords overrun the indistinct ribs giving them a finely wavy appearance. At the sculptural intersections, the cords are lightly thickened, giving them a very weakly beaded appearance. Penultimate whorl with nine spiral cords. Last whorl barrel-shaped, weakly convex in profile, with a wide infrasutural gutter, weakly constricted at the base, bearing 18 narrow spiral cords. Aperture small- to medium-sized, elongate-ovate. Outer lip edge missing; lip callus absent; aperture strongly and deeply lirate, with 16 lirae within; anal canal clearly developed, represented by narrow groove; siphonal canal open, relatively long, narrow, weakly posteriorly recurved. Columella moderately excavated in the mid-portion, with a strong columellar fold at its abapical edge and indistinct tubercles or folds running along the entire outer columellar margin, two elongated folds in the parietal region extending deep within the aperture. Columellar callus thickened, well-delimited, narrowly expanded. Siphonal fasciole sculptured by spiral cords.

DISCUSSION

Although represented by a single specimen, *Amarophos arayaensis* nov. sp. is quite different from all its congeners in having a much larger, more barrel-shaped shell, with a much wider infrasutural gutter. It also has more numerous and less widely spaced axial ribs on the early teleoconch whorls, more numerous spiral cords on the penultimate whorl, and the last whorl is more elongated and far less constricted at the base. The siphonal canal is less strongly posteriorly recurved, the columella is less excavated in the mid-portion, thicker, and with more tubercles or folds along its edge.

Amarophos arayaensis is most similar in shape to *Amarophos bothrus* Woodring, 1964 from the Chagres Formation of Panama, but with a shell twice the size. They differ mainly in the character of the last whorl that is even more elongated and less constricted at the base than in *A. arayaensis*. The infrasutural gutter is wider in *A. arayaensis*, the siphonal canal is straighter, less recurved; the columella is less excavated and the columellar callus is thicker. *Amarophos dentalis* (Olsson, 1922) is quite different, with a more conical spire, a much narrower sutural gutter, and a more rounded last whorl. Of all the *Amarophos* species *A. dentalis* has the most strongly developed axial sculpture. Although always weakly developed in the genus, narrow elevated axial ribs are present on the last whorl of *A. dentalis*, whereas both the penultimate and last whorls in *A. arayaensis* have closely crowded axial lamellae but no elevated ribs.

Paleobiological implications: With the descriptions of *A. woodringi* nov. sp. and *A. arayaensis* nov. sp., the known number of members of this genus is doubled to four. *Amarophos* is an unusual genus in the Caribbean Neogene, because it seems to have been quite restricted in both its geographical and geological distribution. The genus has so far been found only in the Atlantic portion of the Gatunian palaeobiogeographical province (*sensu* Vermeij & Petuch 1986; Landau et al. 2008), and even here it is restricted to the Central American-northern South American Subprovince (of Woodring, 1974; =Limonian Subprovince of Petuch, 1988) and the Colombian-Venezuelan-Trinidad Subprovince (of Woodring, 1974; =Puntagavilanian Subprovince of Petuch, 1988). The faunal province names used herein are those erected by Woodring (1974) and are preferred over those proposed by Petuch (1988; but see Landau

←
Figures 9–11. *Amarophos woodringi* nov. sp. Paratype 2 NHMW 2010/0176/0003 (NHMW coll., ex BL coll.). Height 30.7 mm. Shark Hole Point Formation, Lower Pliocene, Shark Hole Point, Valiente Peninsula, Bocas del Toro region, Panama.
Figures 12–13. *Amarophos bothrus* Woodring, 1964. Holotype USNM 643697. Height 24.7 mm. upper Chagres Formation, Messinian, Upper Miocene, locality 208 (of Woodring, 1964) Mouth of Rio Indios, Panama (reproduced from Woodring, 1964: pl. 47, figs. 1, 2).
Figures 14–16. *Amarophos bothrus* Woodring, 1964. NMB H19489. Height 28.9 mm. Upper Chagres Formation, Messinian, Upper Miocene, locality NMB 18990, Colón. North coast, west of Colón. Approximately 4.4-km air distance west of Río Indio and approximately 900 m east of Punta Gavilán, Morro Rajado.
Figures 17–19. *Amarophos bothrus* Woodring, 1964. NMB H19490. Height 31.1 mm. Upper Chagres Formation, Messinian, Upper Miocene, locality NMB 18990, Colón. North coast, west of Colón. Approximately 4.4-km air distance west of Río Indio and approximately 900 m east of Punta Gavilán, Morro Rajado.
Figure 20. *Amarophos dentalis* Olsson, 1922. Syntype PRI 21124. Height 29.0 mm. uppermost Uscari Formation, Tortonian-Messinian, Upper Miocene, Cocles Creek, Limon Costa Rica (Olsson, 1922: specimen pl. 15, fig. 14).
Figure 21. *Amarophos dentalis* Olsson, 1922. Syntype PRI 21128. Height 27.3 mm. uppermost Uscari Formation, Tortonian-Messinian, Upper Miocene, Cocles Creek, Limon Costa Rica (Olsson, 1922: specimen pl. 15, fig. 18).
Figures 22–24. *Amarophos arayaensis* nov. sp. Holotype NHMW 2010/0176/0004 (NHMW coll., ex BL coll.). Height 41.2 mm. Aramina Formation, Cubagua Group, Lower Pliocene, Upper reddish coarse sandy bed, Cerro Barrigón, Araya Peninsula.

et al., 2008). Geologically, the previous records of the genus are restricted to the Tortonian-Messinian, Upper Miocene (*A. dentalis* and *A. bothrus*). These new records extend the known range into the Lower Pliocene (*A. woodringi* and *A. arayaensis*). There is no further record for the genus.

The origin of *Amarophos* is obscure. Woodring (1964) suggested it might have evolved from *Rhipophos* Woodring, 1964 that occurs in the Upper Miocene Middle and Upper Gatun Formations of Panama but pointed out such a lineage was not possible because they were considered coeval at the time. With the recalibration of the age of many of the Caribbean assemblages, *Amarophos* is indeed slightly younger, with a first appearance in the Tortonian-Messinian rather than the Serravalian-Tortonian for *Rhipophos*. However, in our opinion this lineage is conjectural. Unfortunately, the protoconch that has been used as an important generic character in the *Phos* group of buccinids (i.e. Olsson, 1964) is missing in all *Amarophos* specimens examined.

Acknowledgments. We thank W. Etter, O. Schmidt, and F. Wiedenmeyer (all NMB) for help with access to the Panama Paleontology Project (PPP) collection. Our thanks also to Gregory Dietl (Paleontological Research Institution) for permission to reproduce some images of type material from their database. We acknowledge the following Panamian entities for greatly facilitating fieldwork and for granting the necessary permits to conduct the fieldwork in the Republic of Panama: Autoridad del Canal de Panamá/Panama Canal Authority (ACP) and Dirección de Recursos Minerales del Ministerio de Comercio e Industria (MICI). We thank the Smithsonian Tropical Research Institute (STRI) in Panama, both at Panamá City and at the STRI Bocas del Toro Research Station, for help and guidance in obtaining the necessary permits and for all the logistical laboratory and field support.

LITERATURE CITED

BOUCHET, P. & J. P. ROCROI. 2005. Classification and nomenclator of gastropod families. Malacologia 47(1–2): 1–397.

COATES, A. G., D. F. MCNEILL, M. P. AUBRY, W. A. BERGGREN & L. S. COLLINS. 2005. An introduction to the Geology of the Bocas del Toro Archipelago, Panama. Caribbean Journal of Science 41(3):374–391.

COLLINS, L. S. 1993. Neogene paleoenvironments of the Bocas del Toro Basin, Panama. Journal of Paleontology 67:699–710.

DUQUE-CARO, H. 1990. Neogene stratigraphy, paleoceanography and palaeobiogeography in northwest South America and the evolution of the Panama seaway. Palaeogeography, Palaeoclimatology, Palaeoecology 77(3–4):203–234.

LANDAU, B. M. & C. M. DA SILVA. 2010. Early Pliocene gastropods of Cubagua, Venezuela: taxonomy, palaeobiogeography and ecostratigraphy. Palaeontos 19:1–221.

LANDAU, B. M., G. J. VERMEIJ & C. M. DA SILVA. 2008. Southern Caribbean Neogene palaeobiogeography revisited. New data from the Pliocene of Cubagua, Venezuela. Palaeogeography, Palaeoclimatology, Palaeoecology 257: 445–461.

MACSOTAY, O. & R. C. HERNANDEZ. 2005. Paleoclimatology of the Pleistocene-Holocene using marine molluscs and hermatypic corals from northern Venezuela. Transactions of the 16th Caribbean Geological Conference, Barbados. Caribbean Journal of Earth Science 39:93–104.

OLSSON, A. A. 1964. Neogene mollusks from northwestern Ecuador.. Paleontological Research Institution: Ithaca, New York. 256 pp.

PETUCH, E. J. 1988. Neogene history of tropical American mollusks. Biogeography and evolutionary patterns of tropical western Atlantic Mollusca. Coastal Education and Research Foundation: Charlottesville, Virginia. 217 pp.

VERMEIJ, G. J. & E. J. PETUCH. 1986. Differential extinction in tropical American molluscs: endemism, architecture, and the Panama land bridge. Malacologia 27:29–41.

WATTERS, G. T. 2009. A revision of the western Atlantic Ocean genera *Anna*, *Antillophos*, *Bailya*, *Caducifer*, *Monostiolum*, and *Parviphos*, with description of a new genus *Dianthiphos*, and notes on *Engina* and *Hesperisternia* (Gastropoda: Buccinidae: Pisaniinae) and *Cumia* (Colubrariidae). The Nautilus 123:225–275.

WOODRING, W. P. 1964. Geology & paleontology of the Canal Zone and adjoining parts of Panama. Geology and description of the Tertiary Mollusks (Gastropods: Columbellidae to Volutidae). U.S. Geological Survey Professional paper 306-C, 241–297.

WOODRING, W. P. 1974. The Miocene Caribbean Faunal Province and its Subprovinces. Verhandlungen der naturforschenden Gesellschaft in Basel 84(1):209–213.

The Veliger 51(3):109–116 (November 16, 2012)

THE VELIGER

Population Dynamics of Freshwater Gastropod *Chilina fluminea* (Chilinidae) in a Temperate Climate Environment in Argentina

D. E. GUTIÉRREZ GREGORIC,* V. NÚÑEZ, AND A. RUMI

Consejo Nacional de Investigaciones Científicas y Técnicas, División Zoología Invertebrados, Museo de La Plata, Facultad de Ciencias Naturales y Museo, Universidad Nacional de La Plata, 1900 La Plata, Buenos Aires, Argentina (e-mail: dieguty@fcnym.unlp.edu.ar)

Abstract. The presence and density of gastropods, and the individual growth rate of *Chilina fluminea* snails at Río de la Plata beach, Berisso, Buenos Aires province, Argentina, were analyzed to obtain population data about hosts that could be useful for control of the free-swimming larval stages (cercariae). *Chilina fluminea* has a unique annual reproductive period during winter, whereas other gastropods inhabiting the same area reproduce one to three times a year, but never in winter. Thus, autumn, the season before reproduction and oviposition, is the most adequate season for taking actions to regulate the size of *C. fluminea* populations to reduce possible cases of human schistosomic dermatitis.

INTRODUCTION

The family Chilinidae Dall, 1870 (Gastropoda: Hygrophila) is exclusive to South America, ranging from the Tropic of Capricorn to Cape Horn and the Falkland islands. The family includes the single genus *Chilina* Gray, 1828 with approximately 32 species, 17 of which have been recorded in Argentina (Castellanos and Miquel, 1980; Castellanos and Gaillard, 1981, Gutiérrez Gregoric & Rumi, 2008); the rest are distributed within Chile. From an evolutionary perspective, Chilinidae is among the most primitive of pulmonate gastropods. Dayrat et al. (2001) confirmed the monophyly of Hygrophyla, including the Chilinidae at the base of this clade.

Chilinid species have human health importance because these freshwater gastropods act as intermediate hosts of trematodes, releasing schistosomatid (Plathyhelminthes: Digenea) furcocercarias (cercariae) that usually cause human schistosomic dermatitis (Szidat, 1951; Martorelli, 1984).

Many Argentinean species of *Chilina* are endemic, and their biology and ecological strategies are largely unknown. In general, only a few such studies have been reported in this family: Miquel (1986) studied the life cycle of *Chilina fluminea* Maton (1809) and its gonad evolution; Bosnia et al. (1990) analyzed the growth of *Chilina gibbosa* G. B. Sowerby I, 1841, and its density; Estebemet et al. (2002) analyzed the natural diet for *Chilina parchappii* (d'Orbigny, 1835); Gutiérrez Gregoric et al. (2010) analyzed the growth and density of *Chilina megastoma* Hylton Scott, 1958; and Quijon & Jaramillo (1999) and Quijon et al. (2001) worked on *Chilina ovalis* (Sowerby, 1841) from southern Chile, emphasizing spatial distribution and growth.

The present work focuses on estimating population patterns, such as density, individual growth rate, and recruitment times, of a population of *C. fluminea* in a temperate climate at "La Balandra" beach, Berisso, Buenos Aires province, Argentina. The study established that recruitment times and growth rates of the host allow us to define and assess eventual actions for control of furcocercarias that usually cause human schistosomic dermatitis.

MATERIALS AND METHODS

Samples for this study were collected from the canal of La Balandra beach (34°55′S, 57°43′W). This canal arises from lowlands close to the beach and flows into the Rio de la Plata River and estuary. The sample area selected is located some 150 m from the canal mouth, and it is approximately 7 meters in length and restricted to the left margin of the canal, the only place where a population of *C. fluminea* was recorded. Bulrush (*Scirpus giganteus* Kunth) and yellow iris (*Iris pseudacorus* Linné) grow in the border of the canal.

The study included 24 samples collected between November 2000 and September 2003. Water temperature (Celsius), conductivity (microsiemens), hardness (French degrees, calculated as conductivity/20), total dissolved solids (milligrams per liter), pH, dissolved oxygen (milligrams per liter), and saturated oxygen (percentage) were measured in 23 of the 24 samples.

Gastropods were collected manually from slime soil, rocks, branches, and other objects found at the bottom of the canal bed. Squares of 0.10 m (0.01 m^2) were used as a sample unit (SU). The minimum number of SUs was between 35 and 45, and they settled down with a standard error between 0.07 and 0.16. When the

number of *C. fluminea* found was low, we increased the number of SUs. From August 2001 to October 2002 (10 samples), all molluscs present in SUs also were collected. For three samples (November 2000 and January and December 2001), density could not be estimated because the high water level of the canal did not allow us to use conventional methods. This condition is generally observed when southerly winds affecting the Rio de la Plata ("sudestadas") keep the water level high.

Samples for the study on individual growth rate were measured on site by using a 0.01-mm precision caliber. Because the apex of these gastropods is usually damaged by water streams, only the length of last whorl (LWL) was registered. Once measured, gastropods were returned to their natural environment. Data were divided according to size classes of 1-mm intervals. Polymodal size frequency distribution of each sample was carried out before the analysis of growth values. Frequency distributions corresponding to each cohort were fitted to a normal curve, whose mean and standard deviation were calculated. After cohorts were obtained, individual growth rate was analyzed according to length, following the model of von Bertalanffy (1938). This model has been widely applied for studies on planorbid (Gastropoda: Pulmonata) populations either for experimental designs on site, in the laboratory, or under natural conditions (Loreau & Baluku, 1987; Baluku & Loreau, 1989; Ituarte, 1989, 1994; Rumi et al., 2007, 2009). The model is as follows:

$$LWLt = LWLt\infty\left(1 - e^{-k(t-t_0)}\right)$$

$LWL\infty$ = maximum length of last whorl; k = growth rate constant; t = time, and t_0 = hypothetical time in which length = 0.

Time measured for each sample was divided into parts of 1 yr, following Basso & Kher (1991), Rumi et al. (2007, 2009), and Gutiérrez Gregoric et al. (2010), in the equation

$$t = [(month - 1) \times 30 + sampling\ day]/360 + A$$

A = sampling year. The year in which the study starts is considered as $A = 0$, the following year is $A = 1$, and so on. Thus, $t = 0$ corresponds to January 1, $t = 0.5$ corresponds to July 1, and $t = 1$ corresponds to approximately December 31. Maximum length of the whorl was calculated on mean values of cohorts obtained from decomposition, by using the method of Walford (1946).

For growth rate analysis, samples and cohorts with scarce individuals were not taken into account: August 2001 cohort 1 (n = 1), August 2002 (n = 3), October 2002 (n = 2), December 2002 (n = 3), February 2003 (n = 1), March 2003 (n = 1), June 2003 (n = 4), and August 2003 (n = 3). Only means from cohorts started at the time of the sampling were considered; the cohorts with higher values from November 2000 to June 2001 samples were not taken into account also (six samples). A simple regression analysis between both variables was conducted to compare the results obtained with the results expected. A gradient close to 1 and a high R^2 value (also close to 1) showed good correspondence of data.

To compare these data with data from other species or from the same species in different environments, t_0 was considered as zero and growth rate was expressed as percentage of maximum length of last whorl, as reported by Rumi et al. (2007).

RESULTS

Water temperature at the beach reveals a significant seasonal variation; a difference of almost 13°C can be observed between winter and summer average values. Winter average temperature was 11.6°C, and summer average temperature was 24.1°C. Autumn and spring showed similar average values (16.9 and 16.8°C, respectively; Table 1). Water hardness (French degrees) was 49.9 (very hard water).

Mollusc ensembles that accompanied *C. fluminea* in the canal included the gastropods *Heleobia parchappii* (d'Orbigny, 1835) (Coclhiopidae); *Uncancylus concentricus* (d'Orbigny, 1835) (Ancylidae); *Biomphalaria peregrina* (d'Orbigny, 1835; Planorbidae); *Pomacea canaliculata* (Lamarck, 1822; Ampullariidae); and *Physa acuta* Draparnaud, 1805 (Physidae) and the bivalves *Corbicula fluminea* (Müller, 1774; Corbiculidae); *Musculium argentinum* (d'Orbigny, 1835; Sphaeriidae); and *Limnoperna fortunei* (Dunker, 1857; Mytilidae). The highest density is for registered *U. concentricus* (819 individuals ind/m^2 in October 2002). During October 2001–May 2002, we did not observe oviposition by *C. fluminea* (Table 2). The mean density of *C. fluminea* from November 2000 to September 2003 was 111 ind/m^2, with a maximum value of 300 for January 2002 and a minimum of 0.25 for June 2003 (Figure 1).

Mollusc distribution in canal substrata varied for the species detected. The vertical walls of the canal were mainly colonized by the invading bivalve *L. fortunei.* The bottom of the canal was colonized by *H. parchappii* and *P. acuta.* Floating branches and other objects in the canal were colonized by *U. concentricus* and *L. fortunei. Musculium argentinum* and *Co. fluminea* were found in infaunal environments. *Biomphalaria peregrina* and *P. canaliculata*, both found in low numbers, could not be assigned to any particular area. *Chilina fluminea* was observed in rocky and stony substrates as well as on trunks and vertical walls of the canal. The vertical walls harbored the lowest number of individuals, most of which were found in substrates

Table 1

Mean water quality parameters at La Balandra beach.

Date	Season*	Temperature (°C)	pH	Dissolved O_2 (mg/L)	Saturated O_2 (%)	Conductivity (µS)	Total dissolved solids (mg/L)
December 2000	Su	19.10	6.48	n/d†	n/d	775	392
January 2001	Su	29.20	s/d	n/d	n/d	802	395
February 2001	Su	24.40	6.39	n/d	n/d	807	384
April 2001	A	18.50	7.14	n/d	n/d	1059	532
May 2001	A	14.33	6.52	n/d	n/d	1289	652
June 2001	W	13.66	6.60	n/d	n/d	1691	847
July 2001	W	10.25	6.49	n/d	n/d	871	411
August 2001	W	12.30	6.63	n/d	n/d	1431	736
September 2001	Sp	11.75	6.40	n/d	n/d	n/d	n/d
November 2001	Sp	22.00	6.92	n/d	n/d	n/d	n/d
January 2002	Su	24.30	6.80	1.30	14.90	732	368
April 2002	A	17.80	6.96	1.90	20.00	875	438
May 2002	A	17.30	6.98	2.71	27.90	1214	606
June 2002	W	7.70	7.04	n/d	n/d	989	497
August 2002	W	12.50	6.77	6.50	77.00	1164	552
October 2002	Sp	18.90	7.17	5.92	63.00	1729	867
November 2002	Sp	19.20	7.01	3.25	34.30	736	370
December 2002	Su	30.25	7.35	10.27	137.00	798	393
February 2003	Su	17.50	6.54	3.88	40.00	432	215
April 2003	A	16.50	7.47	9.70	98.70	377	201
June 2003	W	11.70	6.73	5.15	47.00	1194	603
August 2003	W	13.00	6.88	12.30	114.00	1114	562
September 2003	Sp	11.95	7.06	10.00	91.00	882	439

* A = autumn; Sp = spring; Su = summer; W = winter.
† n/d = no data.

that remained continuously under water even when the Río de la Plata waters receded.

Individuals of smaller size were first found in September (class 2, 1–1.99 mm; Figure 2). Samples from August 2002 and June 2003 contained young individuals, although in low numbers. These times were considered as the start of the reproductive efforts. Individuals in classes 10–12 (9–11.99 mm) were found year-round at similar numbers. From November to June–July (winter season), samples showed no young individuals, indicating the absence of new recruitment.

Polymodal size frequency distributions showed similar results, with two well-defined cohorts (Figure 3). There is only one recruitment period during the year (Figure 3). After we determined polymodal size frequency distributions, individual growth rates were analyzed. Two well-defined cohorts were observed during the sampling period: the first cohort started in 2000 and the second cohort started in 2001 (Figure 4). Cohorts of samples collected during 2002 could not be analyzed because of the low number of individuals in the samples. The start of a new cohort could be observed at the end of the sampling period (September 2003; Figures 3, 4).

Maximum length of the last whorl was estimated at 13.5mm. Thus, the 2000 cohort had a $k = 1.50$ and $t_0 = 0.58$, whereas the 2001 cohort, started during the second sampling year, had $k = 1.63$ and $t_0 = 1.62$. The regression coefficient for both cohorts was >0.9. Consequently, growth rate equations for each cohort are as follows:

$$\text{2000 Cohort: } LWLt = 13.5 \text{ mm}\left(1 - e^{[-1.5(t-0.58)]}\right)$$

$$\text{2001 Cohort: } LWLt = 13.5 \text{ mm}\left(1 - e^{[-1.63(t-1.62)]}\right)$$

Because both cohorts started during the same season (winter; similar t_0 values in different years), decomposition data were grouped to follow up the complete growth rate. The smallest modes were considered as year 0 and the highest mode was year 1 (Figure 5). The growth rate curve showed a high regression coefficient ($R^2 = 0.93$) and was defined as follows:

$$LWLt = 13.5 \text{ mm}\left(1 - e^{[-1.52(t-0.58)]}\right)$$

A simple regression analysis between both values was carried out to compare the values observed with the values estimated. This analysis showed a decreasing trend of 0.94 and a high R^2 value (0.97), evidencing the correspondence between observed and expected values.

Maximum length of last whorl percentage of growth

Table 2

Mollusc density (δ; ind/m²) between July 1 and October 2, including *C. fluminea* oviposition density (ovipositions/m²). N, total individuals; $\bar{x}$, mean calculated per SU (= 0.01 m²). SD, standard deviation.

Date	N of SU	Density	*C. fluminea*	Oviposition *C. fluminea*	*H. parchappii*	*U. concentricus*	*L. fortunei*	*P. canaliculata*	*B. peregrina*	*M. argentinum*	*Co. fluminea*	*P. acuta*
August 2001	55	N	24	16	234	159	17	0	1	24	0	1
		$\bar{x}$	0.4	0.3	4.2	2.9	0.3	0	0.02	0.4	0	0.02
		SD	0.6	0.8	22.2	3.8	0.9	0	0.13	2.3	0	0.13
		δ	44	29	425	289	31	0	2	44	0	2
September 2001	63	N	55	58	123	135	174	0	1	0	2	0
		$\bar{x}$	0.9	0.9	2.0	2.1	2.8	0	0.02	0	0.03	0
		SD	0.8	1.5	5.5	2.4	6.3	0	0.13	0	0.2	0
		δ	87	92	195	214	276	0	2	0	3	0
November 2001	39	N	90	0	96	107	200	1	0	1	3	0
		$\bar{x}$	2.3	0	2.5	2.7	5.1	0.03	0	0.03	0.1	0
		SD	2.3	0	6.2	5.0	12.1	0.2	0	0.2	0.3	0
		δ	231	0	246	274	513	3	0	3	8	0
January 2002	36	N	108	0	9	65	68	1	1	0	3	0
		$\bar{x}$	3.0	0	0.3	1.8	1.9	0.03	0.03	0	0.1	0
		SD	2.5	0	0.8	3.3	6.1	0.2	0.2	0	0.4	0
		δ	300	0	25	181	189	3	3	0	8	0
April 2002	50	N	44	0	2	0	119	0	0	0	0	4
		$\bar{x}$	0.9	0	0.04	0	2.4	0	0	0	0	0.1
		SD	0.7	0	0.3	0	7.0	0	0	0	0	0.3
		δ	88	0	4	0	238	0	0	0	0	8
May 2002	67	N	40	3	5	32	276	0	0	0	0	3
		$\bar{x}$	0.6	0.04	0.1	0.5	4.1	0	0	0	0	0.04
		SD	0.7	0.2	0.4	1.0	9.9	0	0	0	0	0.2
		δ	60	4	7	48	412	0	0	0	0	4
June 2002	30	N	4	56	0	93	17	0	0	0	0	0
		$\bar{x}$	0.1	1.9	0	3.1	0.6	0	0	0	0	0
		SD	0.3	2.2	0	5.1	3.3	0	0	0	0	0
		δ	13	187	0	310	57	0	0	0	0	0
August 2002	25	N	3	32	18	82	0	0	3	2	0	58
		$\bar{x}$	0.1	1.3	0.7	3.3	0	0	0.1	0.1	0	2.3
		SD	0.2	1.8	1.2	5.5	0	0	0.2	0.3	0	4.8
		δ	12	128	72	328	0	0	12	8	0	232
October 2002	16	N	21	0	37	131	12	0	0	0	0	41
		$\bar{x}$	1.3	0	2.3	8.2	0.8	0	0	0	0	2.6
		SD	1.2	0	3.4	10.4	1.7	0	0	0	0	4.3
		δ	131	0	231	819	75	0	0	0	0	256

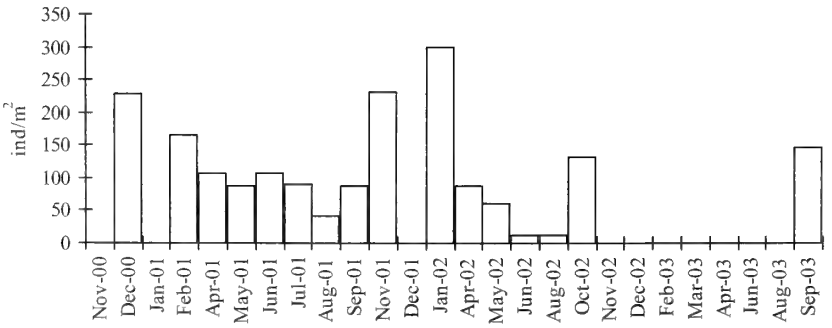

Figure 1. Density of *C. fluminea* at La Balandra beach.

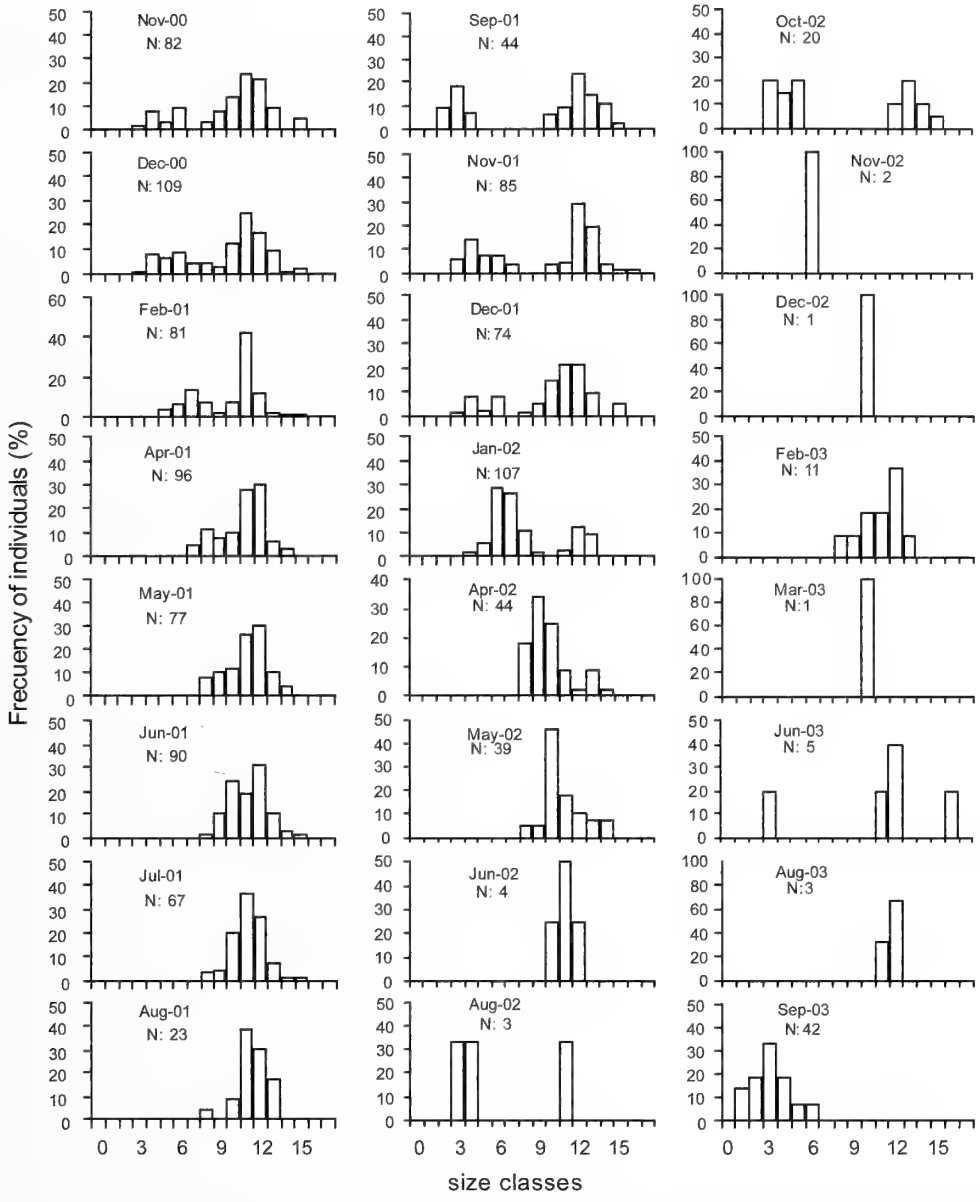

Figure 2. Size–frequency distributions of *C. fluminea*, expressed as percentage of the sample total N, in intervals of 1 mm, along samples at La Balandra beach.

rate is shown in Figure 6. *Chilina fluminea* is observed to reach 78% of its maximum length during the first year of life and 95% after 2 yr. According to samples (Figure 6), life expectancy of this species was estimated as 2.5 yr.

DISCUSSION

In June 2002, the canal selected for samples in this study was dredged, thereby modifying the environment and causing a density decrease in *C. fluminea*. The main reason for this environmental change was the removal of hard substrates (rocks and trunks) from the bottom of the canal; these substrates served not only as attachment sites for adults but also for oviposition. The removal of the brook gullies and bottom stones turned the substrate soft and the water muddy. These factors had significant influence on the stability of *C. fluminea* populations in the area. As depicted in Figure 1, the population density of this species showed a slight recovery only during the last sampling (September 2003), when young individuals could be observed. But *C. fluminea* was not the only species affected by the transformation of the canal; other

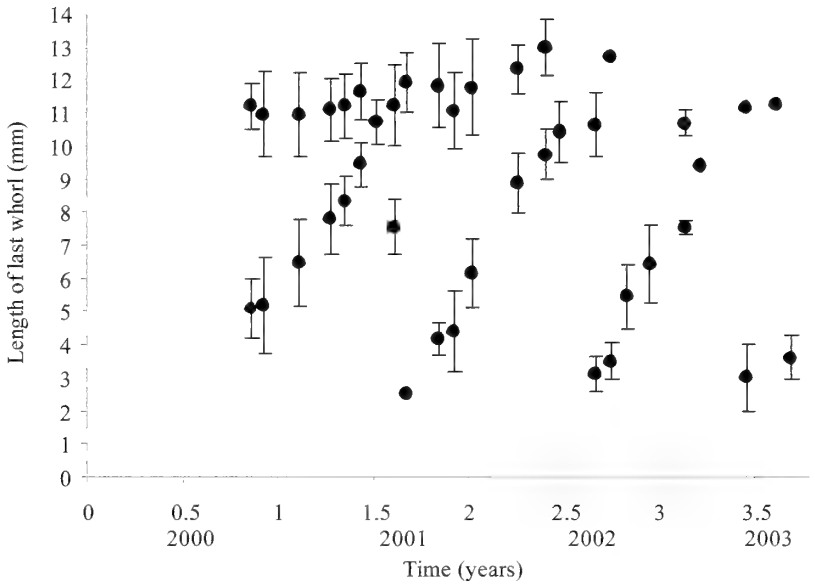

Figure 3. Means (dots) and standard deviations (bars) of the normal curves fitted to each monthly shell-size frequency distribution.

molluscs inhabiting these hard substrates also were affected. For example, *L. fortunei*, an Asian mussel invading South American coasts (Darrigran & Pastorino, 1995), and *H. parchappii* showed significantly decreased density after these environmental changes. However, their population recovery proved to be faster than that of *C. fluminea* (Table 2). These environment disturbances allowed foreign species and those not previously sampled to inhabit the substrate. Thus, the exotic species *P. acuta* showed highly increasing density (230 ind/m^2) and *U. concentricus* increased its average density from 250 to 850 ind/m^2.

Alternatively, the highest density for *C. fluminea* in this environment was recorded during January 2002 (300 ind/m^2) when the temperature reached 24°C. Similar findings were reported by Quijon & Jaramillo

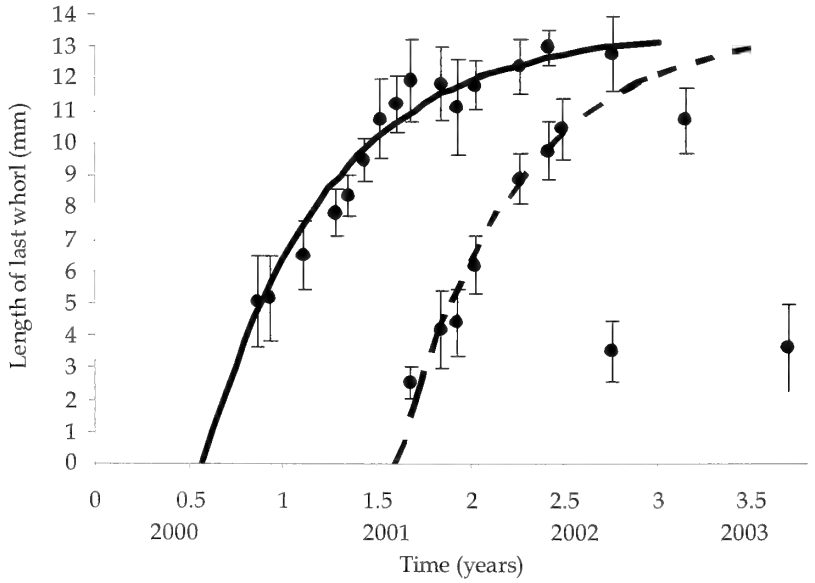

Figure 4. Individual growth for *C. fluminea* in La Balandra beach. Dots represent means observed; bars represent standard deviations. Continuous line represents the theoretical growth curve for the 2000 cohort; broken line represents the theoretical growth curve for the 2001 cohort.

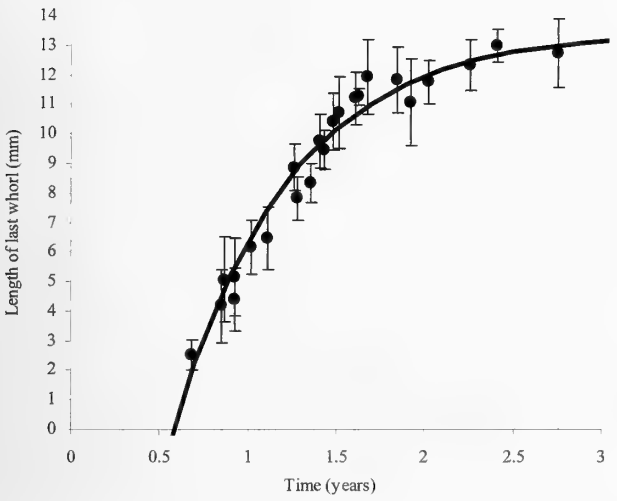

Figure 5. Growth curve for two *C. fluminea* cohorts in La Balandra beach. Dots represent means observed; bars represent standard deviations. The line represents that theoretical growth curve according to the von Bertalanffy model.

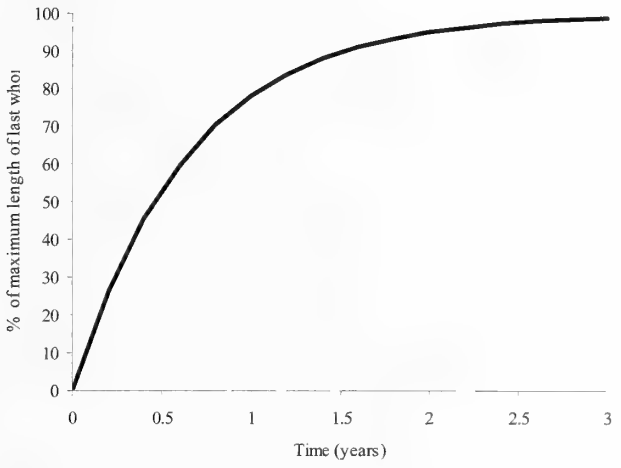

Figure 6. Growth of *C. fluminea* expressed as percentage of maximum length of the last whorl.

(1999) and Quijon et al. (2001) for southern Chile (Lingue River estuary, 39°41′S, 73°13′W), where the highest density values for *C. ovalis* were recorded during January and March, respectively (March temperature, 20°C).

The analysis of *C. fluminea* growth rate showed that the t_0 value corresponded to July. This indicates that the reproduction cycle of this species is limited to winter (June–August), when water temperature descends. These findings agree with those from other studies carried out on the same species inhabiting the same areas (Miquel, 1986).

According to Bosnia et al. (1990), *C. gibbosa*, a species found in Ramos Mexia dam (Río Negro and Neuquén provinces, southern Argentina), reproduces only once a year during the summer. They proposed a sigmoid growth formula for this species in two dam sites; in one of these sites, the cohort starts with 3.39 mm individuals, although at hatching they are usually 0.8 mm in length. In contrast, Gutiérrez Gregoric et al. (2010) concluded that *C. megastoma*, a species found in the Iguazu National Park (Misiones province, Argentina), may reproduce continually because of the low temperature variation throughout the year. However, for *C. megastoma*, its best reproductive period is when temperatures are approximately 15°C, similar to that encountered by *C. fluminea* in La Balandra beach (near 12°C).

Quijon & Jaramillo (1999) and Quijon et al. (2001) also reported a unique annual reproduction period for *C. ovalis* during spring (October, 15–18°C). It is important to emphasize that during winter (approximately 10°C), these authors did not detect any *C. ovalis* in the samples. Quijon et al. (2001) suggested a growth rate formula including a winter delay, with both cohorts first appearing in October (1996 and 1997), with similar growth rate constants, and delay values (growth stoppage) between June and July. In *C. fluminea* this delay was not observed.

Data analyses estimated life expectancy for *Chilina ovalis* in the Lingue river is approximately 3.5 yr (Quijon et al., 2001), for *C. megastoma* is approximately 2 yr (Gutiérrez Gregoric et al., 2010), and 2.5 yr for *C. fluminea* (present study). *Chilina ovalis* and *C. gibbosa* growth rates were similar and lower than those found in the present study. This could be due to the low winter temperature and to the longevity of these two species (3.5 yr); they present a maximum length substantially higher than that of *C. fluminea* (*C. ovalis*, 29 mm; *C. gibbosa*, 26.5 mm). In contrast, *C. megastoma* inhabiting subtropical climates had higher growth rates (k = 1.46–1.96) than *C. fluminea* and reached a higher LWL (18.47 mm).

Moreover, none of the freshwater gastropods from other families studied in Argentina reproduce during winter, regardless of the number of reproductive events of the species: *Drepanotrema kermatoides* (d'Orbigny, 1835) and *Drepanotrema cimex* (Moricand, 1839) (Planorbidae) in Isla Martín García, Río de la Plata (Rumi et al., 2007) have one reproductive event per year; *Drepanotrema lucidum* (Pfeiffer, 1839), *Drepanotrema depressisimun* (Moricand, 1839), and *Biomphalaria occidentalis* (Paraense, 1981) in the province of Corrientes (northeastern Argentina) have more than one reproductive event per year (Rumi et al., 2007, 2009); *Biomphalaria tenagophila* (d'Orbigny, 1835) and *Biomphalaria straminea* (Dunker, 1848) in Salto Grande dam (northwestern Uruguay) have two or more reproductive events per year (Ituarte, 1989, 1994); *B. tenagophila* in La Balandra beach has two or more

reproductive events per year (Rumi et al., 2009); *B. tenagophila* in Atalaya beach (Buenos Aires province) has one reproductive event per year (Rumi et al., 2009); and *B. peregrina* in Punta Lara (Buenos Aires province) has two reproductive events per year (Rumi et al., 2009). All these species inhabit lentic environments, and in very few cases they coinhabit with *C. fluminea*, one reason why it would be necessary to discard that competition exists for niches among these species, and to only be limited to a reproductive strategy.

Planorbid species usually grow faster than chilinid species because, although distributed on all of the continents, their development is significantly improved by warm water. In contrast, the highest number of well-adapted chilinid individuals can be found in the Argentinean Patagonia and southern Chile. Furthermore, average time between oviposition and hatching is shorter for Planorbidae (10 days; Rumi, 1993) than for Chilinidae (28 days; D.E.G.G., personal observations).

It is worthwhile to notice that controls for parasite infection are usually assessed during spring, before the tourist season. The appropriate time for the design of growth regulation strategies for *C. fluminea* populations is autumn (April–May), before their reproductive cycle and oviposition.

Acknowledgments. We thank Andrea Roche for collaboration on some of the sampling. This study was supported by grants from the National University of La Plata (project N470).

LITERATURE CITED

BALUKU, L. & M. LOREAU. 1989. Étude comparative de la dynamique des populations de *Biomphalaria pfeifferi* (Gastropoda, Planorbidae) dans deux cours d'eau du Zaïre oriental. Journal African Zoology 103:311–325.

BASSO, N. G. & A. I. KEHR. 1991. Postmetamorphic growth and population structure of the frog *Leptodactylus latinasus* (Anura: Leptodactylidae). Studies Neotropical Fauna and Environment 26:39–44.

BOSNIA, A. S., F. J. KAISIN & A. TABLADO. 1990. Population dynamics and production of the freshwater snail *Chilina gibbosa* Sowerby 1841 (Chilinidae, Pulmonata) in a North-Patagonian reservoir. Hydrobiologia 190:97–110.

DARRIGRAN, G. & G. PASTORINO. 1995. The recent introduction of a freshwater Asiatic bivalve, *Limnoperna fortunei* (Mytilidae) into South America. The Veliger 38:171–175.

DAYRAT, B., A. TILLIER, G. LECOINTRE & S. TILLIER. 2001. New clades of euthyneuran gastropods (Mollusca) from 28S rRNA sequences. Molecular Phylogenetics and Evolution 19:225–235.

DE CASTELLANOS, Z. A. & M. C. GAILLARD. 1981. Mollusca Gasterópoda: Chilinidae. Fauna de Agua Dulce de la República Argentina, PROFADU (CONICET), Buenos Aires 15(4):23–51.

DE CASTELLANOS, Z. A. & S. E. MIQUEL. 1980. Notas complementarias al género *Chilina* Gray (Mollusca Pulmonata). Neotropica 26:171–178.

ESTEBENET, A. L., N. J. CAZZANIGA & N. V. PIZANI. 2002. The natural diet of the Argentinean endemic snail *Chilina parchappii* (Basommatophora: Chilinidae) and two other coexisting pulmanate gastropods. The Veliger 45:71–78.

GUTIÉRREZ GREGORIC, D. E., V. NÚÑEZ & A. RUMI. 2010. Populations studies of an endemic gastropod from waterfall environment. American Malacological Bulletin 28:159–165.

GUTIÉRREZ GREGORIC, D. E. & A. RUMI. 2008. *Chilina iguazuensis* (Gastropoda: Chilinidae), new species from Iguazú Nacional Park, Argentina. Malacologia 50(1–2): 321–300.

ITUARTE, C. F. 1989. Growth dynamics in a natural population of *Biomphalaria straminea* (Dunker, 1848) from Bella Unión, Artigas, Uruguay. Studies Neotropical Fauna and Environment 24:35–40.

ITUARTE, C. F. 1994. Temporal variation in age structure of a natural population of *Biomphalaria tenagophila* (Gastropoda: Planorbidae) from a rice field irrigation channel system at Artigas, Uruguay. Malacological Review 27:13–21.

LOREAU, M. & L. BALUKU. 1987. Growth and demography of populations of *Biomphalaria pfeifferi* (Gastropoda, Planorbidae) in the laboratory. Journal Molluscan Studies 53:171–177.

MARTORELLI, S. R. 1984. Sobre una cercaria de la familia Schistosomatidae (Digenea) parásita de *Chilina gibbosa* Sowerby, 1841 en el Lago Pellegrini, Provincia de Río Negro, República Argentina. Neotropica 30(83):97–106.

MIQUEL, S. E. 1986. El ciclo de vida y la evolución gonadal de *Chilina fluminea fluminea* (Maton, 1809) (Gastropoda; Basommatophora; Chilinidae). Neotropica 32(87):23–34.

QUIJON, P., H. CONTRERAS & E. JARAMILLO. 2001. Population Biology of the intertidal snail *Chilina ovalis* Sowerby (Pulmonata) in the Queule river estuary, south-central Chile. Estuaries 24:69–77.

QUIJON, P. & E. JARAMILLO. 1999. Gastropods and intertidal soft-sediments: the case of *Chilina ovalis* Sowerby (Pulmonata: Basommatophora) in south-central Chile. The Veliger 42:72–84.

RUMI, A. 1993. Radular variability and life tables of two morpha from *Biomphalaria peregrina* (D'Orb., 1835) (Mollusca Planorbidae). Journal of Medical and Applied Malacology 5:21–30.

RUMI, A., D. E. GUTIÉRREZ GREGORIC & M. A. ROCHE. 2007. Growth rates fitting using the von Bertalanffy model: an analysis in natural populations of *Drepanotrema* spp. (Gastropoda: Planorbidae). Revista de Biología Tropical 55:559–567.

RUMI, A., D. E. GUTIÉRREZ GREGORIC & M. A. ROCHE. 2009. Tendencias del crecimiento individual en poblaciones naturales de *Biomphalaria* spp. (Gastropoda, Planorbidae) en la Cuenca Del Plata, Argentina. Comunicaciones de la Sociedad Malacológica del Uruguay 9(92):185–193.

SZIDAT, L. 1951. Cercarias schistosómicas y dermatitis schistosómica humana en la República Argentina. Comunicaciones del Instituto Nacional de Investigación de las Ciencias Naturales, Ciencias Zoológicas 2(10):129–150.

VON BERTALANFFY, L. 1938. A quantitative theory of organic growth. Human Biology 10(2):181–213.

WALFORD, L. A. 1946. A new graphical method of describing the growth of animals. Biological Bulletin 90:141–147.

The Veliger 51(3):117–130 (November 16, 2012)

THE VELIGER

Sublethal Anesthesia of the Southern Pygmy Squid, *Idiosepius notoides* (Mollusca: Cephalopoda), and Its Use in Studying Digestive Lipid Droplets

LINDA S. EYSTER* AND LISSA M. VAN CAMP†

School of Biological Sciences, Flinders University, Adelaide, South Australia 5001, Australia

Abstract. We immersed southern pygmy squid, *Idiosepius notoides* Berry 1921 (hereafter squid), in three anesthetics (cold seawater, magnesium chloride [$MgCl_2$], and ethanol [EtOH]). Anesthesia was important for inducing both immobility and body transparency, conditions that were required for measuring extracellular lipid droplets. Cold anesthesia (4°C, day 1) led to frequent inking and some mortality. The $MgCl_2$ treatment (1–5%, day 18) did not induce body transparency and was often lethal. The 2% EtOH anesthesia (12–15°C, days 1–12) was most successful: it induced no inking and was followed by 100% recovery and postanesthetic survival (>7 days). There was no difference in induction times for squid anesthetized on day 1 versus day 2 after collection, with loss of body color patterns in ~12 sec followed by loss of mobility at ~30 sec. Time to immobility was related to time to transparency. Size (dorsal mantle length) was not related to time to induction or recovery. Although all squid survived three anesthesias with 2% EtOH, third inductions were significantly slower than first inductions. Anesthesia greatly improved accuracy of locating, counting, and measuring lipid droplets. With sublethal anesthesia, we detected extracellular lipid droplets in the digestive system of all 42 freshly collected squid. Without anesthesia, we failed to see cecal droplets in 20 of 41 squid that had them, and we failed to see digestive gland droplets in five of 23 squid that had them. Light EtOH anesthesia, including repeated treatments, did not seem to move droplets between the digestive cecum and the digestive gland or to induce expulsion of these droplets from the digestive tract.

INTRODUCTION

Cephalopods have complex nervous systems and may show their distress in a variety of ways, such as vigorous movements, skin color changes, and inking. Proper anesthesia is an important and appropriate procedure for calming these active molluscs before handling them for weighing, measuring, or surgical procedures (Moltschaniwskyj et al., 2007). Cephalopod anesthesia has been reported as at "a relatively primitive stage," even though anesthetics have been used for decades on these molluscs (Boyle, 1991).

Anesthesia is physiologically complex and not well understood for any organism, in part because not all anesthetics function the same way at the molecular level, e.g., they may bind into different sites on cellular proteins (Urban, 2002). Although anesthesia is medically defined as treatment that provides insensibility to pain (Urban & Bleckwenn, 2002), the term is often applied in the molluscan literature to any procedure that induces immobility, without reference to pain blockage; we use that latter meaning here.

According to Messenger et al. (1985), the first detailed study of cephalopod anesthesia was provided by Andrews &Tansey (1981). Cephalopod anesthesia typically is accomplished by immersion of the organism in seawater containing the anesthetic, sometimes with the intention of at least temporary survival of the animal (Andrews & Tansey, 1981; Boyle, 1991). Loss of swimming and righting ability, which typically occur before loss of breathing, are considered partial or light anesthesia (Messenger et al., 1985; Boyle, 1991). Loss of respiratory ventilations of the mantle cavity is a marker for induction of full or complete anesthesia (as defined by Young, 1971 in Andrews & Tansey, 1981; Boyle, 1991). Intentional overdoses (via either longer exposure to anesthetics or exposure to higher doses) are intended to humanely kill the cephalopod (e.g., before dissection), and they have been termed terminal anesthesia (Boyle, 1991), overanesthesia, and euthanasia (Moltschaniwskyj et al., 2007). As more humans begin to consider the ethical treatment of cephalopods (Mather & Anderson, 2007), clear information on efficacy of various anesthetics is warranted.

The best anesthetic for cephalopods seems to vary with species. Anesthetics tested on cephalopods include ethanol (EtOH), phenoxyethanol, urethane (ethyl carbamate), magnesium chloride ($MgCl_2$), magnesium sulfate ($MgSO_4$), tricaine mesylate (MS-222), and cold water (as cited in Andrews & Tansey, 1981; Messenger et al., 1985; Moltschaniwskyj et al., 2007; Sen & Tanrikul, 2009). Andrews & Tansey (1981) showed that

* Corresponding author: Department of Science, Milton Academy, 170 Centre Street, Milton, MA USA 02186

† Present address: Wallbridge & Gilbert, 60 Wyatt Street, Adelaide, South Australia 5000, Australia

immersion in cold seawater (~4°C) was superior over the use of EtOH or urethane for relaxing *Octopus vulgaris*. Messenger et al. (1985) determined that $MgCl_2$ was superior to EtOH or urethane; although it was slightly slower, it seemed to be less traumatic on members of the five cephalopod genera they tested, including species of cuttlefish, squid, and octopods. In contrast, O'Dor et al. (1990) reported that EtOH was less stressful than $MgCl_2$ for producing light anesthesia in the squid species *Loligo pealei*, *Loligo opalescens*, and *Illex illecebrosus*. More recently, Berk et al. (2009) tested an ice bath and MS-222 in *L. pealei*, discarding both procedures after high distress and mortality and opting instead for rapid intubation without anesthesia.

The world's smallest squid (~0.5–3.0-cm mantle length) are placed in the family Idiosepiidae and include approximately a half dozen species. These Indo-Pacific cephalopods, despite their small size and lack of fishery importance, have recently become the topic of research (Boletzky, 2005), including analyses of nervous systems (Shigeno & Yamamoto, 2002), egg masses (Kasugai & Ikeda, 2003), life history traits (Tracey et al., 2003), extracellular lipid droplets (Eyster & van Camp, 2003), embryonic brains (Yamamoto et al., 2003), external digestion (Kasugai et al., 2004), and adhesive organ histochemistry (Byern et al., 2008).

During our initial study of yellowish, hydrophobic, sudanophilic spheres detected in the lumen of digestive organs of southern pygmy squid, *Idiosepius notoides* Berry 1921 (Eyster & van Camp, 2003; hereafter squid), we avoided chemical anesthesia because it might cause movement of material between adjacent digestive organs (Bidder, 1966). In that prior work, we confirmed the lipoid nature of these droplets; they are noteworthy because cephalopods apparently have limited capacity to metabolize or store lipids, relying instead on carbohydrate and protein metabolism for their energy sources (Hochachka et al., 1975; Storey & Storey, 1983; O'Dor & Webber, 1986). Although these droplets were detected in the lumen of digestive organs, it is unclear whether the droplets are metabolized, function in buoyancy, or are metabolic waste. We wanted to determine the frequency of occurrence of these small extracellular droplets and to follow their presence over time in live squid, so we needed a sublethal method of immobilizing the squid.

In cephalopods, including *Idiosepius* species, body color patterns are produced by muscles acting on pigment-containing sacs of the chromatophores (Boyle, 1991; Hanlon, 2010). Because our captive squid were often active and darkly pigmented (Figure 1), we needed a procedure that would not only immobilize the animals but also cause mantle tissue to relax to an almost transparent, uncolored state so that we could see through it to locate, count, and measure lipid droplets in live squid. In addition, we wanted an anesthetic procedure that was (1) quick and light (reducing anesthetic stress to the squid and allowing us to measure more droplets on the same day), (2) did not cause expulsion of the oil droplets out of the digestive system, (3) allowed the squid to recover normal swimming and feeding behavior after treatment, and (4) allowed posttreatment survival of at least 1 wk so that the squid and lipid droplets could be studied over that time. Here, we report successful responses of squid to immersions in EtOH, with additional notes on lipid droplets, development of anesthetic tolerance, and testing with $MgCl_2$ and with cold (4°C) seawater.

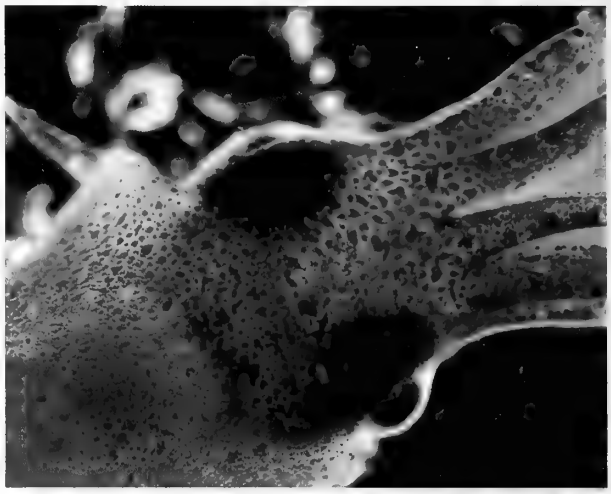

Figure 1. Head region of squid in seawater before anesthesia. Pigment-containing chromatophores are expanded, producing dark patterns; no papillae are noted. All squid shown in Figures 1–4, 7, and 12 were 6–9 mm in dorsal ML.

MATERIALS AND METHODS

Collection and Maintenance of Squid

Southern Pygmy squid are small (~2-cm dorsal mantle length) cephalopods that attach to seagrasses by use of glue glands located on the upper body (Norman, 2000). We collected these squid by seining over seagrass beds in several locations in South Australia.

For cold anesthesia tests, squid were collected near Myponga, South Australia, in the summertime (January 11, 2004) and acclimated to the laboratory at near field temperature (~22°C) for 1 day before testing. The rest of the squid in this study were collected at Noarlunga Reef, south of Adelaide, in the fall (April 21, 2002 [=day 0]). These squid were kept in an aquarium with recirculating seawater (~14–16°C; ~40 ppt salinity; 12:12-hr light:dark cycle) before and after testing.

To keep track of individual squid after testing began, we housed them singly in plastic screw cap straight-sided jars (~450 mL). To provide each squid with

flowing water, we replaced the central half of each lid and the entire bottom of each jar with plastic 2-mm gauge mesh. We then submerged the numbered jars on their sides in a flow-through tank attached to the recirculating seawater system.

We provided food to half the squid during week 1. Just before feeding time, all holding jars were cleaned out. Then, the holding jar of each fed squid was provided with 10 live field-collected mysid shrimp (daily through day 7). This feeding schedule was based on our videotaped observations that (1) the maximum number of mysids caught in one meal by isolated *I. notoides* before they stopped feeding was 10 and that (2) squid were more likely to feed when new food arrived; active but left-over shrimp frequently were ignored. In week 2, each squid was given five large store-bought brine shrimp daily (because poor weather prevented field collection of additional mysids). All squid in this work were starved on days of anesthesia before treatment.

Transfer and Immersion of Squid

On testing days, we transferred the holding jars from the aquarium building to the laboratory in large, water-filled trays. To reduce stress on the squid, we kept each squid submerged in seawater inside its holding jar until its testing time, and then we transferred it quickly to anesthetic solution (see below), returned it to fresh seawater as soon as measurements were completed, and maintained it in fluids between 12 and 16°C (except for 4°C treatments). We limited air exposures primarily because we observed that small air bubbles could become trapped in the mantle cavity and that these bubbles could resemble colorless oil droplets when viewed through the mantle.

To remove a squid from its holding jar, the jar was inverted (so that the removable lid was now on the bottom) and a glass dish (Petri dish) placed under the jar lid. As we lifted the jar out of the transport tray, water drained from the jar except for an ~1-cm-deep layer in the lid, held in by the glass dish. We unscrewed the lid from the jar and placed the glass dish (containing lid and squid) under a dissecting microscope for viewing. Previous testing showed that these shallow dishes were tall enough and held enough water to retain and submerge the squid.

Transfer of squid into anesthetic solutions (EtOH or $MgCl_2$) was accomplished by waiting until the squid swam over the central meshed portion of the jar lid. We then quickly lifted the lid out of the seawater, keeping the squid supported on the mesh grid of the lid. Next, we immediately inverted the lid over a small culture dish that was convexly full of anesthetic solution (~10 mL) so that the squid was immediately immersed in anesthetic solution. Compared to collecting and transferring each squid by small dip net or by hand, this rapid inversion–transfer method was faster and seemed less stressful for and damaging to the squid (based on absence of inking responses, absence of hyperactive swimming behavior, and subsequent health). If the squid did not instantly detach from the mesh, we gently squirted it with the same anesthetic solution until release. Exposure time was counted from the first second that the squid touched the anesthetic solution, even if the squid did not initially release from the mesh lid.

Anesthesia with Cold Seawater, EtOH, and $MgCl_2$

Cold seawater: On day 1 after collection, we transferred squid into cold seawater to determine whether the sudden temperature change from 22°C (room temperature) to 4°C would induce immobility, color change, movement of lipid droplets in the digestive system, or various combinations of responses. All squid were sexually mature (two females, eight males) and ranged from 6- to 19-mm dorsal mantle length (ML; mean = 11 mm). After lipid droplets became visible through the skin, the locations of the droplets were noted; locations were noted again at the end of the 60-sec immersion. Time to loss of mobility and time to loss of body color patterns were recorded as for EtOH immersions (see EtOH). After removal from the cold water, each squid was examined up to 4 min after treatment. No artificial ventilation was attempted if squid stopped breathing.

EtOH: The majority of our study involved 2% EtOH in filtered seawater (volume/volume) as the anesthetic. A few squid were exposed to 4% EtOH (see Repeated Anesthesia). The EtOH solutions were prepared fresh daily and used at 12–15°C to approximate the maintenance temperature; a solution was never reused. We recorded time (seconds) that we kept each squid immersed (=exposure time). Exposure time (123 ± 34 sec [mean ± SD]) was not constant because it varied with how long it took to measure each squid (ML), and then to locate, count, and measure visible lipid droplets (diameters).

For each squid immersed in 2% EtOH (or cold seawater), we recorded time to reach two induction markers: (1) complete loss of swimming (no jetting and no finning) and (2) complete loss of body color patterning (head and arms not included). These particular anesthetic stages were important for us because we needed stationary squid to make measurements and transparent squid to view the lipid droplets present in the digestive organs. We did not need any deeper anesthesia in this particular study, so we did not purposefully continue anesthesia until squid stopped respiratory ventilations.

Because newly collected cephalopods can be more susceptible to anesthesia than squid adapted to the laboratory (Messenger et al., 1985), we compared time to induction and time to recovery for squid anesthetized day 1 (24–30 hr after collection; n = 18) versus day 2 (43–47 hr after collection; n = 24). Average exposure times were ~2 min and were comparable on day 1 (2.2 min) and day 2 (1.9 min; unpaired *t*-test, $P = 0.12$).

$MgCl_2$: We immersed squid (n = 3) into 2.5–5% $MgCl_2$ in seawater (16°C, day 18). For one squid, $MgCl_2$ was added dropwise (1 drop/20 sec) to reach 1% at 10 min, followed by immersion for two more minutes. Solutions were prepared fresh before use, by mixing Merck hexahydrate ($MgCl_2 \cdot 6\ H_2O$) into distilled water and then mixing that solution with seawater (Messenger et al., 1985). After treatment, squid were moved to fresh seawater for recovery. If a squid stopped ventilating during the recovery phase, the mantle cavity was artificially flushed with seawater by using a pipette. Because these squid are so small (they are easily propelled around the culture dish when squirted by the pipette and cannot be easily held to administer artificial ventilations), when the upper body surface was sticky enough, a glass coverslip was attached to the squid; we held onto the coverslip to keep the opening of the mantle cavity oriented toward the pipette tip.

Impact of Anesthesia on Digestive Lipid Droplet Detection and Location

Bidder (1966) stated that anesthesia may cause movement of liquids between digestive organs of cephalopods. To address the question of whether light anesthesia moved these lumenal droplets of unknown function, we recorded the location of oil droplets at the beginning and end of the cold anesthesia tests as well as just before and then during 2% EtOH immersions. We used only newly collected squid (day 1or 2 after collection) to decrease other health issues that might impact outcome.

Just before the first EtOH immersion, we examined each animal microscopically (~×10) while it swam freely in its jar lid (sitting inside the glass dish); we hoped to locate lipid droplets visible during brief periods of squid inactivity that were accompanied by flashes of skin transparency. During the flashes, we also estimated the number of droplets at each location. To increase the number of squid we could test over a 24-hr period, we limited the preanesthesia microscopic viewing of each squid; if the mantle did not become transparent within 15 min, we proceeded to EtOH immersion. Each squid was carefully examined (~×10) while it was anesthetized, and the actual number of lipid droplets in each of three locations (cecum, left side of digestive gland, right side of digestive gland) was recorded and compared with that of the preanesthetic records. After measuring each squid (ML) and its lipid droplets (diameters), we immediately put it into a bucket (~8 L) of seawater to dilute and flush away the anesthetic. We later tested the impact of repeated anesthesia on the same squid (see Recovery from Anesthesia).

Recovery from Anesthesia

Timing of recovery from anesthesia began when treated squid entered fresh seawater. We defined full recovery as resumption of active swimming. Because preliminary work showed that (1) no squid resumed swimming in <60 sec after immersion in 2% EtOH ended and that (2) later during recovery, a squid sometimes looked immobilized (it had not moved) but it swam abruptly if gently prodded, we poked squid during their recovery phase. Beginning at 60 sec into recovery time, each squid was prodded gently with a glass rod once every 30 sec until it swam actively (either between proddings or at a prodding); to reduce stress on the squid, we did not prod more frequently.

Repeated Anesthesia: Second – Fifth Immersions

We hoped to track lipid droplets over time in individual squid to examine whether the droplets moved between organs, changed in volume, or were expelled from squid. Because such experiments required that squid be anesthetized more than once, we recorded squid responses to a variety of reanesthesia treatments.

The first, second, and third anesthesias all used 2% EtOH and occurred on days 1–2, 8, and 9–12 after collection, respectively. We compared three anesthetic markers for the first versus third EtOH anesthesias: (1) time to loss of swimming ability, (2) time to loss of body color patterns, and (3) time to full recovery. We also recorded location and number of lipid droplets (all anesthesias), volume of lipid droplets (first and third anesthesias), and squid survival rate (all anesthesias).

Because squid did not seem to become transparent as readily during third EtOH anesthesia, we raised the fourth EtOH treatment concentration to 4% for a few squid (n = 4). These four squid were immersed in 2% EtOH on days 1, 8, and 11 and then 4% EtOH on day 18. The fourth EtOH immersions lasted 1.5–2.5 min. No squid in our study was anesthetized more than five times or >3 wk after collection.

To compare the possible impact of nonconsecutive versus consecutive anesthesia, we exposed a few squid to each treatment pattern. Most reanesthesias were on nonconsecutive days, occurring three to four times over ~2.5 wk. For consecutive reanesthesia, squid (n = 4)

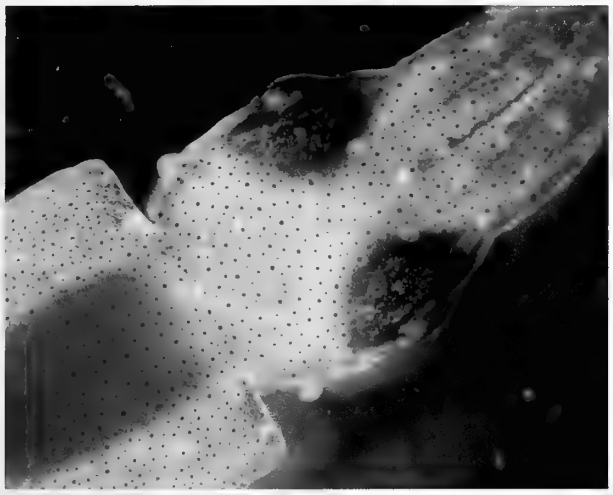

Figure 2. Head region of squid in postanesthesia recovery phase, showing minimized chromatophores, blue and green reflections from iridophores, and papillae in cheek areas.

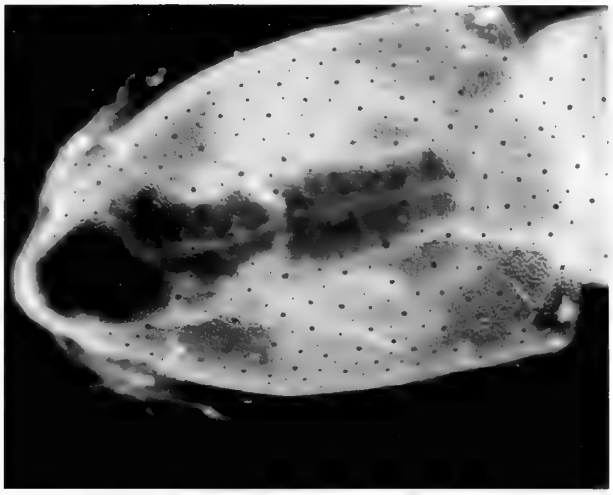

Figure 3. Body of EtOH-anesthetized squid, with transparent mantle that allows view of digestive organs.

were anesthetized first on day 1, fed mysids daily through day 7, and then reanesthetized daily on three to four consecutive days (days 8–10 or 8–11). On day 11, only one squid was reanesthetized; the other three squid looked unhealthy (i.e., less active, hypoventilating, or hyperventilating) and were sufficiently transparent to be examined without anesthesia. The four squid chosen for consecutive daily anesthesia were not selected at random but were chosen because on day 8 they were still very active and contained conspicuous lipid droplets. During consecutive anesthesia testing, the squid were housed individually between anesthesia treatments in glass bowls (100-mL static filtered seawater) so that we might detect lipid droplets if they were expelled. Aeration of cultures was avoided to avoid possible disruption of any expelled lipid into smaller droplets and also so that the surface of the water was more easily examined for oil droplets (Eyster & van Camp, 2003). Each bowl was cleaned, and the water was replaced daily with fresh aerated seawater at the same temperature.

Statistical Analyses

Data on squid dorsal MLs, induction times, exposure times, and recovery times were analyzed by unpaired *t*-tests, F-tests, Wilcoxon matched pairs tests, or Wilcoxon signed ranks tests.

RESULTS

Cold Seawater Treatment

Squid lost mantle color patterns very quickly after immersion in 4°C seawater, but they also inked frequently. Of the 10 squid tested, seven released ink, usually during the second half of their immersion minute. Squid in 4°C seawater lost their color patterns (in ~4 sec) before they stopped moving (in ~19 sec). After immersion, two squid with ink in the mantle cavity stopped breathing and died, so survival rate after these cold immersions was 80% (no artificial ventilation was attempted).

First EtOH Anesthesia (2% EtOH)

Body color patterns: The skin of untreated squid (Figure 1) had blackish and brownish patterns produced by chromatophore organs; blue and green colors were observed in untreated (Figure 1) as well as treated squid (Figure 2). The density of blackish and brownish colors in untreated squid (except during occasional flashes of transparency) prevented viewing of many lipid droplets located in the digestive system. However, in the first EtOH immersions, the squid quickly paled. In the time (~2 min) that it took to measure the squid and its lipid droplets, the most common skin response was transparency (Figure 3) over the entire squid body. Squid also produced a "bathroom-window translucency" (Figure 2), but the level of transparency shown in Figure 3 was sufficient and necessary to allow detection and measurement of lipid droplets in the digestive system.

Other color pattern changes involved some variation of paling. Some squid (three of 42) lost the black or brown patterns but turned opaque white (not transparent); compare the splotchy brown pattern on a white background in $MgCl_2$ (Figure 4).Three other squid paled when the color in the chromatophore sacs reduced to approximately half of their expanded surface area but did not minimize further. Some squid became transparent over most of the body but with

Figure 4. Body of squid in 3.75% $MgCl_2$, showing splotchy color pattern. The body is white but not transparent; some chromatophores are expanded and others are minimized.

colored patches remaining (i.e., they did not pale uniformly and completely). For example, in several squid, the ventral mantle became transparent, but the dorsal mantle between the fins did not become transparent or did not become transparent as quickly or as completely. Unfortunately, this was the key area that needed to be transparent for us to measure cecal oil droplets.

Time for the squid to develop skin transparency during the first EtOH immersion averaged 11–12 sec (range, 0.5–38 sec; Table 1). Time to reach transparency was equally quick for squid acclimated to the laboratory for 1 versus 2 days before anesthesia (Table; unpaired *t*-test, P = 0.893).

Time from immersion until the squid lost body color patterns (=time to transparency) was not related to squid size (Figure 5). That is, dorsal mantle length (range, 3.7–8.9 mm) was not related to time to reach this anesthetic state (F-test, $P = 0.598$).

No inking occurred in squid (n = 42) that were immersed in 2% EtOH at approximately the same temperature as their maintenance temperature and that were transferred by the rapid inverted lid method.

Movements: Untreated squid in small glass dishes without vegetation swam actively by jetting and finning, but they never jetted out of those dishes. Untreated squid never settled or crawled on the dish bottom, but they would attach underneath a floating piece of plain or marker-colored Parafilm® or plain glass coverslip (Figure 7). Treated squid soon lost mobility (Table) and rested on the dish bottom. No squid stopped respiratory ventilations or heart contractions during the first EtOH immersions.

Recently collected squid (day 1 or 2) continued swimming in 2% EtOH for approximately half a minute (33 ± 12 sec [mean ± SD]); only one squid kept swimming longer than 1 min (Figure 6). How long a squid swam in 2% EtOH was not related to squid size (Figure 6). Over the ML range of 3.7 to 8.3 mm, size was not related to time between immersion and immobility (F-test, $P = 0.92$).

Time to immobility was related to time to transparency (n = 37). The slope of the line in Figure 8 is significantly nonzero (F-test, $P = 0.0007$), suggesting that squid that took longer to lose body color also took longer to lose mobility.

Recovery: During recovery from the first EtOH anesthesia, only one squid stopped respiratory ventilations (apnea); ventilations paused for ~20 sec and then resumed without human intervention. Full recovery from the first EtOH anesthesia was therefore 100% (n = 42), followed by 100% postanesthetic survival of approximately a week (before the second EtOH anesthesia occurred on day 8).

More than 20% of squid in first recovery (n = 9), regained dark pigmentation on the head while the body was still transparent. Before regaining mobility, four squid produced prominent papillae on the head, with one or two papillae near each eye, one near each "cheek" (Figure 2), or both. Although we did not measure time to recovery of body color patterns or

Table 1

Anesthetic induction times (including time to loss of body color patterns [transparency] and time to loss of swimming ability [immobilization]), exposure times, and postanesthesia recovery times for squid after the first (day 1 or 2) and third immersion in 2% EtOH (days 11–12), both at 12–15°C. Time values are averages.

Day after collection	Time to transparency (sec)	Time to immobilization (sec)	Exposure time (min)	Recovery time (min)	No. of squid
1	11.3	38	2.2	3.5	18
2	11.8	30	1.9	3.2	24
11 and 12	>90*	46	2.4	4.1	10

* Because most squid during third anesthesia never became fully transparent, time to transparency is given in this table as greater than the minimum exposure time.

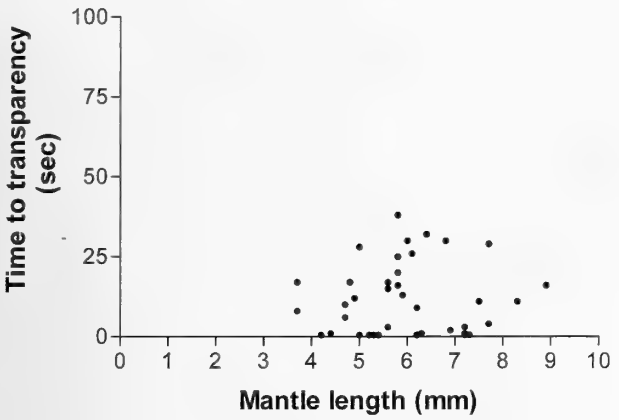

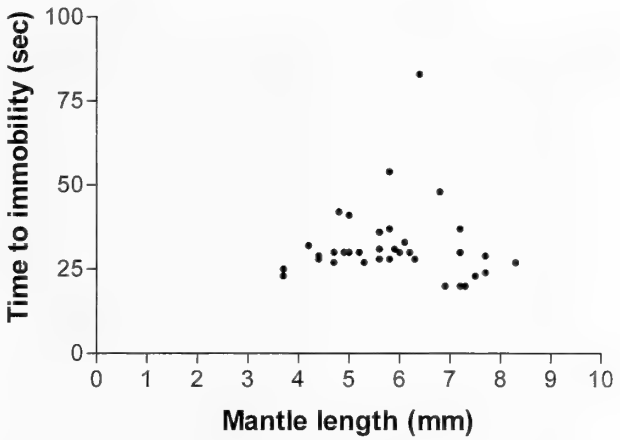

Figures 5–6. Anesthetic induction of the squid during its first immersion in 2% EtOH. Squid size (as dorsal ML) was not related to anesthetic induction measured either as time (seconds) for squid to lose body color and become transparent (see Figure 5) or measured as time to lose swimming ability (see Figure 6). To aid comparison, data are graphed on the same scale for both anesthetic markers.

feeding ability, squid did regain apparently normal behaviors: they swam effectively, caught and ate arthropod prey, and produced and maintained skin color patterns during the week between the first and second anesthesias.

Most squid (71%) resumed active jetting and finning in 2–4 min (range, 1.3–7.5 min) after the first anesthesia (Figure 9). Time to recover swimming ability was not related to length of immersion in the anesthetic solution (range, ~1–4 min; F-test, $P = 0.57$). The first postanesthetic locomotion of four squid (including two papillated squid) was not by finning or jetting; these squid moved instead by walking on the dish bottom (by arm crawling).

Larger squid did not recover from anesthesia faster or slower than smaller squid over the range from 3.7 to 8.9 mm ML (Figure 9). Squid size (ML) was not related to time to full recovery of active swimming (F-test, $P = 0.632$).

For squid acclimated to the laboratory for 1 versus 2 days before the first anesthesia (Table), there was no difference in mean recovery times (unpaired t-test, $P = 0.443$). However, recovery times for day 1 squid were more variable; variances for day 1 versus day 2 were significantly different (F-test, $P = 0.009$).

Figure 7. Body of live, nonanesthetized squid attached to under surface of floating glass coverslip, showing retention of chromatophore expansion in the mantle region near the dorsal adhesive glands; the rest of the body has temporarily lost color and become somewhat transparent.

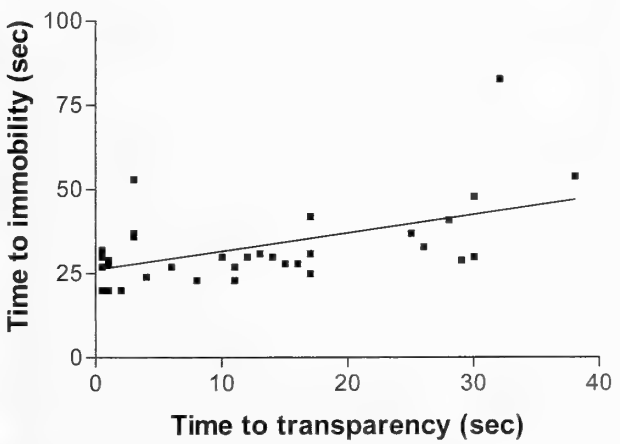

Figure 8. Relationship between time required for squid to lose body color (time to transparency) versus time to lose swimming ability (time to immobility) during first anesthesia with 2% EtOH days 1–2 after collection. The slope of the line is significantly nonzero (F-test, $P = 0.0007$).

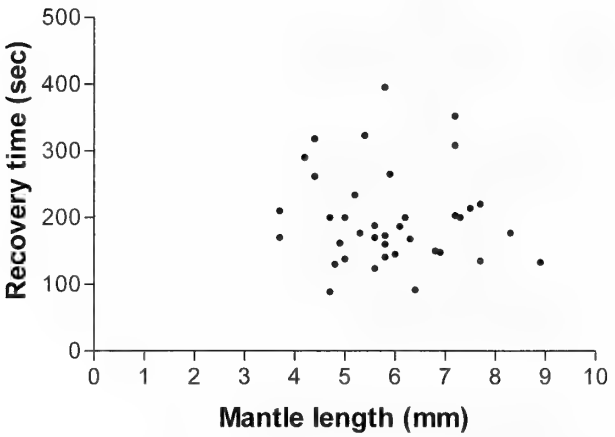

Figure 9. Squid body size (dorsal ML) versus time to recover swimming ability after first anesthesia (in 2% EtOH). Squid size (ML) was not related to time to full recovery (F-test, $P = 0.632$).

Repeated EtOH Anesthesias

Induction: Repeated EtOH anesthesias were similar in some ways and different in other ways from the first anesthesia (Table). Immersions in EtOH led to changes in body color pattern and mobility, but squid anesthetized more slowly during their third than first anesthesia (Figures 10, 11). For example, 90% of the squid (nine of 10) retained skin color patterns longer during their third EtOH immersion than they had during the first EtOH immersion (Figure 10). Time to body transparency for the third anesthesia averaged >90 sec compared with ~14 sec for first exposure for these same 10 squid (two-tailed Wilcoxon matched pairs test, $P = 0.004$). In the third anesthesia, seven of the 10 squid never became completely transparent during the time it took to measure them and to locate and measure visible lipid droplets. Consequently, the order of our two anesthetic induction markers was full body color loss before swimming loss in all squid (n = 42) during the first anesthesia and was reversed to swimming loss before full body color loss during the third anesthesia (n = 10). (Because transparency was not fully achieved in most squid during the third anesthesia, time to transparency for statistical testing and in Figure 10 was recorded as equal to the immersion time, a more conservative set of values.)

During the third EtOH anesthesia, squid took significantly longer to lose their swimming ability than they had during their first anesthesia (two-tailed Wilcoxon matched pairs test, $P = 0.027$). They could still swim ~46 sec after immersion during their third anesthesia compared with ~28 sec during their first anesthesia (Figure 11).

Recovery: In the first, second, and third anesthesias in 2% EtOH, squid immersed for a few minutes recovered in a few minutes. Recovery averaged 3.3 min after the first anesthesia and 4.1 min after third anesthesia

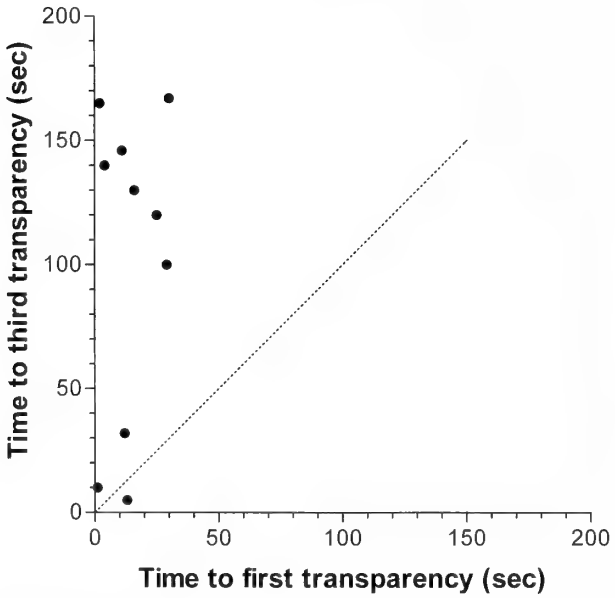

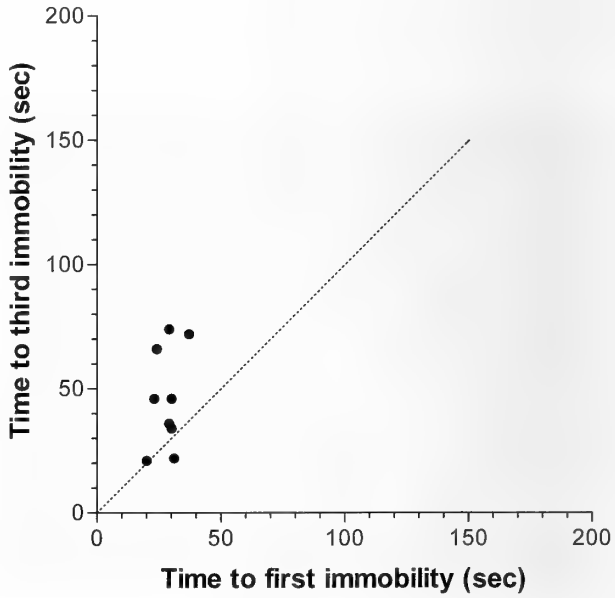

Figures 10–11. Comparison of times to reach two anesthetic induction markers during first anesthesia (2% EtOH, day 1 or 2) versus third anesthesia (day 11 or 12) for squid (n = 10). During the third anesthesia, squid took longer to lose body color patterns (see Figure 10) and longer to lose swimming ability (see Figure 11) than they had during the first anesthesia. All data above the dotted reference line represent slower inductions in the repeated anesthesias. To aid comparison of time to the two induction markers, data in Figures 10, 11 are graphed to the same scale.

(Table); these recovery times were not significantly different (two-tailed Wilcoxon matched pairs test, $P = 0.81$), but squid began to look less healthy after the third anesthesia.

No squid completely stopped respiratory ventilations during the first, second, or third immersion, but in recovery from the third anesthesia one squid was artificially ventilated with seawater for 8 min before it resumed breathing on its own. Survivorships for the first, second, and third EtOH anesthesias were 100%, with intervention on behalf of that one squid.

Fourth anesthesia: After it became apparent that squid seemed to be developing resistance to repeated 2% EtOH anesthesia, we tested some squid in a higher EtOH concentration and some in $MgCl_2$ solutions. Preliminary data (n = 4 squid) suggest that the fourth anesthesia (doubled to 4% EtOH) induced loss of skin color and loss of mobility comparably to the first anesthesia (using 2% EtOH), in that complete loss of body color patterns and loss of mobility occurred in both EtOH concentrations and occurred in that same order. Average time to transparency was 17 sec (cf. 12 sec in 2% EtOH, first anesthesia) and average time to immobility was 27 sec (cf. 30 sec in 2% EtOH, first anesthesia). Based on our small sample size, it seems that 4% EtOH as the anesthetic during the fourth anesthesia was faster at inducing color loss and immobility than was 2% EtOH during the third anesthesia. One squid died soon after the fourth anesthesia in 4% EtOH. The fourth anesthesia with $MgCl_2$ is described separately under $MgCl_2$ Treatment.

$MgCl_2$ Treatment

Squid (n = 4) immersed in $MgCl_2$ solutions (up to 12 min) did slow down but never became transparent throughout the mantle. In $MgCl_2$ solution, skin coloration became patchy, with the body sometimes transparent and sometimes white (Figure 4). Squid could still swim at 1 min after immersion in $MgCl_2$ solutions; they might rest on the dish bottom, but they would swim if they were gently prodded.

The one squid immersed in the highest $MgCl_2$ concentration (5%) showed an abnormal curved posture accompanied by jerky movements. Its mantle was not transparent and it retained a band of color mid-dorsally. Each tentacle displayed a prominent yellow stripe.

In 3.75% $MgCl_2$, the single squid tested had not become transparent at 8-min immersion, when it stopped respiratory ventilations. This squid was moved immediately to fresh seawater, and its mantle cavity was flushed using a pipette for 8 min before the squid ventilated on its own. It next hyperventilated (~100 times/min for several minutes). Ventilation slowed over the next 4 min and then stopped; the heart stopped and the body turned opaque white.

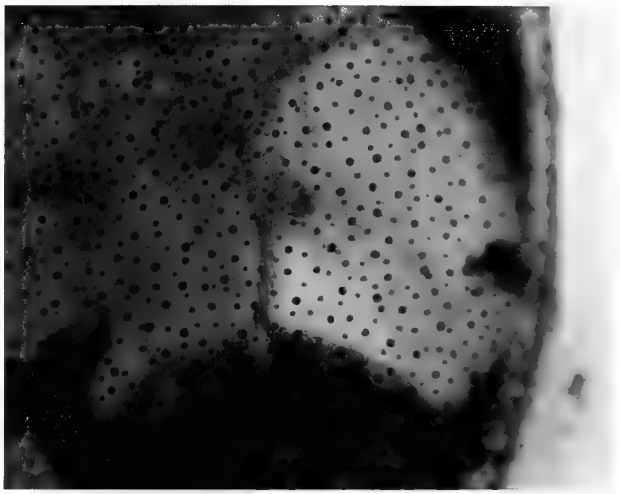

Figure 12. Cluster of droplets visible in the digestive cecum of a live, intact EtOH-anesthetized squid with retracted chromatophores and no colored body pattern. These dark yellow but small droplets were not detected several minutes earlier, before the squid was anesthetized.

In total, three of four squid stopped respiratory ventilations during or shortly after $MgCl_2$ treatment. None of these three squid survived the fourth anesthesia, despite up to 60 min of artificial ventilation per squid in fresh seawater. The sole squid that survived for several days after $MgCl_2$ treatment was the only squid exposed to $MgCl_2$ added dropwise (over a 10-min period to a final concentration of 1% $MgCl_2$, followed by 2 min in 1% $MgCl_2$). By 12 minutes, that squid was sluggish enough to be measured, but it was not fully immobilized. After 2 min recovering in fresh seawater, it began active finning and jetting and had a darkly pigmented mantle.

Impact of Anesthesia on Lipid Droplet Detection, Movement, and Retention

Without using anesthesia, we detected (during the 15-min allotted viewing time) extracellular lipid droplets in the digestive system in 25 of 42 live, intact squid on day 1 or 2 after collection. A few minutes later (per squid), using 2% EtOH anesthesia, we detected lipid droplets in all 42 squid. Comparatively large and dark yellowish droplets (see Eyster & van Camp, 2003;fig. 1a) were never missed in nonanesthetized squid. Droplets that we missed seeing tended to be comparatively small (Figure 12), pale yellow to colorless, or exhibited both traits. When we did not use anesthesia, we failed to detect droplets in both known locations: the digestive ceca and the digestive glands.

Just before the first EtOH anesthesia (days 1–2), lipid droplets were detected in the digestive cecum in 21 of 42 squid (50%). A few minutes later (per squid) cecal lipid droplets were seen in 41 of 42 anesthetized squid (98%), including all 21 squid that had visible cecal droplets before anesthesia. The one squid in which we did not detect cecal droplets (before or during its anesthesia) seemed healthy and was of average size (6.8 mm ML).

Just before the first EtOH anesthesia (days 1–2), lipid droplets were seen in the digestive gland in 18 of 42 squid (43%). In anesthetized squid, droplets were again detected in the digestive gland of those 18 squid plus five additional squid (55%).

In no case (on either day 1 or 2) were lipid droplets seen in a digestive organ just before anesthesia but then not found in that same organ during anesthesia. Also, no shifting of droplets between cecum and digestive gland was detected while the squid were immersed in the anesthetic solutions. Fluid seemed to flow from digestive gland to cecum in one anesthetized squid, but no droplets were seen in the digestive gland before or during the apparent flow.

Amongst squid that did have lipid droplets when anesthetized days 1–2 and that were re-examined ~1 wk later (second anesthesia), no starved individuals had any visible lipid droplets (n = 21) but all fed squid did (n = 20). In addition, the sum total lipid droplet volume detected in fed squid (in digestive gland plus digestive cecum) was greater on day 8 (after the second anesthesia) than the volume detected on days 1–2 (n = 20 squid; Wilcoxon signed ranks test, $P = 0.01$).

Total visible extracellular lipid droplet volume decreased in squid exposed to consecutive EtOH anesthesias (days 8–10 or 11) and starved during those days (Figure 13). Both cecal and digestive gland droplets were seen in all four squid on day 8 (during the second anesthesia), in three squid on day 9 during the third anesthesia, in two squid on day 10 (fourth anesthesia), and in one of the four squid on day 11. Lipid droplet volume decreased to zero or almost zero over several days of treatment, not after just one anesthesia event (Figure 13). No oil droplets were detected on the water surface in individual culture dishes.

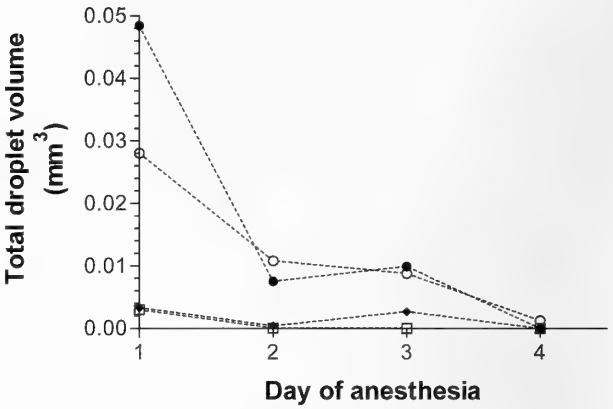

Figure 13. Extracellular lipid droplet volume (sum total volume of droplets in the digestive gland and the digestive cecum) in four squid exposed to starvation and repeated consecutive anesthesia administered 3–4 days in a row (with 2% EtOH, days 8–11 after collection).

DISCUSSION

Context for Using Chemical Anesthesia on Squid

In our previous work on extracellular lipid droplets in squid (Eyster & van Camp, 2003), we did not use chemical anesthesia for fear that it would induce movement of the digestive contents, as suggested by Bidder (1966). Instead, we placed squid in room temperature seawater into the freezer to the point of their immobility; then we decapitated them and cut them open to remove their lipid droplets. As our work continued and we began to examine lipid in numerous live squid over time, we needed a quicker and reliably sublethal method of repeatedly immobilizing the squid. Besides chilling, we tried other ways to observe a live squid microscopically in its relaxed, transparent state. For example, we confined individual squid under a small clear inverted dish about twice their length in diameter, but this caging method induced hyperactivity, and the duration of transparency did not last long enough for us to locate and count the oil droplets. Because captive squid typically spent many hours each day attached to the undersides of vegetation by their dorsal adhesive glands, we experimented with small floating pieces of transparent Parafilm and microscope coverslips (glass) in the observation dishes. In the absence of vegetation, nonanesthetized squid attached readily (in a few minutes) to the underside of these floating materials; after attaching, the animals often paled, allowing us to look for oil droplets in the digestive organs. Although this method avoided most stresses to the squid, the floating material jiggled as the squid ventilated, making accurate microscopic measurements difficult, and although the squid paled they were not always sufficiently translucent to allow viewing of the lipid droplets. While attached, the portion of the squid skin closest to the floating coverslip did not always pale as much as the rest of the squid (Figure 7) and transparency in that area of the body was critical for revealing all of the lipid droplets. Because waiting for a squid to pale enough on its own was very time-consuming and times of transparency were often too brief to allow detection of droplets, we finally used chemical anesthesia, as reported here. It was not our intention to conduct a thorough comparative study of anesthetic responses for

Southern Pygmy squid; we share a summary of the various responses of our squid to the anesthetics we used.

This is apparently the first description of sublethal anesthesia in idiosepiids, the world's smallest cephalopods. Anesthetic effects noted in our squid included (listed here in no particular order, without reference to order of induction, frequency of occurrence, or induction agent), (1) abnormal body posture, (2) suppression of jetting and finning movements, (3) paling of skin either in patches or to almost transparency, (4) decrease in mantle cavity ventilation rate, (5) cessation of respiratory ventilations, (6) inking, (7) loss of heart contractions, and (8) death. Previous studies have shown that side effects of cephalopod anesthesia include all of the above-mentioned effects as well as muscle contraction (with cold anesthesia), hyperactivity, hyperventilation, waves of skin color changes, attacks by other individuals, and attempts to escape (Hanlon et al., 1983; Messenger et al., 1985; Boyle, 1991).

Efficacy of EtOH as an Anesthetic

As Hanlon et al. (1983) and O'Dor et al. (1990) reported for other loliginid squid species, EtOH was a quick and effective light anesthetic for our squid. Time to both of our induction markers was rapid, typically occurring within ~0.5 min for first exposure to 2% EtOH in seawater. Stress from 2% EtOH immersion seemed low in squid based on normal body postures, lack of hyperactivity, lack of hyperventilation, rapid recovery times, quick return of feeding behavior, and absence of any inking in a large number of animals (n = 42). We do not know whether the respiratory movements seen in immobilized squid were effective or not, but even at the maximum exposure time (3.5 min), no squid stopped respiratory ventilations while submerged in 2% EtOH. We do not know whether anesthesia affected the digestive system, but treatment did not prevent recovered squid from capturing and eating prey or from surviving (with or without food) for 1 wk after treatment. In fact, fed squid ML grew an average of 0.4 mm during the week between their first and second EtOH anesthesias.

Although the present study shows that a few minutes immersion in 2% EtOH–seawater solution was an effective nonlethal anesthetic procedure for our squid, EtOH treatment can be traumatic or lethal for some cephalopods. For example, 60% of *Octopus vulgaris* hyperventilated and made escape attempts, and inking was common during 3–4-min exposures to 2% EtOH (Andrews & Tansey, 1981). EtOH (1.5%) was lethal for 20% of the squid *Illex illecebrosus* (Webber & O'Dor, 1986). For the congener *Idiosepius paradoxus*, 3% EtOH in seawater was used as an anesthetic before fixation for immunocytochemistry (Shigeno et al., 2008), but it is unclear whether those squid were anesthetized until loss of movement, loss of respiratory ventilations, or death. Even with very large cephalopods (e.g., cuttlefish up to 1 kg and octopods up to 9 kg; Zielinski et al., 2001), 2% EtOH solutions can be used for euthanasia.

Our two indicators of anesthetic induction (loss of ability to move and loss of ability to produce and sustain body color patterns) were relatively unambiguous markers with detectable end points. Because we exposed squid to EtOH only for as long as needed to measure their MLs and their visible microscopic oil droplets, we did not continue immersion until full anesthesia was reached; we assume that loss of respiration would be more stressful on the squid. An additional criterion to assess induction of anesthesia is whether the animal responds to the pinching of skin above the eye (Andrews & Tansey, 1981). However, because of the small size of our squid, eyelid pinches to assess anesthetic induction state were not attempted.

Of all induction and recovery information, data on time to loss of swimming ability were most closely clustered; almost half of the squid (20/42) stopped swimming between 27 and 32 sec after their first immersion in 2% EtOH in seawater. Recovery times were more variable than induction times, possibly in part because recovery was more difficult to assess. Because loss of ventilation was not used as an induction marker, resumption of ventilation could not be used for a recovery marker. It was apparent when the squid stopped swimming, but the point at which normal swimming behavior resumed or could have resumed was more subjective and reported values are subject to ±15-sec uncertainty. Also, some squid (15%) resumed movement by arm crawling before they resumed swimming. It is unclear whether these squid could have jetted as early as they crawled.

Compared with specimens acclimated to the laboratory, newly caught specimens of some cephalopods seem more susceptible to anesthesia, meaning that they suffer from more negative side effects. Therefore, cephalopods are usually held in the laboratory for a while before being tested. Twenty-four hours is considered an adequate acclimation period, but little information is available on this topic (Boyle, 1991). Here, we obtained no evidence that squid maintained in the laboratory for 2 days were less stressed during 2% EtOH anesthesia than were squid held for only 1 day before anesthesia. Thus, 1 day of acclimation before light EtOH anesthesia seems adequate for these squid.

Exposure time (i.e., how long it took us to measure the squid and its droplets) was 2.2 min on day 1 and 1.9 min on day 2. Although these times are not significantly different, the shorter time on the second

day of anesthetizing squid may be due to increased human efficiency rather than anything related to the squids' acclimation to the laboratory.

Repeated EtOH Anesthesia: Time to Induction, Order of Induction, and Health and Recovery

Squid often took longer to induce on subsequent EtOH immersions than during the first anesthesia, suggesting development of resistance to anesthesia, the specific anesthetic, or both. Our data do enable us to confirm whether the difference is due to repeated anesthetic events (previous anesthetic history), to change(s) in the squid during the time they were held in the laboratory, or both. For example, we did not compare first induction responses for day 1 versus day 8 of captivity. However, it seems more likely that squid would be less healthy after longer captivity and might therefore be less resistant, not more resistant, to induction, as shown here.

With the first EtOH anesthesias, loss of skin body color patterns in squid always preceded loss of swimming. With later EtOH exposures, this order was not maintained. For example, during the third anesthesia most squid lost mobility before reaching full transparency. Andrews & Tansey (1981) reported that order of induction events was the same in first urethane versus later urethane anesthesia (although the number of exposures is unclear).

Squid exposed to three EtOH anesthesias over 10 days seemed subjectively healthier than squid exposed to three EtOH anesthesias in three consecutive days; so, spacing of anesthesia may affect squid health, but we cannot rule out the impact of starvation that occurred on days of anesthesia. We knew from previous work (Eyster & van Camp, 2003) that some squid can survive without feeding for a couple weeks, but we have no data on impact of periodic starvation on their health. Squid (n = 4) maintained in a way similar to that of squid exposed to consecutive anesthesia in our study, but without anesthesia (i.e., in static culture in fingerbowls without food; Eyster & van Camp, 2003), looked healthier than anesthetized squid after 3 days, suggesting the repeated anesthesia did have a deleterious effect on the animals.

Despite some apparent development of resistance to EtOH anesthesia, as shown by changes in induction times and patterns, we consider reanesthesia with EtOH successful. Reanesthesia of cuttlefish with $MgCl_2$ was reported as successful (with full recovery; work of Kier et al., in preparation, as cited in Messenger et al., 1985), but repeated EtOH or urethane immersions were traumatic for octopus (Messenger et al., 1985).

Because our data suggest that anesthetized squid became resistant to induction by 2% EtOH, we performed one small trial test with 4% EtOH and one small trial with $MgCl_2$ (four squid each). Squid mortality in 4% EtOH was much higher (one of four squid) compared with that at 2% EtOH (zero of 42 squid); however, the squid exposed to 4% EtOH had been in the laboratory approximately 2 wk longer and thus were probably not as healthy. They also already had been exposed to 2% EtOH three times before their 4% EtOH treatment. Although induction times at 4% EtOH were similar to initial 2% EtOH induction, recovery times were more than twice as long, suggesting greater stress on the squid.

Cold Seawater and $MgCl_2$ Anesthesias

Although we had previously used chilled squid (Eyster & van Camp, 2003), we had only used lethal exposures (before incisions to remove droplets for testing). Although squid rarely inked when cooled slowly in a dish of room temperature seawater placed into the freezer, squid placed directly into 4°C seawater in the present work inked frequently (seven of 10). Based on our preliminary data, we cannot recommend sudden immersion in cold water for this squid, although retesting at other times of year may be worthwhile; perhaps the temperature drop from 22 to 4°C was too great and a smaller drop might be less stressful. Cold anesthesia may be ruled out for some cephalopods; for example, *Sepioteuthis lessoniana* should be kept at approximately 12°C during shipping (Ikeda et al., 2004). Cold anesthesia has been used successfully for 6.5-hr transports of the live squid *Todarodes pacificus*, although longer exposures (10–11-hr immersions) were fatal (Bower et al., 1999). Also, although cephalopods may survive cold anesthesia, it may be less effective in relaxing muscles (Andrews & Tansey, 1981).

$MgCl_2$ has been reported previously to be an effective anesthetic for a variety of cephalopods, including cuttlefish, squid, and octopods (Messenger et al., 1985). However, the smallest cephalopods they tested were 120 g or 50 mm ML, approximately 5 times longer than our squid and approximately 100 times more massive. Messenger et al. (1985) found $MgCl_2$ to have few traumatic side effects and to cause only one death (one of 17 animals) and only one inking. They also noted initial hyperventilation in all cephalopods; we did not note this particular side effect for squid immersed in $MgCl_2$.

Here, $MgCl_2$ was not as useful as EtOH for inducing minimized chromatophores in squid or for immobilizing the squid. Induction was slower than in EtOH, and these longer immersions were accompanied by loss of respiration that was followed by low percentage of recovery. Because we did not test response of recently collected squid to $MgCl_2$, we cannot rule out the possibility that this poor response was aggravated by

health of the squid (they had been in captivity ~19 days), previous anesthetic history (three previous EtOH anesthesias), or both. However, four other squid also held in the laboratory for ~19 days, and also previously exposed to EtOH anesthesia three times, suffered only 25% mortality in 4% EtOH compared with 75% mortality in $MgCl_2$.

Extracellular Lipid Droplets and Impact of Anesthesia and Reanesthesia

Eyster & van Camp (2003) reported extracellular lipid droplets in the digestive system in two freshly collected squid. Here, we expand that sample size and report droplets in all 42 freshly collected squid (examined days 1–2 without postcollection feeding).

We showed previously that these lipid droplets persisted in three squid starved for 7 days before sacrifice; squid starved longer had no detectable lipid droplets (Eyster & van Camp, 2003; Table). Here, we confirm loss of lipid drops by day 8 in starved squid, although squid were not checked for droplets on days 3–7. Although all starved squid (n = 21) had lost all visible droplets by day 8 and all fed squid (n = 20) contained visible droplets on day 8, we cannot determine whether those droplets demonstrate persistence of the original lipid observed on days 1–2, production of new lipid from mysid consumption, or both.

Anesthesia was important to our study of the lipid droplets in squid. Brief EtOH anesthesia greatly improved accuracy of data on location, number, and size of extracellular lipid droplets because it rapidly induced squid immobility and loss of mantle color patterns. For example, without anesthesia we failed to see cecal droplets in 20 of the 41 squid and digestive gland droplets in 5 of 23 squid that had them a couple minutes later when the squid were in a nonmobile, transparent, anesthetized state. We stated previously (Eyster & van Camp, 2003) that in cold-anesthetized squid, cecal droplets were easier to see than were digestive gland drops. This was because the cecum lumen was not obscured with dark material as was the digestive gland. Surprisingly, in the present study, we apparently missed cecal drops more frequently than digestive droplets when we tried to locate them without the aide of anesthesia.

We were concerned that anesthesia might induce these unusual extracellular oil droplets to move between organs, be expelled, or both (Bidder, 1966). However, we obtained no evidence that a single EtOH anesthetic event, anesthesia repeated on nonconsecutive days, or anesthesia repeated on consecutive days led to expulsion of these droplets from the digestive system. The fact that three of four squid still had lipid droplets during their third day of consecutive anesthesia suggests that light anesthesia did not lead to expulsion of droplets. We can rule out the idea that the lipid viewed on these days was formed from new meals because these four squid were not fed during anesthetic treatment days. It is unlikely that these squid expelled all of their old extracellular oil and made new oil droplets; preliminary work by Eyster & van Camp (2003) suggested that droplets can appear (in squid without apparent drops) approximately 3 hr after feeding.

It is harder to determine whether anesthesia induced any movement of oil drops between digestive ceca and digestive glands (than to determine whether drops were expelled) because both organ types already may contain these extracellular lipid droplets before anesthesia. This point is relevant to interest in where oil might possibly be stored versus possibly digested. Just before anesthesia, drops seemed to be in the same organ that they were found in during anesthesia. It is difficult to assess oil drop movement due to anesthesia because it is difficult to locate all drops without anesthesia, especially if the squid was too active or too darkly pigmented during the observation period or the drops were too small or colorless to be detected when the squid was moving slowly. Because the oil droplets can fuse or split, total droplet volume, not just droplet number, must be considered. Although data on repeated anesthesia 10–14 days after the first exposure do not suggest movement of droplets during anesthesia, we cannot rule out movement after recovery. Our data suggest that short exposures to 2% EtOH might not move these droplets between organs, but clear confirmation of organ-to-organ transfer of oil induced by anesthesia may require individual squid with digestive gland drops but no cecal drops, or vice versa.

Our work does not rule out catabolism of some of the oil, movement of some droplets between digestive organs, or expulsion of some small droplets from the squid, but it does seem to rule out EtOH-induced movement of all drops out of any particular digestive organ, or expulsion of all droplets after a single or even repeated immersion in 2% EtOH. This work clearly shows the advantage and safety of using EtOH anesthesia for calming and immobilizing Southern Pygmy squid.

Acknowledgments. We are grateful for the use of the Flinders University laboratory facilities of J. N. Havenhand and for the boats of J. Robertson and A. R. Dyer. Thanks to Oliver Pechenik for help with data entry and graph preparation. This research was supported in part by a sabbatical leave and a research grant from Milton Academy to L.S.E.

LITERATURE CITED

ANDREWS, P. L. R. & E. M. TANSEY. 1981. The effects of some anesthetic agents in *Octopus vulgaris*. Comparative Biochemistry and Physiology 70C:241–247.

Berk, W., J. Teperman, K. D. Walton, K. Hirata, M. Sugimori & R. R. Llinas. 2009. Oral administration of pharmacologically active substances to squid: a methodological description. Biological Bulletin 216:1–6.

Bidder, A. M. 1966. Feeding and digestion in cephalopods. Pp. 97–124 in K. M. Wilbur & C. M. Yonge (eds.), Physiology of Mollusca. Vol. II. Academic Press: New York.

Boletzky, S. V. (Convenor). 2005. *Idiosepius*: ecology, biology and biogeography of a mini-maximalist. Phuket Marine Biological Center Research Bulletin 66:11–22.

Bower, J. R., Y. Sakurai, J. Yamamoto & H. Ishii. 1999. Transport of the ommastrephid squid *Todarodes pacificus* under cold-water anesthesia. Aquaculture 70:127–130.

Boyle, P. 1991. The UFAW Handbook on the Care & Management of Cephalopods in the Laboratory. Universities Federation for Animal Welfare: Potters Bar, United Kingdom. 63 pp.

Byern, J. V., L. Rudoll, N. Cyran & W. Klepal. 2008. Histochemical characterization of the adhesive organ of three *Idiosepius* spp. species. Biotechnic and Histochemistry 83(1):29–46.

Eyster, L. S. & L. M. Van Camp. 2003. Extracellular lipid droplets in *Idiosepius notoides*, the southern pygmy squid. Biological Bulletin 205:47–53.

Hanlon, R. T. 2010. How squid change color. http://www.mbl.edu/publications/pub_archive/Loligo/squid/skin.2.html. Accessed December 26, 2010.

Hanlon, R. T., R. F. Hixon & W. H. Hulet. 1983. Survival, growth and behaviour of the loliginid squids *Loligo plei*, *Loligo pealei* and *Lolliguncula brevis* (Mollusca: Cephalopoda) in closed sea water systems. Biological Bulletin 116:637–685.

Hochachka, P. W., T. W. Moon, T. Mustafa & T. W. Storey. 1975. Metabolic sources of power for mantle muscle of a fast swimming squid. Comparative Biochemistry and Physiology 52B:151–158.

Ikeda, Y., Y. Ueta, I. Sakurazawa & G. Matsumoto. 2004. Transport of the oval squid *Sepioteuthis lessoniana* Férussac, 1831 in Lesson 1830–1831 (Cephalopoda: Loliginidae) for up to 24 h and subsequent transfer to an aquarium. Fisheries Science 70:21–27.

Kasugai, T. & Y. Ikeda. 2003. Description of the egg mass of the pygmy cuttlefish, *Idiosepius paradoxus* (Cephalopoda: Idiosepiidae), with special reference to its multiple gelatinous layers. The Veliger 46(2):105–110.

Kasugai, T., S. Shigeno & Y. Ikeda. 2004. Feeding and external digestion in the Japanese pygmy squid *Idiosepius paradoxus* (Cephalopoda: Idiosepiidae). Journal of Molluscan Studies 70:231–236.

Mather, J. A. & R. C. Anderson. 2007. Ethics and invertebrates: a cephalopod perspective. Diseases of Aquatic Organisms 75:119–129.

Messenger, J. B., M. Nixon & K. P. Ryan. 1985. Magnesium chloride as an anesthetic for cephalopods. Comparative Biochemistry and Physiology 82C:203–205.

Moltschaniwskyj, N. A., K. Hall, M. R. Lipinski, J. E. A. R. Marian, M. Nishiguchi, M. Sakai, D. J. Shulman, B. Sinclair, D. L. Sinn, M. Staudinger, R. Van Gelderen, R. Villaneuva & K. Warnke. 2007. Ethical and welfare considerations when using cephalopods as experimental animals. Reviews in Fish Biology and Fisheries 17:455–476.

O'Dor, R., H. O. Pörtner & R. E. Shadwick. 1990. Squid as elite athletes: locomotory, respiratory, and circulatory integration. Pp. 481–504 in D. L. Gilbert, W. J. Adelman, Jr. & J. M. Arnold (eds.), Squid as Experimental Animals. Plenum Press: New York.

Norman, M. 2000. Cephalopods: A World Guide. ConchBooks: Hackenheim, Germany. 320 pp.

O'Dor, R. K. & D. M. Webber. 1986. The constraints on cephalopods: why squid aren't fish. Canadian Journal of Zoology 64:1591–1605.

Sen, H. & T. T. Tanrikul. 2009. Efficacy of 2-phenoxyethanol as an anaesthetic for musky octopus, *Eledone moschata* (Lamarck 1799), (Cephalopoda: Octopodidae). Turkish Journal of Veterinary Animal Sciences 33(6):463–467.

Shigeno, S. & M. Yamamoto. 2002. Organization of the nervous system in the pygmy cuttlefish, *Idiosepius paradoxus* Ortmann (Idiosepiidae, Cephalopoda). Journal of Morphology 254(1):65–80.

Shigeno, S., T. Sasaki, T. Moritaki, T. Kasugai, M. Vecchione & K. Agata. 2008. Evolution of the cephalopod head complex by assembly of multiple molluscan body parts: evidence from *Nautilus* embryonic development. Journal of Morphology 269(1):1–17.

Storey, K. B. & J. M. Storey. 1983. Carbohydrate metabolism in cephalopod molluscs. Pp. 92–137 in P. W. Hochachka (ed.), The Mollusca I. Metabolic Biochemistry and Molecular Biomechanics. Academic Press: London, United Kingdom.

Tracey, S. R., M. A. Steer & G. T. Pecl. 2003. Life history traits of the temperate mini-maximalist *Idiosepius notoides*, (Cephalopoda: Sepioidea). Journal of the Marine Biological Association of the United Kingdom 83:1297–1300.

Urban, B. W. 2002. Current assessments of targets and theories of anesthesia. British Journal of Anesthesia 89: 167–183.

Urban, B. W. & M. Bleckwenn. 2002. Concepts and correlations relevant to general anesthesia. British Journal of Anesthesia 89:3–16.

Webber, D. M. & R. K. O'Dor. 1986. Monitoring the metabolic rate and activity of free-swimming squid with telemetered jet pressure. Journal of Experimental Biology 126:205–224.

Yamamoto, M., Y. Shimazaki & S. Shigeno. 2003. Atlas of the embryonic brain in the pygmy squid, *Idiosepius paradoxus*. Zoological Science 20(2):163–179.

Young, J. Z. 1963. The number and sizes of nerve cells in *Octopus*. Proceedings of the Zoological Society of London 140:229–245.

Zielinski, S., F. J. Sartoris & H. O. Pörtner. 2001. Temperature effects on hemocyanin oxygen binding in an Antarctic cephalopod. Biological Bulletin 200:67–76.

The Veliger 51(3):131–136 (November 16, 2012)

THE VELIGER

A New Species of *Harpa* (Gastropoda: Volutoidea) from the Neogene of the Dominican Republic: Paleobiogeographical Implications

BERNARD LANDAU*

Departamento e Centro de Geologia da Universidade de Lisboa. Campo Grande, 1749-016 Lisboa, Portugal and International Health Centres, Avenida Infante de Henrique 7, Areias São João, P-8200 Albufeira, Portugal (e-mail: bernielandau@sapo.pt)

FRANCK FRYDMAN

4, square Saint Irénée, 75011 Paris, France

CARLOS M. DA SILVA

Departamento e Centro de Geologia. Universidade de Lisboa. Campo Grande, 1749-016 Lisboa, Portugal

Abstract. A new species of *Harpa*, *H. daisyae* is described from the Upper Miocene Cercado Formation of the Dominican Republic. The genus in the tropical American Neogene is discussed, phylogenetic groups within the genus are suggested, and paleobiogeographic implications commented.

INTRODUCTION

The rich and diverse Neogene assemblages from the northern Dominican Republic have been known for >150 yr (Sowerby, 1850). More recently, these assemblages have been studied in a systematic way as part of the "Dominican project," and these results published in a series of papers that appeared in Bulletins of American Paleontology (Vokes, 1989, 1998; Jung & Petit, 1990; Jung, 1994; Freiheit & Greary, 2009). For an account of the history and methodology of the various Dominican collecting ventures, see Vokes (1989).

This paper is the first of a series of papers describing new gastropod taxa from these Dominican assemblages belonging to taxonomic groups already monographed by the Dominican project but discovered subsequent to the publication of these works. These new taxa also represent the result of 20 yr collecting in the Dominican Republic by one of us (B.L.).

The genus *Harpa* in the Dominican Neogene was revised by Vokes in 1998. The presence of fossils belonging to the genus *Harpa* in the Dominican Republic Neogene was first noted by Gabb (1873); the specimens were later described by Pilsbry (1922) as *Harpa americana*. This species is represented by two specimens from an unnamed unit in the López section of the Yaque del Norte River, ascribed to the same age of the Cercado Formation, Upper Miocene by Vokes (1998). We here describe a second *Harpa* species co-occurring in these deposits. It is also from the López section, from sandy unit close to the river bed toward the east bank and probably is also of the same age as the Cercado Formation (Vokes, personal communication). The bed of the Yaque del Norte River is very dynamic and the units exposed change accordingly. Conglomerates, coarse-to-fine sands, and clays are exposed at different sections of the river bed when the river is at its lowest, and the specimen described here was found in a bed composed of fine yellow sands situated approximately 2.9–3 km upstream of the mouth of Angostura Gorge (Figure 1), Rio Yaque del Norte, with sparsely scattered fossils of molluscs, mostly *Vokesimurex messorius* (Sowerby, 1841), and a few other molluscs, none of which were stratigraphic index taxa.

For a more detailed geological and stratigraphic setting and geographic location of the study, see Saunders et al. (1986;23–30).

MATERIALS AND METHODS

The material described here is from the Bernard Landau collection, which will be housed in the Naturhistorisches Museum Wien (NHMW collection [coll.]), Vienna, Austria. Type material is deposited in the Naturhistorisches Museum Wien (NHMW coll.), Vienna, Austria.

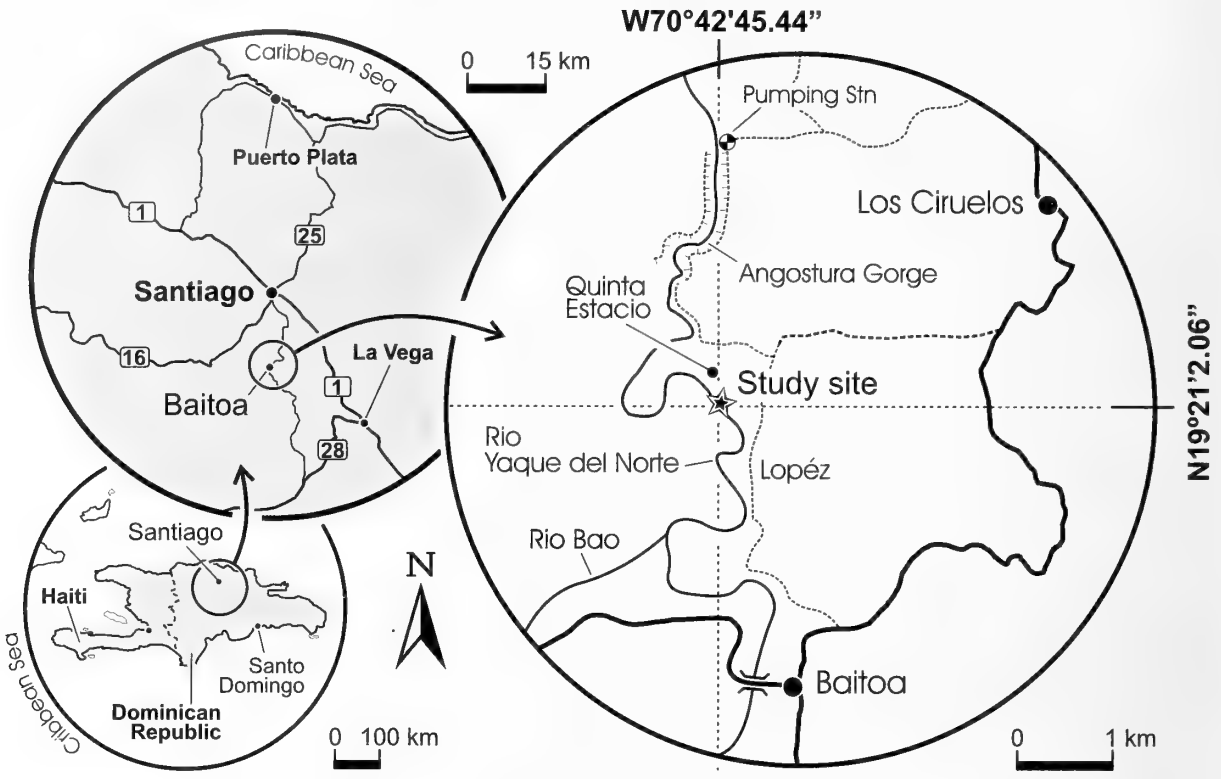

Figure 1. Geographic location of study area.

SYSTEMATIC PALAEONTOLOGY

VOLUTOIDEA

HARPIDAE Bronn, 1849

Harpinae Bronn, 1849

Harpa Röding, 1798

Harpa daisyae nov. sp.

(Figures 2–5)

Type material and dimensions: Holotype; NHMW 2009z0076/0001, height 22.5 mm.

Etymology: Small and pretty, like my daughter Daisy (B.L.).

Type locality: Lopez section, Rio Yaque del Norte, upstream of the mouth of Angostura Gorge, Dominican Republic (Saunders et al., 1986;fig. 23; and Figure 1).

Type stratum: Unnamed unit of the same age of the Cercado Formation (Upper Miocene).

Diagnosis: A small-shelled *Harpa*, with a multispiral protoconch of smooth rounded whorls, and a low spired teleoconch with, an elongated last whorl, very narrow and relatively close-set axial ribs, weak spiral sculpture of roughly equal strength to the axial growth lines giving the shell surface a finely reticulate pattern, outer lip smooth, without barbs.

Description: Shell very small for genus, ovate; spire low, depressed, rapidly increasing in size; last whorl and aperture very large. Protoconch poorly preserved with nucleus missing, multispiral, high dome-shaped, tilted slightly at an angle to the main axis of the shell, composed of at least three smooth whorls. Last protoconch whorl inflated, bearing three strongly prosocline riblets toward the protoconch–teleoconch boundary, which is sharply delimited by a sinusoid scar. Teleoconch consists of three whorls with a narrow, almost horizontal subsutural platform, broadly rounded below with the periphery at the adapical suture. Axial ornament strongly predominant, consisting of 11 very narrow elevated ribs, opistocyrt on the first teleoconch whorl, straight below, 13 on the last whorl. The ribs are reflected abaxially at the shoulder, fuse with the adapical portion of the preceding whorl to cover the adapical suture entirely. A small auricle develops on the axial ribs at the shoulder on the second half of the penultimate whorl and last whorl. Spiral sculpture consists of very weak, narrow, irregular cords cut by close-set axial growth lines giving the surface a finely reticulate pattern. Last whorl very large, 90% of

total height, barrel-shaped. Aperture large, 78% total height, elongate. Outer lip slightly thickened by labral varix, weakly flared abapically, not barbed on the edge, smooth within; anal canal relatively wide, rounded, shallow; siphonal canal open, short, slightly recurved. Parietal callus expanded, closely adherent, thin, clearly delimited; columellar callus slightly thicker, somewhat detached over the siphonal fasciole. Siphonal fasciole broad, rounded, with the axial sculpture deflected onto it as elevated scales.

Comparison: *Harpa daisyae* nov. sp. is the smallest adult *Harpa* shell known from the Tropical American Neogene. It is most similar in size and shape to the Recent *Harpa gracilis* Broderip, W. J. & G. B. I Sowerby, 1829 (Figures 6, 7) that is mainly a Polynesian species but that also occurs at Clipperton Island in the eastern Pacific (Rehder, 1973), but this *Harpa* has an even more elongated shell, with a higher spire and the outer lip is more flared abapically. Like *H. gracilis*, it has a smooth outer lip with no barbs. Of the Tropical American species, *Harpa isthmica* Vokes, 1984 is the most similar (Figures 8–10), but the latter species has a wider, less elongated shell, with more numerous axial ribs that form a small spine at the shoulder rather than a rounded auricle as in *H. daisyae*. According to the original description, the protoconch of *H. isthmica* is keeled (Vokes, 1984: 57), whereas that of *H. daisyae* has uniformly rounded whorls. *Harpa myrmia* Olsson, 1931 and *Harpa crenata* Swainson, 1822 (Figures 11, 12) both have much broader shells and more widely spaced axial ribs with spines at the shoulder, and in *H. crenata* a double set of spines.

GENUS *HARPA* IN THE TROPICAL AMERICAN NEOGENE

The genus *Harpa* in the Tropical American Neogene has attracted a fair amount of attention and was comprehensively covered by Vokes (1984). Five species of *Harpa* Röding, 1798 have been described from the tropical American Neogene, and although fairly widespread in the Tropical American deposits, it is invariably rare in abundance; therefore, new records are worthy of mention to reveal the Neogene history and palaeobiogeography of the genus.

Harpa first appears in the Cenozoic of tropical America in the Lower Oligocene Chira Formation of Peru (Olsson, 1931) represented by *Harpa myrmia*, characterized by its extremely heavy ribs and broad extension of the axial ribs of the last whorl; these ribs are appressed against the previous whorl and completely cover the suture and most of the penultimate whorl. Chronostratigraphically, the next occurrence is in the Lower Miocene Cantaure Formation of Venezuela. Identified as *Harpa myrmia* by Gibson-Smith & Gibson-Smith (1982), it also has heavy axial ribs, with extensions covering the suture. The width of the ribs are somewhat variable (Gibson-Smith & Gibson-Smith (1982: figs. 1, 2), and three further specimens (B.L coll.) have relatively narrower ribs, whereas the shell described in Gibson-Smith & Gibson-Smith (1982;fig. 3) has broad ribs, similar to the Peruvian specimen. As noted by Vokes (1984), more Peruvian material is needed to confirm whether the two specimens are conspecific.

Harpa americana Pilsbry, 1922 from the Cercado Formation, Upper Miocene of the Dominican Republic has a relatively elongated shell, with low, nodular varices and a nonpolished surface. It is known from only two specimens (Vokes, 1998), and our collecting efforts have not brought any more specimens to light. *Harpa isthmica* Vokes, 1984 from the Agueguexquite Formation, Middle Pliocene of Mexico (Caribbean) has more numerous and heavier ribs, and a smoother surface to the shell. One of us (B.L.) has found a specimen ascribed to *Harpa isthmica* in the Ground Creek Formation on Bastimentos Island, Bocas del Toro, Panama (Figures 8–10) dated as Plio-Pleistocene Boundary (Coates et al., 2005).

Lastly, the living *H. crenata* is characterized by having a more inflated last whorl and fewer axial ribs, with secondary nodes anterior to the shoulder that become prominent shoulder spines, giving a "double-shouldered" aspect to the shell (Vokes, 1984); and by having barbs on the edge of the outer lip. There are differences also in the protoconch, consisting of 3.5 whorls in *H. crenata* and *H. isthmica* and 4.5 whorls in *H. americana* (although this is somewhat contradictory; the original description gives an "embryonic whorl count of 3.0"; Pilsbry, [1922]: 337), whereas Vokes [1984: 57] states 4.5 whorls). The presence of *H. crenata* was recorded in the Lower Pliocene Esmeraldas Formation of Ecuador (Pitt, 1981; Vokes, 1984). The specimen illustrated by Vokes (1984: pl. 1, fig. 5) as *H. crenata* with some hesitation is rather elongated for the species and lacks the "double-shouldered" aspect to the shell. The second specimen illustrated by Pitt (1981: 155: fig. 1) is also atypical for *H. crenata*, and although broader, in our opinion both represent specimens of *H. americana*. *Harpa crenata* does, however, occur in the Lower Pliocene Araya Formation of Venezuela on Cubagua Island (Figure 11) and the Araya Peninsula (Figure 12; Landau et al., 2008).

Vokes (1984) suggested a phylogeny in which *H. myrmia* was a distinct lineage on account of having the sutures crossed by extensions of the ribs, not known in any other species. She suggested it derived from the ancestral *Eocithara* line and left no descendants. In the Caribbean, Vokes (1984) suggested that *H. isthmica* was most similar and possibly ancestral to the Recent West African *H. doris* Röding 1798. She suggested that *H. americana* gave rise to *H. crenata*, and its Early

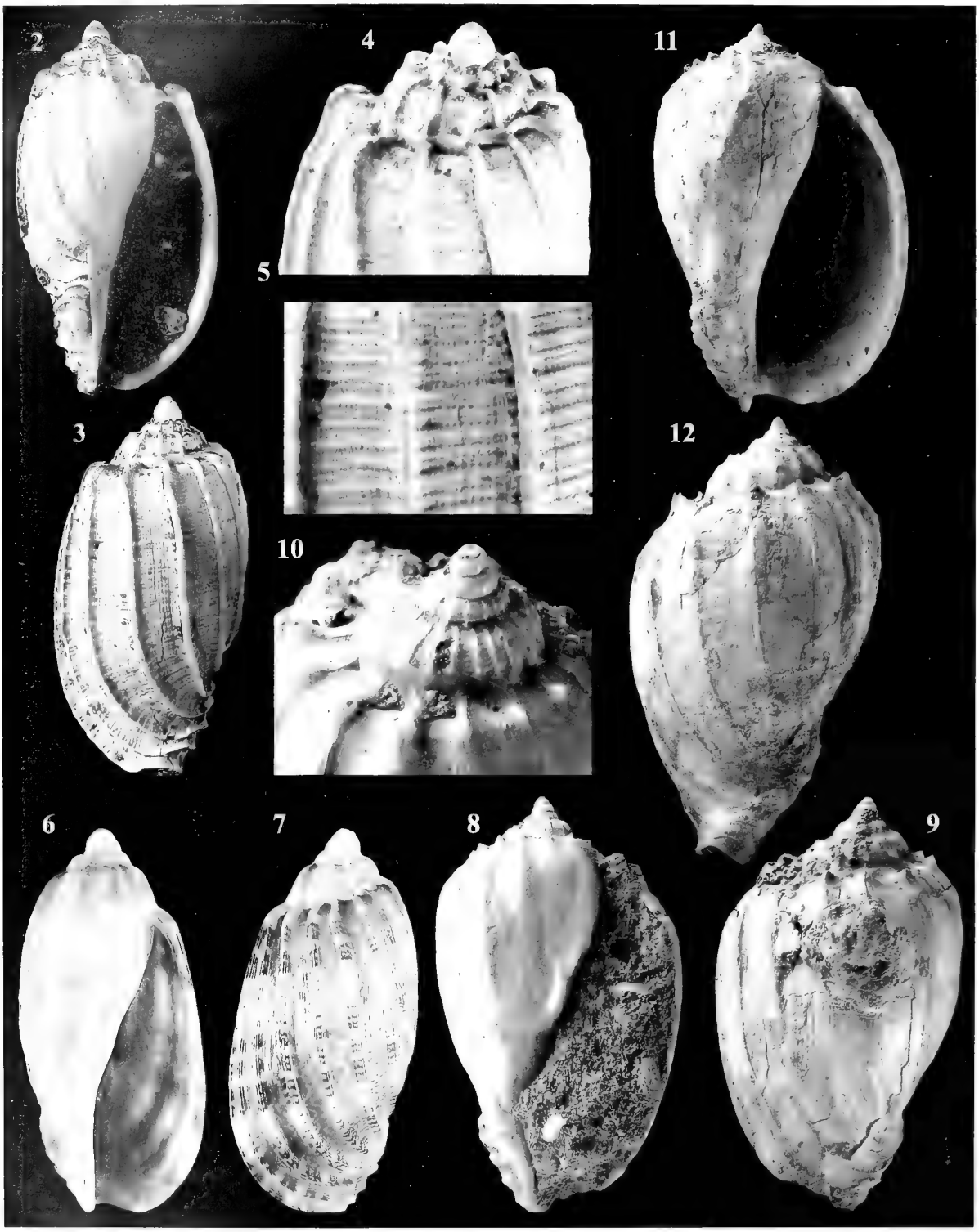

Figures 2–5. *Harpa daisyae* nov. sp. Holotype; NHMW 2009z0076/0001 (ex. B.L. coll.), height 22.5 mm. Unnamed unit of same age as Cercado Formation (Upper Miocene), sandy bed just upstream of the mouth of Angostura Gorge, Rio Yaque del Norte, Dominican Republic. Figure 4. Detail of spire and protoconch. Figure 5. Detail of surface sculpture last whorl.
Figures 6–7. *Harpa gracilis* Broderip, W. J. & G. B. I Sowerby, 1829 (coll. G. T. Poppe). Height 22.8 mm. French Polynesia. Tuamotous Archipelago.

Pliocene relative in Ecuador. Although these extensions to the ribs covering the suture are most marked in *H. myrmia*, they are also present to a lesser degree in *H. isthmica* and *H. daisyae*. Based on close similarities in shell morphology between *H. daisyae* and the Recent Indo-Pacific and eastern Pacific *H. gracilis*, it is likely that the two species are phylogenetically related, although we must stress that the fossil record of *Harpa*, especially in the Indo-Pacific, is very incomplete,

The presence of typical *H. crenata* specimens in the Lower Pliocene of Cubagua Island (Araya Formation) of Venezuela complicates the issue. In our opinion, the shells illustrated by and Pitt (1981) and Vokes (1984) from the Esmeraldas Formation of Ecuador are more typical of *H. americana*. It is likely that *H. americana* existed on both the Atlantic and Pacific portions of the Gatunian palaeobiogeographic province. *Harpa crenata* was restricted to the southern part of the province in the Pliocene and at some stage expanded its range to the Pacific side of the palaeobiogeographic province, with its distribution subsequently restricted to the Pacific after the closure of the Central American seaway.

Harpa is important from a palaeobiogeographic angle, because it is a good example of the group Woodring (1966) called paciphiles, i.e., taxa that were present throughout the Gatunian Neogene Province (see Vermeij & Petuch, 1986; Landau et al., 2008), but that suffered a range contraction after the closure of the Central American Seaway and subsequently became restricted to the Pacific side of their original distribution. With the description of *H. daisyae* nov. sp., we now have Caribbean fossil representatives of both the living eastern Pacific groups of *Harpa*: *H. daisyae* in the *H. gracilis* group, characterized by small, elongated shells with no barbs on the abapical portion of the outer lip; and *H. crenata*, one of the few living paciphile species (see Landau et al., 2009) in the Caribbean Lower Pliocene, in the *Harpa* group, with barbs on the abapical portion of the outer lip. *Harpa* is also an example of a typically tropical and subtropical genus that seems to have been widespread in the Neogene Gatunian Province but never extended its range into the neighboring Caloosahatchian Province to the north, despite this province also being tropical to subtropical (see Vermeij & Petuch, 1986; Landau et al., 2008).

From an ecostratigraphic point of view, *Harpa* is also important, because it is one of the few paciphile taxa that survived the first pulse of paciphile Caribbean disappearances at the end of the Early Pliocene, at approximately 3.5 Ma, before the disappearance of paciphiles from the Caribbean near the end of the Early Pleistocene, at approximately 1 Ma (Landau et al., 2009: fig. 2), and thus one of the paciphile taxa characteristic of the ecostratigraphic Gatunian Neogene Paciphile Molluscan Unit 2 of Landau et al. (2009).

Acknowledgments. Our thanks to Geraat J. Vermeij (Department of Geology, University of California, Davis) for critical review and to Guido Poppe for pictures of *H. gracilis*.

LITERATURE CITED

COATES, A. G., D. F. MCNEILL, M. P. AUBRY, W. A. BERGGREN & L. S. COLLINS. 2005. An introduction to the Geology of the Bocas del Toro Archipelago, Panama. Caribbean Journal of Science 41:374–391.

FREIHEIT, J. R. & D. H. GREARY. 2009. Neogene paleontology of the northern Dominican Republic. 23. Strombid gastropods (genera *Strombus* and *Lobatus*; Mollusca: Gastropoda: Strombidae) of the Cibao Valley. Bulletins of American Paleontology 376:1–54.

GABB, W. M. 1873. On the topography and geology of Santo Domingo. Transactions of the American Philosophical Society 15:49–259.

GIBSON-SMITH, J. & W. GIBSON-SMITH. 1982. The genus *Harpa* (Mollusca: Gastropoda) in northern South America. Tulane Studies in Geology and Paleontology 17:157–158.

JUNG, P. 1994. Neogene Paleontology in the Northern Dominican Republic 15. The genera *Columbella*, *Eurypyrene*, *Parametaria*, *Conella*, *Nitidella*, and *Metulella* (Gastropoda: Columbellidae). Bulletins of American Paleontology 106(344):1–45.

JUNG, P. & R. E. PETIT. 1990. Neogene Paleontology in the northern Dominican Republic. 10 The Family Cancellariidae (Mollusca: Gastropoda). Bulletins of American Paleontology 98(334):87–115.

LANDAU, B. M., G. VERMEIJ & C. M. SILVA. 2008. Southern Caribbean Neogene palaeobiogeography revisited. New data from the Pliocene of Cubagua, Venezuela. Palaeogeography, Palaeoclimatology, Palaeoecology 257:445–461.

LANDAU, B. M., G. VERMEIJ & C. M. SILVA. 2009. Pacific elements in the Caribbean Neogene gastropod fauna: the source-sink model, larval development, disappearance, and faunal units. Bulletin de la Société géologique de France 180:249–258.

←

Figures 8–10. *Harpa isthmica* Vokes, 1984. NHMW 2009z0077/0002 (ex. B.L. coll.), Height 35.2 mm. Plio-Pleistocene Boundary, Ground Creek Formation, Bastimentos Island, Bocas del Toro, Panama. Figure 10. Detail of spire and protoconch.
Figure 11. *Harpa crenata* Swainson, 1822. NHMW 2009z0077/0003 (ex. B.L. coll.), Height 66.2 mm. Early Pliocene, Araya Formation, Cubagua Group, Cañon de las Calderas, Cubagua Island, Nueva Esparta State, Venezuela.
Figure 12. *Harpa crenata* Swainson, 1822. NHMW 2009z0077/0004 (ex. B.L. coll.), Height 61.8 mm. Lower Pliocene, Amina Formation, Cubagua Group, Cerro Barrigón, Araya Peninsula, Sucre State, Venezuela.

OLSSON, A. A. 1931. Contributions to the Tertiary paleontology of northern Peru. Part 4. The Peruvian Oligocene. Bulletins of American Paleontology 17(63):97–218.

PILSBRY, H. J. 1922. Revision of W. M. Gabb's Tertiary Mollusca of Santo Domingo. Proceedings of the Academy of Natural Sciences of Philadelphia 73:305–435.

PITT, W. 1981. Two new gastropod occurrences in the Ecuadorian Neogene. Tulane Studies in Geology and Paleontology 16:155–156.

REHDER, H. A. 1973. The family Harpidae of the world. Indo-Pacific Mollusca 3:207–247.

SAUNDERS, J. B., P. JUNG & B. BIJU-DUVAL. 1986. Neogene paleontology in the Northern Dominican Republic. Part 1. Field surveys, lithology, environment and age. Bulletins of American Paleontology 89(323):1–79.

SOWERBY, G. B. [second of the name]. 1850. Descriptions of some new species found by J. S. Heniker, esq. In: MooreJ. C. (ed.), On some tertiary beds in the Island of San Domingo; from notes by J. S. Heniker, esq., with remarks on the fossils. Geological Society of London, Quarterly Journal 6:39–53.

VERMEIJ, G. J. & E. J. PETUCH. 1986. Differential extinction in tropical American molluscs: endemism, architecture, and the Panama land bridge. Malacologia 27:29–41.

VOKES, E. H. 1984. The genus *Harpa* (Mollusca: Gastropoda) in the New World. *Tulane Studies in Geology and Paleontology* 18:53–60.

VOKES, E. H. 1989. Neogene paleontology in the northern Dominican Republic. Part 8. The family Muricidae (Mollusca: Gastropoda). Bulletins of American Paleontology 97(332):5–94.

VOKES, E. H. 1998. Neogene paleontology in the northern Dominican Republic. Part 18. The superfamily Volutacea (in part) (Mollusca: Gastropoda). Bulletins of American Paleontology 113(354):5–54.

WOODRING, W. P. 1966. The Panama land bridge as a sea barrier. Proceedings of the American Philosophical Society 110:425–433.

The Veliger 51(3):137–144 (November 16, 2012)

THE VELIGER

The Mucus of the Mollusk *Phyllocaulis boraceiensis*: Biochemical Profile and the Search for Microbiological Activity

A. R. TOLEDO-PIZA

Malacology Laboratory, Butantan Institute, Avenida Vital Brazil, 1500, São Paulo, Brazil

I. LEBRUN

Biochemistry and Biophysics Laboratory, Butantan Institute, Avenida Vital Brazil, 1500, São Paulo, Brazil

M. R. FRANZOLIN

Bacteriology Laboratory, Butantan Institute, Avenida Vital Brazil, 1500, São Paulo, Brazil

E. NAKANO

Malacology Laboratory, Butantan Institute, Avenida Vital Brazil, 1500, São Paulo, Brazil

O. A. SANT'ANNA

Immunochemistry Laboratory, Butantan Institute, Avenida Vital Brazil, 1500, São Paulo, Brazil

AND

T. KAWANO*

Malacology Laboratory, Butantan Institute, Avenida Vital Brazil, 1500, São Paulo, Brazil

Abstract. Many invertebrates, including the mollusks, have been researched as potential source of compounds with antibiotic activity. Biochemical profile of the mucus from the slug *Phyllocaulis boraceiensis* was studied to determine if this species presents any fraction containing this sort of compound. Assays to quantify lipids, proteins, or peptides, free glucose or associated with other substances, were performed through establishment of the electrophoretic profile, high-performance liquid chromatography (HPLC), and mass spectrometry. The data were: lipids = 6.9×10^{-5} mg/mL; protein = 1.15×10^{-4} mg/mL; few amino acids were detected, probably because the molecules degraded; free glucose = not detected; glucose in association with other substance = 600 µg/mL. In the HPLC assay, some bands of protein were detected correlating with the electrophoretic profile. The mass spectrometry showed a major proteic component of 17.5 kDa molecular weight. Any direct bactericidal or bacteriostatic effect was detected facing distinct bacteria of medical interest such as *Escherichia coli* and *Staphylococcus aureus*. It could be hypothesized that eventual active compounds are masked in the mucosal matrix of the secretion. Probably the *P. boraceiensis* mucus acts as a physical barrier, hindering the entrance of microorganisms in the body, does not act on the microorganisms assayed—or even does not present microbicidal property.

INTRODUCTION

Natural products have been historically a source of therapeutic drugs, and >30 biologically active compounds have been collected from a variety of quite distinct marine species (Shen et al., 2000), including some peptides released by mollusks of the genus *Conus* Linnaeus 1758 as defense against predators. A peptide isolated from *Conus magus* Linnaeus 1758 secretion was efficient to control pain in terminal phase of HIV-infected individuals and in cancer patients (Stix, 2005).

In the advent of new infectious diseases, as for previous ones that develop significant resistance to the current available antibiotics, many authors are working with an enormous variety of animal species of which active molecules may reveal microbicidal properties.

Terrestrial gastropods, such as snails and slugs, produce a complex mixture of components in the body

*Corresponding author: T. Kawano: tkawano@usp.br.

mucus (Deyrup-Olsen & Martin, 1982). These fluid secretions are produced by skin gland cells located in the back pedal region (Ruppert & Barnes, 1996), whose functions are to prevent desiccation (Deyrup-Olsen et al., 1983), reduce friction in locomotion (Denny, 1989), and protect the body against mechanical injuries or noxious substances (Triebskorn & Ebert, 1989).

Mucus was composed of mucopolysaccharides that are heteropolysaccharides frequently composed of two monosaccharide units, where at least one present is an acid group, carboxylic or sulfuric. The negatively charged molecules are water soluble, forming a viscous solution that could be added to a protein, producing substances similar to gelatin, which are mucoproteins or mucins. There are variations in the chemical composition of mucins and mucopolysaccharides among the mollusk species. The presence of sulfate acid group could be one of characteristics of the mollusk's mucopolysaccharide, in contrast to the viscous secretion of vertebrates with acid characteristic by reason of sialic acid residue (Livingstone & Zwaan, 1983).

In spite of quite fragile structure and humid skin, mollusks are fairly resistant to infections by microorganisms, suggesting the presence of some bactericidal factor(s) in the mucus (Iguchi et al., 1982). The same authors also described bactericidal activity expressed by the *Achatina fulica* (Férussac, 1821) mucus as in gram-positive (*Bacillus subtilis* and *Staphylococcus aureus*) as in gram-negative bacteria (*Escherichia coli* and *Pseudomonas aeruginosa*). Meanwhile, a lectin isolated from *A. fulica* mucus was not responsible for antibacterial activity when used in a crude form (Iguchi et al., 1982). A glycoprotein named achacin extracted from *A. fulica* mucus presented an antibacterial action in gram-positive and gram-negative bacteria but only in growing-phase colonies (Otsuka-Fuchino, 1992). This protein is also produced by the yeast *Pichia pastoris*, and presents an antibacterial action with large spectra; this effect occurred also with recombined achacin, which inhibited growth of various bacteria species (Ogawa, 1999).

The mucus released by the slugs *Phyllocaulis boraceiensis* (Thomé, 1972) was analyzed for its potential bactericidal activity on *Staphylococcus aureus*, *Pseudomonas aeruginosa*, and *Escherichia coli* cultures being supported by the characterization of its biochemical profile.

MATERIAL AND METHODS

Collection and Preparation of the Mucus

Thirty specimens of *P. boraceiensis* were collected in Taboão da Serra (SP, Brazil) and were used in the experiments for 3 yr. Mucus was obtained by stimulating pedal tissues of the slug without damage as described previously by Pakarinen (1994). Each mucus sample was obtained from four specimens, which were maintained freely moving on a glass plate with saline solution (NaCl: 0.06%) during 5 min. The secretion was collected using a spatula and stored in plastic tubes at −80°C. To perform the experiments, mucus was solubilized using acetonitrile (1:3) and the extracted sample was lyophilized.

Sodium Dodecyl Sulfate–Polyacrylamide Gel Electrophoresis (SDS-PAGE)

Electrophoresis of the lyophilized mucus was carried out as proposed by Laemmli's methods (Laemmli, 1970) using 12.5% SDS-PAGE. The molecular markers used vary between 36 and 205 kDa. Protein bands are visualized by silver staining.

High-Performance Liquid Chromatography (HPLC)

A sample of *P. boraceiensis* mucus was extracted with acetonitrile and subjected to HPLC in a C_{18} reversed-phase column (4.6 × 250 nm, Beckman 5-µL Ultrasphere ODS) connected to a chromatography system (HP series 1100) apparatus. The gradient was developed from 5 to 90% (in 50 min) solvent A (water + trifluoroacetic acid 0.1%) and solvent B (acetonitrile 90% + 10% solvent A) after initial profile peaks were purified. The main peaks were isolated, stored at −20°C, and assessed.

Microbiological Activity from the Mucus of *P. boraceiensis*

The strains of *Escherichia coli* ATCC 25922, *Pseudomonas aeruginosa* ATCC 27853, and *Staphylococcus aureus* ATCC 25923 were stored at −80°C in tryptic soy broth (TSB) supplemented with 20% glycerol at the Bacteriology Laboratory, Butantan Institute. Bacteria were cultivated in TSB at 37°C (Koneman et al., 1997). After 16 to 18 h of incubation, precultures were diluted in physiologic saline (NaCl 0.85%) to 1–2 × 10^8 cells/mL (0.5 McFarland) and spread on the medium with sterile swabs. A filter (Whatman No. 541) paper disc embedded in 10 µL of each test solution (peak 1 and 2, and pool 7 isolated from chromatography system, lyophilized and solubilized in sterile saline—NaCl, 0.06%—pure and in a new sample processed and diluted at the concentrations of 10, 50, 100, and 500 µg/mL and crude mucus) was laid on the plate. After incubation at 37°C and at room temperature during 24–72 h, plates were observed for the presence or absence of growth inhibition.

In order to analyze the bactericidal activity of the crude mucus (with and without ultraviolet treatment),

in which 10 mL of crude mucus was added to 30 mL of saline solution (NaCl 0.06%) and exposed to ultraviolet light for 40 min for sterilization at room temperature and at 37°C, *Pseudomonas aeruginosa* ATCC 27853, a microorganism commonly found in the environment, was used. Bacterial strain was cultivated in TSB at 37°C at 180 rpm for 3 hr. A microbial suspension was made in physiologic saline (0.85%) equivalent to 1–2 × 10^8 cells/mL (0.5 McFarland) and diluted to 1–2 × 10^2 cells/mL. This bacterial suspension was spread in plates with tryptic soy agar (TSA) with a sterile swab. Crude mucus was inoculated in precultivated plates and was incubated at 37°C and at room temperature during 24–72 hr. The plates were observed for presence or absence of growth inhibition.

Positive and negative controls were done, keeping the plates and the tubes with and without inoculum, for the same periods and under identical incubation conditions. The growth control of bacteria was made in TSA plates and TSB tubes. The sterility test of the samples (with and without ultraviolet treatment) was made in thioglycollate broth.

Protein Determination

Protein concentration was determined by Bradford's method (Bradford, 1976) using bovine serum albumin as standard (Bio-Rad Co.). Ten samples of crude mucus were analyzed (100 µL in each one) and the results were captured in a spectrophotometer (Pharmacia Ultrospesc 2000) with adjusted wavelength to 595 and 280 nm. A standard curve was produced (not shown).

Lipid Determination

Lipid concentration in each sample was determined using Chabrol & Charonaat method as proposed by Collet & Etienne (1965) with some modifications. Ten samples of crude mucus were analyzed, and 50 µL of each one were used and the results captured in a spectrophotometer (Pharmacia Ultrospesc 2000) with adjusted wavelength to 530 nm. A standard curve was produced (not shown).

Peptide Determination

Peptide concentrations were determined through the total hydrolysis of the mucus with 6.0 M HCl at 110°C for 24 hr and then removed by vacuum. Amino acids were derivatized with phenyl-isothiocyanate (Merck) and identified by chromatography using HPLC equipment from HP Series 1100 (column 4.6 × 25 cm, Bèckman 5-µL Ultrasphere ODS-PTH). The comparison was made using a standard solution with the concentration as described previously by Heinrikson & Meredith (1984).

Free Glucose Determination

Free glucose in the sample was determined as proposed by Lima et al. (1977). Twelve microliters of each one of 10 samples of crude mucus were analyzed. The absorbance was captured in a spectrophotometer (Pharmacia Ultrospesc 2000) with adjusted wavelength to 625 nm. A standard curve was produced (not shown).

Glucose Associated with Other Substances Determination

Glucose associated with other substances was determined as proposed by Chaplin & Kennedy (1994). Four samples of crude mucus were analyzed. The absorbance was captured in a spectrophotometer (Pharmacia Ultrospesc 2000) with adjusted wavelength to 490 nm. A standard curve was produced (not shown).

Mass Spectrometric Analyses

Molecular mass analyses of mucus were performed on a MALDI-TOF mass spectrometry on an Ettan MALDI-TOF/Pro system (Amersham Biosciences, Sweden), using a-cyano-4-hydroxycinnamic acid as matrix.

RESULTS

To extract possible active compounds of mucus and prepare a homogenized solution, several solvents were assayed: saline solution (NaCl) 1 M; ethyl alcohol (C_2H_5OH); dimethyl sulfoxide (C_2H_6OS) 20%; and acetonitrile (C_2H_3N). No alteration was observed when mucus was added to the saline solution or ethyl alcohol; when dimethyl sulfoxide was added, fragmentation occurred but without homogenization. When acetonitrile was added, the result was satisfactory: mucus was homogeneous with 30% of yield and a little residue was discarded. Acetonitrile was used as a good solvent being easily removed by lyophilization. This solution was subjected to overnight agitation in the proportion of 1:3 (mucus:acetonitrile) under 8°C and lyophilized.

Twelve microliters of five samples of crude mucus were subjected to SDS-PAGE analysis under 110°C for 15 min (Figure 1), showing an amount of proteins in the mucus.

With lyophilized extracted mucus, 250 µL was solubilized in Milli-Q water to obtain chromatographic profile (Figure 2) using HPLC equipment. Four peaks and three pools were separated. A small amount of

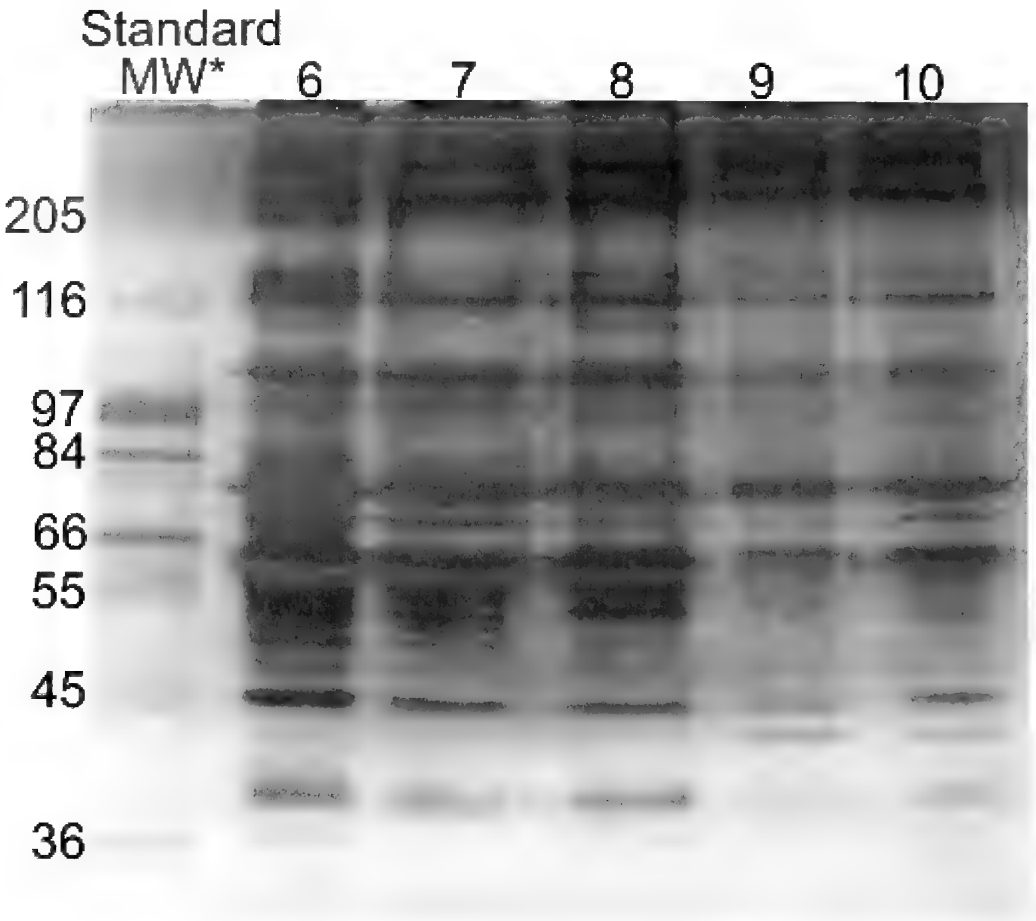

Figure 1. The SDS-PAGE analysis of five crude mucus samples of *P. boraceiensis* using acrylamide (12.5%). Protein bands were stained with silver nitrate.

peaks 1 and 2 and pool 7 were used by microbiological assays.

After 24 hr of incubation, microbial growing was similar to the control plates in both situations. The control for the crude mucus was performed to certify the samples' quality, and *Escherichia coli* and *Bacillus* sp. grew after incubation. The samples isolated from chromatography did not present contamination; there was also no difference between samples incubated at room temperature and/or at 37°C in all experiments realized.

The protein determination performed by Bradford (1976) methods with 10 samples of crude mucus showed an average concentration of 1.15×10^{-4} mg/mL, SE of 0.591×10^{-4} mg/mL, and standard deflection $\pm 1.87 \times 10^{-3}$ g/mL when subjected to spectrophotometer with adjusted wavelength to 595 nm. However, when subjected to spectrophotometer with adjusted wavelength to 280 nm, the average concentration was 0.404×10^{-3} mg/mL, SE of 0.649×10^{-5} mg/mL, and standard deflection $\pm 0.2052 \times 10^{-3}$ g/mL. Only proteic trace was detected in both.

Lipid determination of 10 samples of crude mucus showed an average concentration of 6.9×10^{-5} mg/mL, SE of 4.39×10^{-5} mg/mL, and standard deflection $\pm 1.39 \times 10^{-5}$ mg/mL.

Three samples (2, 3, and 4), from the same 10 samples used before, were subjected to an amino acid determination with no hydrolyzed mucus; no amino acid residue was detected, only a small quantity of glycosides. When the analyses were performed with five hydrolyzed samples (6, 7, 8, 9, and 10), the substance showed to be a peptidic–proteic compound whose average composition is shown in Table 1. Samples 8 and 9 were excluded because of the extreme values.

The data obtained with free glucose determination were negative. However, the data obtained from four samples subjected to glucose associated with other substances determination shows a large amount of glucose, 600 µg/mL.

The mass spectrometry (Figure 3) showed four molecular ions, the biggest peak with molecular weight of 17.5 kDa and other peaks of 8.695, 35.229, and 6.512 kDa.

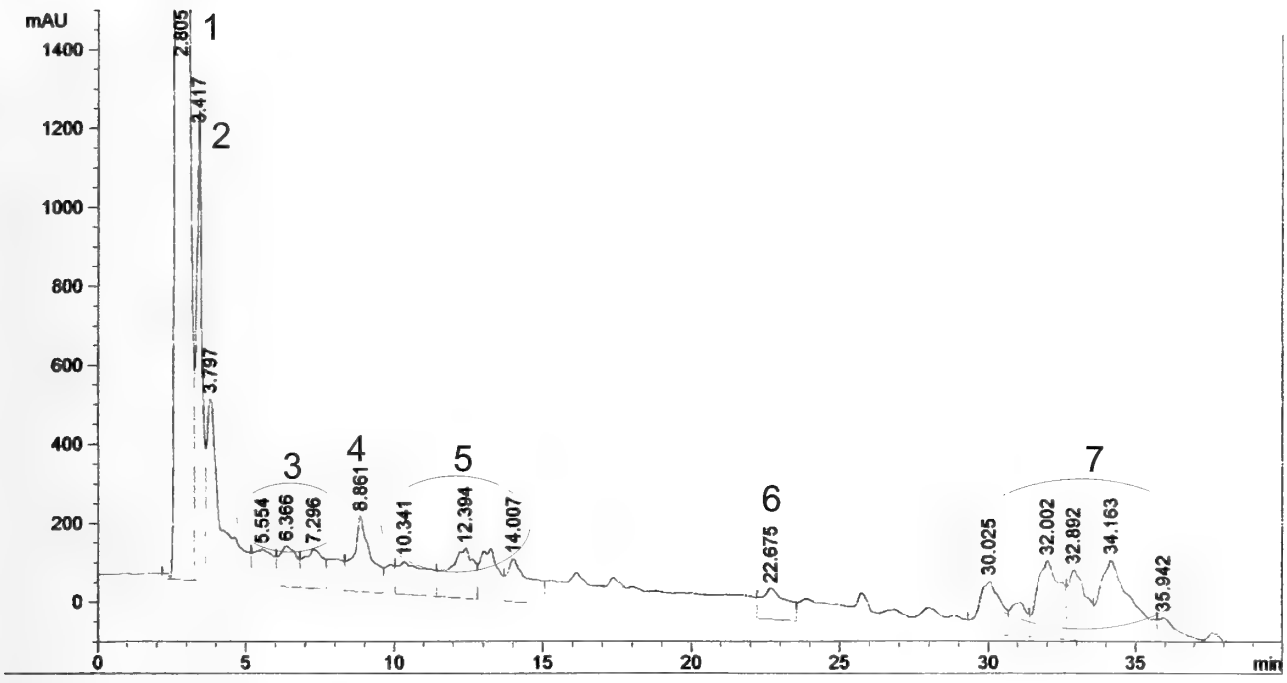

Figure 2. Chromatographic profile of lyophilized *P. boraceiensis* mucus using HPLC equipment with linear gradient varying between 5 and 90%, identifying the peaks (1, 2, 4, and 6) and "pools" (3, 5, and 7).

DISCUSSION

At first it was tried to apply crude mucus in plates with *Escherichia coli* and *Staphylococcus aureus* culture, but no mucus diffusion was observed in the agar. So, to avoid a false-negative result, a method to dissolve mucus was standardized without losing its characteristics.

Twelve microliters of five samples of crude mucus were subjected to 12.5% SDS-PAGE analysis under 110 mV during 90 min, showing a great number of protein bands, ranging from 34 to 300 kDa of molecular weight. The amount and variety of bands observed were greater than those observed by other authors. Quantification of possible bioactive compounds isolated from *Aplysia dactylomela* (Rang, 1828) mucus showed predominant molecular mass of 66 and <20.1 kDa; however, between 18.0 and 36 kDa were not observed (Melo et al., 1998); also, a fraction of it, named dactylomelin-P, was isolated with molecular weight of 60 kDa (Melo et al., 2000). *Achatina fulica* mucus shows a band from 70 to 80 kDa (Kubota et al., 1985) and *Aplysia californica* (Cooper, 1863) shows a unique band of 60 kDa (Yang et al., 2005). The bands obtained after SDS-PAGE reveal some similar pattern, suggesting the presence of related compounds.

Bradford's method (Bradford, 1976) allowed detection of proteic concentration of around 1.15×10^{-4} mg/mL, SE 0.591×10^{-4} mg/mL, and standard deflection $\pm 1.87 \times 10^{-3}$ mg/mL when the spectrophotometer was adjusted with wavelength to 595 nm. This substance expresses some particular characteristics such as a mucosal matrix, suggesting that some molecules can be masked. Other protein determination was performed using the same method but now with spectrophotometer adjusted with wavelength to 280 nm and the concentration was 4.04×10^{-4} mg/mL, SE 0.649×10^{-5} mg/mL, and standard deflection $\pm 0.2052 \times 10^{-3}$ mg/mL. In both methods, protein quantity was low compared to the results obtained from electrophoresis after staining that showed a large amount of proteic bands when compared to the intensity of the staining of standard. Probably, both methods of protein determination were inefficient to determine proteins in this sort of substance, possibly because glucose presence in the "core" of molecules. Lipid determination in crude mucus showed an average concentration of 6.9×10^{-5} mg/mL; this low value suggests that there is only residual lipid. The high amount of glucose associated with other substances could interfere in the microbicidal activity of the mucus, acting as a nutrient in the growing medium to the bacteria used.

The peptides determination with no hydrolyzed mucus did not detect free amino acid residues, only a small quantity of glycosides, probably a product from mucosal matrix. However, when a hydrolyzed sample was used, residues of all amino acids were detected. There was a good relationship between amino acid concentration and intensity of bands in the electrophoresis.

Table 1

Peptide concentration of *P. boraceiensis* crude mucus.

	Sample no.					
Amino acid	6 (mM/mL)	7 (mM/mL)	8 (mM/mL)	9 (mM/mL)	10 (mM/mL)	Average (mM/mL)
Asx	0.675	0.357	0.126	7.872	0.357	0.463
Glx	0.522	0.279	0.108	1.325	0.279	0.360
Ser	2.865	0.449	0.234	4.076	0.449	1.254
Gli	2.551	0.719	0.386	2.185	0.719	1.330
His	2.036	1.219	0.409	4.391	1.219	1.491
Ala	1.495	0.627	0.719	1.024	0.627	0.916
Treo	0.955	1.491	0.788	1.711	1.491	1.312
Arg	0.355	0.211	0.062	0.559	0.211	0.259
Pro	4.162	6.988	5.225	5.393	6.988	6.046
Tir	1.259	0.641	0.279	1.219	0.641	0.847
Val	0.707	0.766	0.278	1.750	0.563	0.679
Met	0.500	0.861	0.204	3.020	0.771	0.711
½ Cys	2.262	1.413	0.275	5.161	1.413	1.696
Iso	0.978	0.487	0.137	2.383	0.487	0.650
Leu	0.958	0.634	0.160	1.964	0.634	0.742
Fen	5.247	0.952	0.287	4.143	0.952	2.384
Lis	0	0.333	0.092	0.101	0	0.333

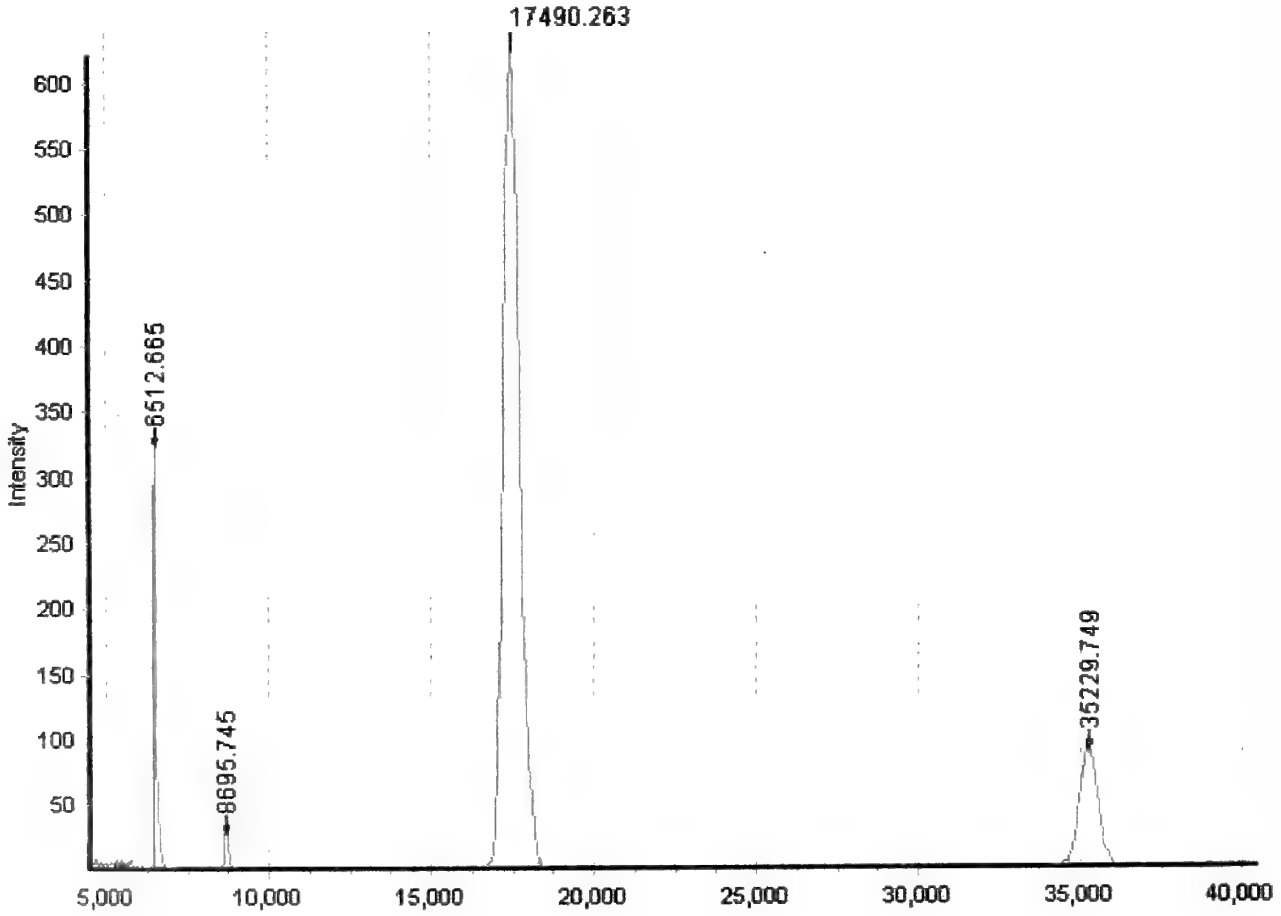

Figure 3. Mass spectrometry profile of *P. boraceiensis* mucus.

Mass spectrometry exhibited four molecular ions, the greatest peak with molecular weight of 17.5 kDa and others of 8.695, 35.229, and 6.512 kDa. Low ones after chromatography and various bands obtained by electrophoresis suggest the presence of polymeric shapes of the compounds in the mass spectra: a monomer is 8.695 kDa, while the most abundant is the 17.5 kDa, probably a dimer of 35.229 kDa, and a monomer fragment with 6.512 kDa. In the electrophoresis system, protein bands up to 300 kDa were detected, also suggesting stable aggregates formation. It was impossible to separate these aggregates with SDS and β-mercaptoethanol, and probably they could interfere in the microbiological results.

Using those fractions isolated by chromatography from the crude mucus, several microbiological experiments were carried out with distinct concentrations of lyophilized mucus facing both gram-positive and gram-negative bacteria species. Control colonies were performed to certify the crude samples' quality; *Escherichia coli*, *Staphylococcus aureus*, and *Pseudomonas aeruginosa* grew normally after incubation. The samples isolated from chromatography did not present contamination. The lyophilized mucus was incapable of avoiding bacterial growth, and these data were quite different from those of Melo et al. (1998) that reduced by 40% *Pseudomonas aeruginosa* growth when exposed to *Aplysia dactylomela* mucus as well as those from Iguchi et al. (1982), who observed an expressive rising reduction of *Staphylococcus aureus*, *Bacillus subtillis*, *Escherichia coli*, and *Pseudomonas aeruginosa* colonies when exposed to *Achatina fulica* mucus. All lyophilized mucus was subjected to homogenization using acetonitrile, a toxic solvent that could be responsible for inactivation of possible active molecules in the mucus. So, to discard this hypothesis, new experiments were made using crude mucus; the same results were observed.

In body secretion of *Dolabella auricularia* (Lightfoot, 1786), a microbicidal compound named dolabellanin B2 was found, which showed a growth inhibition in 12 different microorganisms, including *Staphylococcus aureus* and *Escherichia coli* (Iijima et al., 1995). Growth inhibition of *Staphylococcus aureus*, *Pseudomonas aeruginosa*, and *Proteus vulgaris* was observed in crude samples of *Aplysia dactylomela* mucus as well as in the dialyzed sample (Melo et al., 1998). Dactylomelin-P, a protein extracted from *Aplysia dactylomela* mucus, was able to express bactericidal action when applied to *Staphylococcus aureus* colonies (Melo et al., 2000). When *Aplysia californica* mucus was applied to *Escherichia coli*, *Pseudomonas aeruginosa*, *Salmonella typhimurium*, *Vibrio harveyi*, *Bacillus subtilis*, *Streptococcus pyogenes*, and *Staphylococcus aureus* colonies, growth inhibition was observed (Yang et al., 2005). *Phyllocaulis boraceiensis* mucus does not confirm these results when applied as microbicidal agent.

Possible bioactive compounds originating in *P. boraceiensis* mucus could be labile and lose its characteristics as soon as being exuded; or the incubation temperature for the bacteriological analyses could contribute to this inactivation. In order to solve these questions, an experiment was performed using *Pseudomonas aeruginosa*, a microorganism commonly isolated from the environment also able to develop in varied temperatures. Assuming the plasticity of molecule expression by invertebrates, a prespread plate was exposed to crude mucus immediately after its collection and incubated during 24 hr at room temperature and another plate at 37°C, but the same results were obtained. Thus, it is possible to infer that *Phyllocaulis boraceiensis* mucus acts basically as a physical barrier, hindering the entrance of microorganisms in the body. Nevertheless, bioactive molecules could still be concealed in mucosal matrix, which could not be removed efficiently.

Acknowledgments. FAPESP and CAPES for the financial support. Center for Applied Toxinology (CAT/CEPID) is gratefully acknowledged.

LITERATURE CITED

BRADFORD, M. M. 1976. A rapid and sensitive method for the quantitation of microgram quantities of proteins utilizing the principle of protein-dye binding. Analytical Biochemistry 72:248–254,

CHAPLIN, M. F. & J. F. KENNEDY. 1994. Carbohydrate Analysis: A Practical Approach. 2nd ed. Oxford University Press: New York.

COLLET, J. & J. ETIENNE. 1965. Determination of serum lipids by the sulfo-phosphovanillic method of E. Chabrol and R. Charonnat. Bulletin de l'Academie Nationale de Medecine 149:331–338.

DENNY, M. W. 1989. Invertebrate mucous secretions: functional alternatives to vertebrate paradigms. Symposia of the Society for Experimental Biology 43:337–366.

DEYRUP-OLSEN, I. & A. W. MARTIN. 1982. Surface of exudation in terrestrial slugs. Comparative Biochemistry and Physiology 72C:45–51.

DEYRUP-OLSEN, I., D. L. LUCHTEL & A. W. MARTIN. 1983. Components of mucus of terrestrial slugs (Gastropoda). American Journal of Physiology 243:448–452.

HEINRIKSON, R. L. & S. C. MEREDITH. 1984. Amino acid analysis by reverse-phase high-performance liquid chromatography: precolumn derivatization with phenylisothiocyanate. Analytical Biochemistry 136:65–74.

IGUCHI, S. M. M., T. AIKAWA & J. MATSUMOTO. 1982. Antibacterial activity of snail mucus mucin. Comparative Biochemistry and Physiology 72A:571–574.

IIJIMA, R., J. KISUGI & M. YAMAZAKI. 1995. Antifungal activity of aplysianin E, a cytotoxic protein of sea hare (*Aplysia kurodai*) eggs. Developmental & Comparative Immunology 19:13–19.

KONEMAN, E. W., S. D. ALLEN, W. M. JANDA, P. C. SCHRECKENBERGER & W. C. WINN, JR. 1997. Diagnostic

Microbiology. Color Atlas and Textbook. 5th ed. Lippincott: Philadelphia.

KUBOTA, Y., Y. WATANABE, H. OTSUKA, T. TAMIYA, T. TSUCHIYA & J. J. MATSUMOTO. 1985. Purification and characterization of an antibacterial factor from snail mucus. Comparative Biochemistry and Physiology 82C: 345–348.

LAEMMLI, U. K. 1970. Cleavage of structural proteins during the assembly of the head of bacteriophage T4. Nature 227: 680–685.

LIMA, A. O., J. B. SOARES, J. B. GRECO, J. GALIZZI & J. R. CANÇADO. 1977. Métodos de Laboratório Aplicados à Clínica. 5th ed. Editora Guanabara Koogan: Rio de Janeiro.

LIVINGSTONE, D. R. & A. ZWAAN. 1983. Carbohydrate metabolism of gastropods. Pp 177–242 in K. M. Wilbur (ed.), The Mollusca—Metabolic Biochemistry and Molecular Biomechanics. Academic Press: London.

MELO, V. M. M., A. B. G. DUARTE, A. F. F. U. CARVALHO, E. A. SIEBRA & I. M. VASCONCELOS. 2000. Purification of a novel antibacterial and haemagglutinating protein from the purple gland of the sea hare, *Aplysia dactylomela* Rang, 1828. Toxicon 38:1415–1427.

MELO, V. M. M., A. M. FONSECA, I. M. VASCONCELOS & A. F. F. U. CARVALHO. 1998. Toxic, antimicrobial and hemagglutinating activities of the purple fluid of the sea hare *Aplysia dactylomela* Rang, 1828. Brazilian Journal of Medical and Biological Research 31:785–791.

OGAWA, M., S. NAKAMURA, T. ATSUCHI, T. TAMIYA, T. TSUCHIYA & S. NAKAI. 1999. Macromolecular antimicrobial glycoprotein, achacin, expressed in a methylotrophic yeast *Pichia pastoris*. FEBS Letters 448:41–44.

OTSUKA-FUCHINO, H., Y. WATANABE, C. HIRAKAWA, T. TAMIYA, J. J. MATSUMOTO & T. TSUCHIYA. 1992. Bactericidal action of a glycoprotein from the body surface mucus of giant African snail. Comparative Biochemistry and Physiology 101C:607–613.

PAKARINEN, E. 1994. The importance of mucus as a defence against carabic beetles by the slugs *Arion fasciatus* and *Deroceras reticulatum*. Journal of Molluscan Studies 60: 149–155.

RUPPERT, E. E. & R. D. BARNES. 1996. Zoologia dos Invertebrados. 6th ed. Editora Roca Ltda.: São Paulo.

SHEN, G. S., R. T. LAYER & R. T. MCCABE. 2000. Conopeptides: from deadly venoms to novel therapeutics. Drug Discovery Today 5(3):98–106.

STIX, G. 2005. Toxina contra a dor. Scientific American Brazil 38:80–85.

TRIEBSKORN, R. & D. EBERT. 1989. The importance of mucus production in slugs reaction to molluscicides and the impact of molluscicides on the mucus producing system. Pp. 373–378 in I. Henderson (ed.), Slugs and Snails in World Agriculture. Proceedings of British Crop Protection Council, 41, Guildford, April 1989. Lavenham Press Limited: Lavenham, U.K.

YANG, H., P. M. JOHNSON, K. C. KO, M. KAMIO, M. W. GERMANN, C. D. DERBY & P. C. TAI. 2005. Cloning, characterization and expression of scapin, a broadly antimicrobial FAD-containing L-amino acid oxidase from ink of the sea hare *Aplysia californica*. Journal of Experimental Biology 208:3609–3622.

The Veliger 51(3):145–164 (November 16, 2012)

THE VELIGER

Three New Species of Aeolid Nudibranchs (Opisthobranchia) from the Pacific Coast of Mexico, Panama, and the Indopacific, with a Redescription and Redesignation of a Fourth Species

SANDRA MILLEN

Department of Zoology, University of British Columbia, 6270 University Boulevard, Vancouver, BC, Canada V6T 1Z4
(e-mail: millen@zoology.ubc.ca)

AND

ALICIA HERMOSILLO

Universidad de Guadalajara, Centro Universitario de Ciencias Biológicas y Agropecuarias, Las Agujas, Zapopan, Jalisco, México
(e-mail: alicia_hg@prodigy.net.mx)

Abstract. Three new species of aeolid nudibranchs are described and another species is redescribed and redesignated based on specimens collected at several localities of the tropical eastern and Indopacific. *Dondice galaxiana* sp. nov. is a facelinid aeolid, distinct from other species for its light brown and cream colored body with four dark brown spots containing bright turquoise centers between each cluster of cerata and a few similar spots on the sides. The cerata are light brown or pinkish tan with white cnidosacs and a brown ring below the cnidosacs. They are in raised arch-shaped clusters. The mottled brown and cream oral tentacles are long, the short rhinophores have disk-shaped annulations, and the unarmed penis has a prominent penial gland. The generic placement of another facelinid species was problematic and was therefore assigned as a new genus, *Adfacelina* gen. nov. *Adfacelina medinai* sp. nov. has cerata in arches with multiple rows. The penis is blunt tipped, bearing one outer row of tiny conical spines and there is no accessory gland. The external coloration is pink with opaque yellow blotches covering the body, cerata, rhinophores, and oral tentacles. Our phylogenetic analysis suggests this genus is close to the genera *Dondice* and *Facelina*. *Phestilla hakunamatata* Ortea, Caballer & Espinoza, 2003, is redescribed and placed in the facelinid genus *Hermosita* because it has a cleioproctic anal position, a radula with slender denticles, two bursae, and a fleshy papilla beside the penis. Both the familial and generic placement of the fourth species was problematic. It has the external appearance and notal flange of a flabellinid and the anus is acleioproctic. Internally it has a unidentate radula and the penis is armed with a chitinous spine. External coloration of *Unidentia angelvaldesi* sp. nov. varies with diet from orange shades or white with a series of purple lines and opaque white markings on the body, rhinophores, cerata, and oral tentacles. A phylogenetic analysis suggests that this species should be placed in a new genus, *Unidentia* gen. nov., and that this genus is more closely allied to other uniseriate, acleioproctic aeolids of the genus *Piseinotecus* than members of the family Facelinidae.

Resumen. Se describen tres especies nuevas de nudibranquios aeólidos, una especie más es redescrita y su asignación genérica cambiada con base en especimenes colectados en localidades del Pacífico oriental y el Indopacífico. *Dondice galaxiana* sp. nov. es un aeólido facelinido distinto de otras especies por su coloración café claro y crema con cuatro puntos café oscuro con centros azul turquesa entre cada grupo de ceratas y algunos puntos similares en los laterales. Los ceratas son café claro o rosado con cnidosacos blancos y un anillo café proximal a los cnidosacos. Los ceratas se encuentran en grupos elevados en forma de arco. Los tentáculos orales son largos y moteados de color café y crema; los rinóforos son cortos con anulaciones en forma de discos, la glándula penial es prominente, y el pene no está armado. La asignación genérica de otro facelinido fue problemática por lo que se asignó al género nuevo, *Adfacelina* gen. nov. *Adfacelina medinai* sp. nov. tiene ceratas en arcos de filas múltiples. La punta del pene es chata, con una línea externa de espinas cónicas diminutas sin glándula accesoria. La coloración externa es rosa con manchones amarillo opaco cubriendo completamente ceratas, rinóforos, y tentáculos orales. Nuestro análisis filogenético sugiere que el género es cercano a los géneros *Dondice* y *Facelina*. *Phestilla hakunamatata* Ortea, Caballer y Espinoza, 2003, es redescrita y asignada en el género de facelinido *Hermosita* por tener el ano en posición cleiopróctica, rádula con dentículos delgados, dos bursas, y una papilla carnosa a un lado del

pene. Tanto la asignación genérica como de familia de la cuarta especie fue problemática. Tiene la apariencia externa y falange notal de un flabelinido, el ano siendo acleiopróctico. Internamente tiene rádula uniserrada y el pene armado con una espina quitinosa. La coloración externa de *Unidentia angelvaldesi* sp. nov. varía según su alimentación de tonos anaranjados a blanco con una serie de líneas moradas y patrones de blanco opaco en el cuerpo, rinóforos, cerata, y tentáculos orales. El análisis filogenético sugiere que esta especie debería ser asignada a un género nuevo, *Unidentia* gen. nov. y que este género se encuentra más cercanamente relacionado a los aeólidos acleiopróctico, uniserrados del género *Piseinotecus* que los miembros de la familia Facelinidae.

INTRODUCTION

A survey was undertaken by the junior author of the opisthobranch mollusks of Bahía de Banderas, on the Pacific coast of Mexico. Results indicated 20 range extensions (Hermosillo-González, 2003) and a total of 96 species. Several of these species were undescribed, and additional species have since been added by Hermosillo & Behrens (2005) to a current total of 141 reported by Hermosillo-González (2006). Some ranges were extended further south as a result of a visit to Panama (Hermosillo, 2004; Hermosillo & Camacho-García, 2006).

Subsequent descriptions by Angulo-Campillo & Valdés (2003), Ortea et al. (2003), Hermosillo & Valdés (2004), Gosliner & Bertsch (2004), Dayrat (2005), Hermosillo & Valdés (2007a, b), and Millen & Hermosillo (2007) have added 13 new species. Photographs of these and several, as yet undescribed, species can be found in three recent books: Behrens & Hermosillo (2005), Camacho-García et al. (2005), and Hermosillo et al. (2006). This paper describes three additional aeolid nudibranch species and redescribes and reassigns the genus of *Phestilla hakunamatata* Ortea, Caballer & Espinosa, 2003 to the genus *Hermosita* Gosliner & Behrens, 1986.

The four species in this paper have a uniseriate radula and a jaw with one row of denticles on the masticatory margin. Three of the species have the anus in the cleioproctic position (among the posterior cerata) and belong in the family Facelinidae Bergh, 1890. The other species has its anus in the interhepatic area, in an acleioproctic position, an anterior notal brim, and well-developed ramified oral glands, all features that are not found in the Facelinidae. It has been placed in the family Unidentidae fam. nov. and assigned a new genus, *Unidentia* gen. nov.

MATERIALS AND METHODS

Collection and observations were conducted by scuba diving and intertidally. The material examined is deposited at the Department of Invertebrate Zoology and Geology of the California Academy of Sciences, San Francisco (CASIZ), the Malacology Section of the Natural History Museum of Los Angeles County (LACM), and the Museum of Zoology of the University of Costa Rica (MZUCR-INB).

Specimens were relaxed in a 7% magnesium chloride solution in freezing seawater and preserved in 70% ethanol. Specimens were dissected by a right lateral incision from back to front just above the foot, and the internal features were examined and drawn using a dissecting microscope with a camera lucida. The buccal mass was removed and placed in 10% sodium hydroxide until the radula and jaws were isolated from the surrounding tissue. The radula and jaws were then rinsed in water, dried, and mounted for examination. Scanning electron micrographs were made with a Hitachi S-4700FE scanning electron microscope.

Features of living animals were recorded in the field by digital photography, both *in situ* and in aquarium photographs with a Nikon Coolpix 995 camera. For underwater photography, a YS-90 Sea and Sea and an INON slave strobe were used, with white balance set on daylight. For aquarium photographs, only the INON slave strobe was used with the same white balance setting. No color correction was used.

SPECIES DESCRIPTIONS

Family FACELINIDAE Bergh, 1890

Genus *Dondice* Marcus, Er. 1958

Dondice galaxiana Millen & Hermosillo, sp. nov.

(Figures 1A, F, 2, 3)

Material: Holotype: CASIZ 176810, 7 mm long, Puerto Vallarta, Noche Iguana, Bahía de Banderas, 28 April 2002, at 15 m depth on a rock wall. Collected by S. Millen. **Paratypes:** LACM 3042, 5 mm long, Mismaloya, Bahía de Banderas, 8 March 2004, at 17 m depth. LACM 194198, 5 mm long, Île Clipperton, 19 April 2007, at 70–90 m depth on a coral detritus slope. Collected by Jeff Bozanic. MZUCR-INB0001496600, 1 specimen, 4 mm long, Roca la Viuda, Puntarenas, Costa Rica, 26 January 1998, at 7–10 m depth. Collected by A. Berrocal. **Other material:** 2 specimens, 6 and 5 mm, dissected, collected with the holotype. 1 specimen, 4 mm, Mismaloya, Bahía de Banderas, 13 June 2004. 1 specimen, 7.5 mm, Mismaloya, Bahía de Banderas, 26 May 2004.

Etymology: The specific name of this species, *galaxiana*, is given because of its otherworldly appearance.

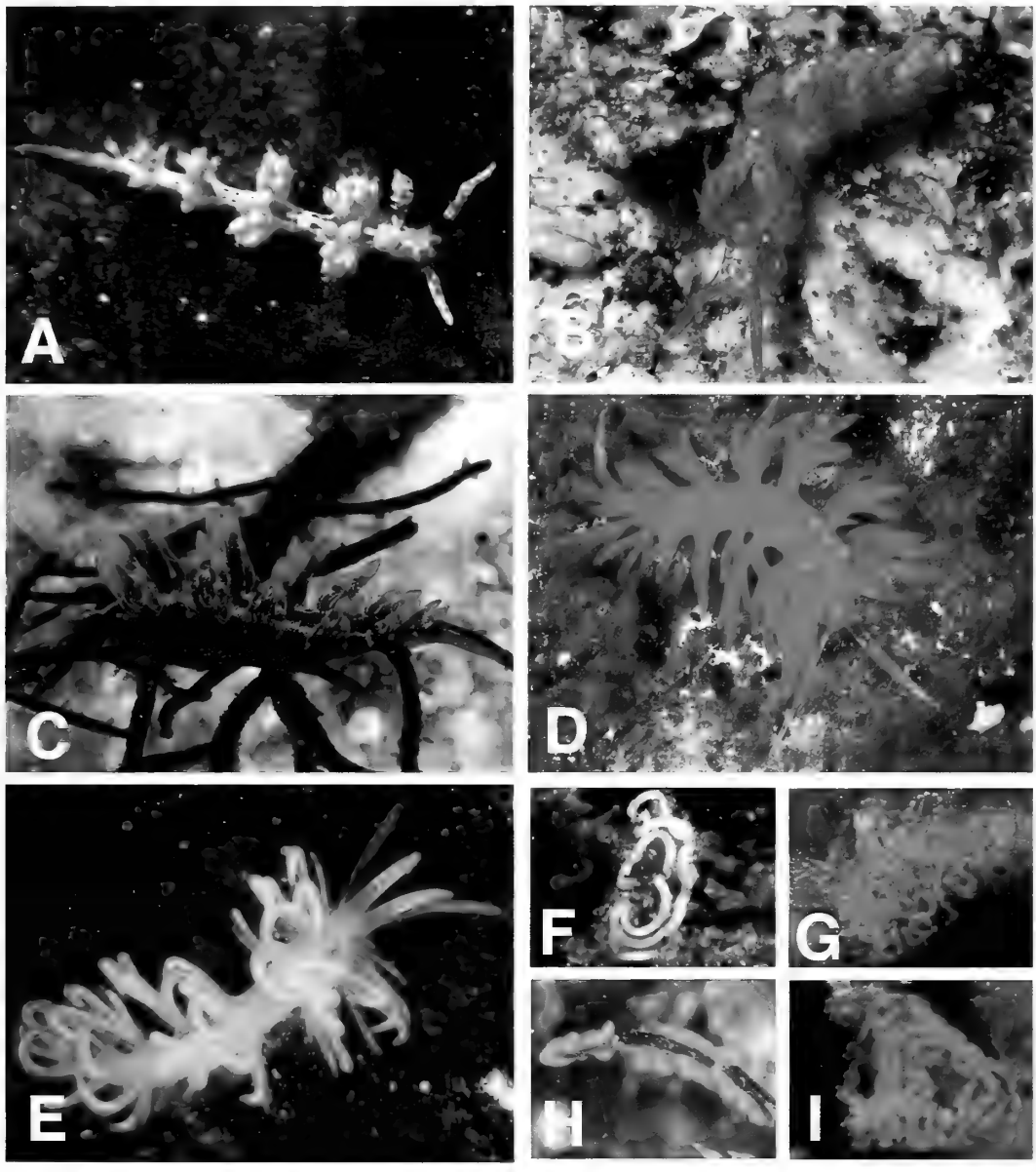

Figure 1. Photographs of living aeolids taken in the field: **A**, *Dondice galaxiana* sp. nov., 8 mm long, Bahía de Banderas, Mexico; **B**, *Adfacelina medinai*, 11 mm long, specimen (CASIZ 175779) from Bahía de Banderas, Mexico; **C**, *Hermosita hakunamatata* from Bahía de Banderas, Mexico; **D**, *Unidentia angelvaldesi*, dark variation (CASIZ 176809), specimen from Bahía de Banderas, Mexico; **E**, *Unidentia angelvaldesi*, pale variation, specimen from Tulamben, Bali; **F**, Spawn of *D. galaxiana*; **G**, Spawn of *A. medinai*; **H**, Spawn of *H. hakunamatata*; **I**, Spawn of *U. angelvaldesi*, dark variation.

External morphology: This aeolid reaches up to 7.5 mm in preserved length. Living size: 8 mm, 1 mm wide, and 1.25 mm high (Figures 1A, 2A). The body is slender, with laterally bulging areas at the clusters of cerata. The rhinophores are short, ending with a cylindrical tip. There are usually 6 or 7 (4–8) large dish-shaped annulations, continuous anteriorly, widest laterally and notched posteriorly. The oral tentacles are slightly longer than the rhinophores, cylindrical and slender. They originate dorsal to the oral surface. The cerata are arranged in tight horseshoe-shaped clusters on raised cushions. The anterior-most two have up to 20 cerata in alternating double rows, whereas the other arches have one row of cerata. There is one precardiac cluster and two to three posterior ones plus a row of 2–3 cerata. The cerata are slender and cylindrical, up to 3 mm in length, with long pointed cnidosacs and granular cores (Figure 2B). The head is oval, slightly

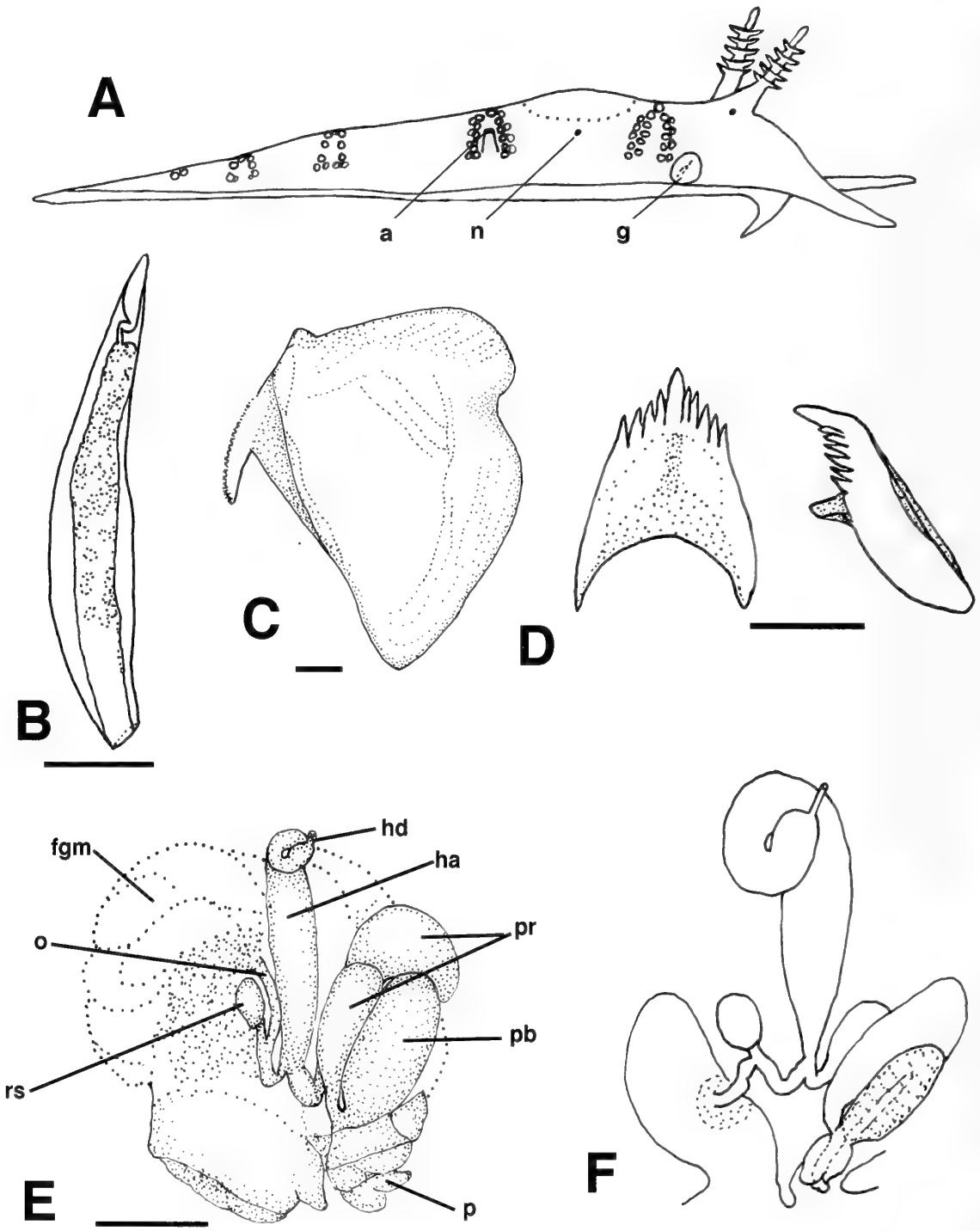

Figure 2. *Dondice galaxiana* sp. nov. from Bahía de Banderas, Mexico: **A**, Right lateral view showing position of ceratal insertions, stylized drawing; **B**, Ceras; **C**, One jaw; **D**, Radular tooth; **E**, Camera lucida drawing of the reproductive system; **F**, Stylized drawing of the reproductive system. Abbreviations: **a**, anus; **fmg**, female gland mass; **g**, genital apertures; **ha**, hermaphroditic ampulla; **hd**, hermaphroditic duct; **n**, nephroproct opening; **o**, oviduct; **p**, penis; **pb**, penial bulb; **pr**, prostate; **rs**, receptaculum seminis. Scale bars: B = 0.5 mm; C = 0.1 mm; D = 50 μm; E = 0.5 mm.

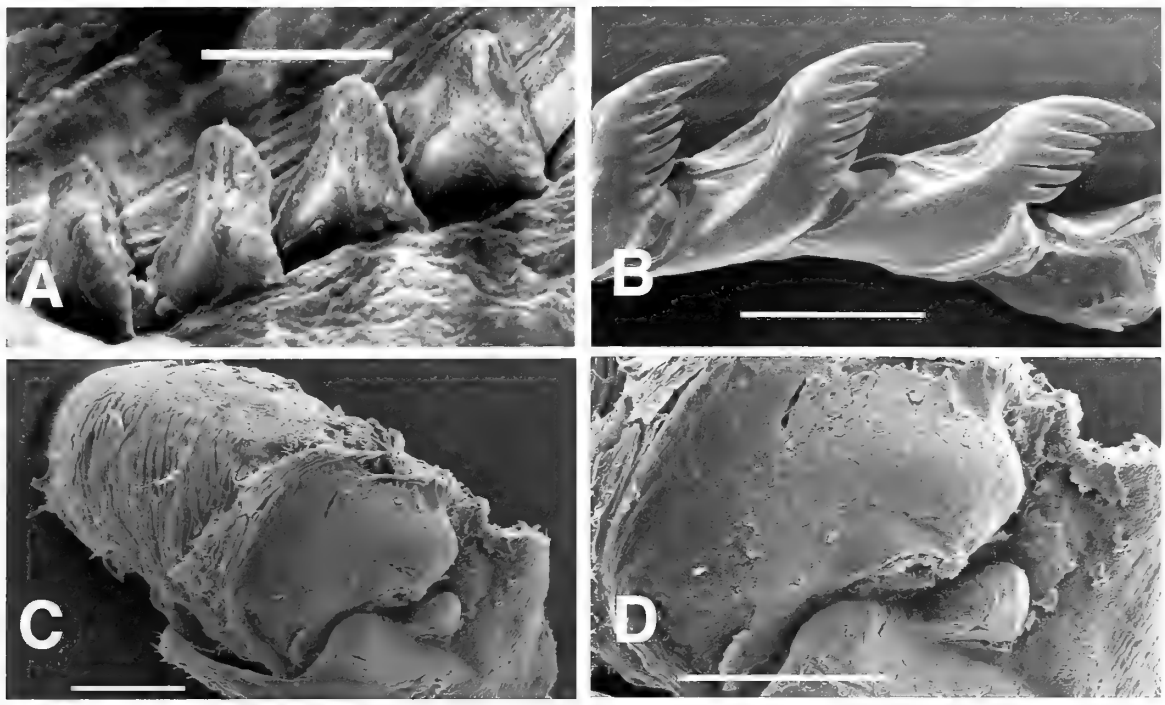

Figure 3. Scanning electron micrographs of *Dondice galaxiana* sp. nov. from Bahía de Banderas, Mexico: **A**, Denticles on masticatory flange of a jaw; **B**, Radular teeth; **C**, Penis and penial sac; **D**, Close-up of penis. Scale bars: A = 10 μm; B = 50 μm; C = 100 μm; D = 100 μm.

wider than long; the mouth is a vertical slit. The foot is bilabiate but not notched and extended into well-defined propodial tentacles up to 1 mm in length. The foot is narrow; each flange is as wide as the attached portion. The portion of the foot posterior to the body cavity is pointed, 1.5 mm long, flat and slender. A diagonal flap separates the genital openings and there is a posteriorly directed, triangular flap anterior to them. They are located below and anterior to the anterior most limb of the prehepatic ceratal arch. The anus is cleioproct, located within the first posthepatic arch. The renal opening is just under the heart, midway in the interhepatic space.

Coloration: The body color is translucent cream with rhomboid-shaped patches on the dorsum between the cerata. The center of each rhombus is light opaque cream surrounded by a light brown band and contains four equidistant bright turquoise spots forming a square. Next to each of these turquoise spots, there is a larger dark olive to black spot. In some specimens, the turquoise spots are so faint they can barely be distinguished next to the dark spots. The rest of the body is covered with random bright white specks, the number varying among specimens, with some completely devoid of them. The sides of the body have dark reddish brown patches that join near the cerata, further defining the rhombus. Some light cream patches with dark brown spots are also found on the sides. The cerata are light pinkish brown with a subterminal brown band and darker reddish brown cores. The surfaces of the cerata are covered with random white spots. The rhinophores have a clear base followed by a brown area and an opaque cream club. The head, at the base of the rhinophores, is clear, allowing the dark eyes to be seen. The remaining cephalic area follows the same coloration pattern as the body. The oral tentacles are the same color as the body, with dark brown irregular blotching at the bases and lighter blotching along the length, ending with clear tips.

Internal anatomy: The buccal mass has a muscular lip disk with a thin, chitinized ring. There are no compound oral glands, but solitary labial glands surround the mouth. The jaws (Figure 2C) are covered with black melanophores in the epithelium, concentrated dorsally and ventrally. They are pale yellow with a notched posterior margin.The masticatory margin bears a single row of approximately 20 well-developed, triangular denticles (Figure 3A).

The radular formula is 15–16 (1); the teeth are amber colored and located in a slightly protruding radular sac. Each rachidian tooth has an elongate cusp bearing one or two denticles and there are 4–6 triangular denticles

flanking the cusp (Figures 2D, 3B). The teeth are approximately 110 μm in length. The salivary glands have a long, narrow duct and are large with a flattened, irregular shape. The esophagus is a short tube leading into a large, oval, striated stomach. The posterior hepatic duct lies dorsal to the ovotestis, the wide, striated intestine forms a deep ∪ along the side of the ovotestis and ends at the anus, located high within the first posterior hepatic arch.

The central nervous system has large, oval, fused cerebropleural ganglia, connected closely together by a narrow commissure. There are short stalks to large rhinophoral ganglia in the bases of the rhinophores. The eyes are almost sessile. Small statocysts lie behind each eye. The oval pedal ganglia are about half the size of the cerebropleurals and connected to them by a short commissure and to each other by a longer commissure. The smaller, oval buccal ganglia lie beneath the esophagus and are connected to each other by a moderately long commissure.

The ovotestis is composed of smooth grape-like lobules containing both male and female acini. The long, narrow ovotestis duct widens slightly into a tubular ampulla, which runs the length of the female gland mass and then bifurcates into an oviduct and a vas deferens (Figure 2E, F). The vas deferens immediately becomes prostatic, with a wide glandular portion looping against and entering the base of a large penial sac. The penial sac and prostate appear as one structure. The penial sac is smooth and muscular externally; internally it is glandular with a central hollow. The sac and vas deferens terminate in a short, blunt, muscular, unarmed penis. When everted, the vas deferens projects anteriorly with a posterior bulge and a lateral flap. The oviduct enters a small, round, seminal receptacle and then continues a short distance to enter the female gland mass. The female gland mass is convoluted and white with a central, folded, bright yellow albumen gland.

Natural history: This species is known from Bahía de Banderas, Île Clipperton (Kaiser, 2007) and Costa Rica (Camacho-García et al., 2005). It is found in the shallow subtidal, under or over rocks with good hydroid coverage, from March to June in Bahía de Banderas. It has been photographed eating a reddish-orange athecate hydroid, possibly *Eudendrium*. The egg mass, observed in May, is a white string coiled around the hydroid (Figure 1F).

Discussion: The genera of Facelinidae having multiple rows of arch-shaped cerata on pedicles and no penial armature are listed in Millen & Hamann (1992: table 1). None of these genera exactly fit the present species, nor do any of the genera with arches bearing a single row of cerata. The rhinophores of this species are unusual in their cup-like annulations, similar to those of *Nanuca* Marcus, 1957. *Dondice galaxiana* differs from *Nanuca* in the ceratal arrangement, the presence of propodial tentacles, heart and kidney, and in arrangement of the reproductive system. The jaws have external black pigment, one row of masticatory denticles, and a posterior notch, as is found in *Caloria elegans* (Alder and Hancock, 1845) and *Dondice occidentalis* (Engel, 1925). *Caloria* Trinchese, 1888, has cerata in rows and simple rhinophores, whereas *Dondice* has weakly annulate rhinophores and multiple rowed arches on pads. The genus *Dondice* is unique in that it has a penial gland and a large penis containing the prostate. This new species has a prostate stuck against the penial bulb and entering the distal part of the penial bulb. In *D. occidentalis* and the similar *Dondice parguarensis* Brandon & Cutress, 1985, there is an external sperm groove spiraling down the penis to the tip, covered by a flap (personal observation, Millen), whereas in the new species, the penial bulb and prostate join distally and the short, muscular penis extends from the penial bulb. This species is provisionally placed in the genus *Dondice,* which is the only genus with cerata in arches with multiple rows and having a separate, unstalked penial gland and unarmed penis. They also are similar in that the jaws are notched and covered with black tissue and the teeth have pointed, denticulate cusps and lateral denticles. Penial glands are also found in the genus *Facelina* Alder and Hancock, 1855, which has cerata in rows and simple arches, but the penial glands in this genus enter the penial sac and are quite different in shape being bulbous with a long stalk.

Family Facelinidae Bergh, 1890

Genus *Adfacelina* Millen & Hermosillo, gen. nov.

Generic diagnosis: Cleioproctic aeolids with lamellate rhinophores and well-developed propodial tentacles. Pre- and postcardiac cerata in arches with multiple rows of cerata. Uniseriate radula with a prominent cusp and several strong lateral denticles. Jaw with one row of denticles on the masticatory margin and without a posterior notch. One copulatory bursa. Penis wide, with a blunt, lobate tip, bearing one outer row of tiny papillae.

Etymology: The name *Adfacelina* underscores the fact that this species has a series of papillae in a position similar to the chitinous spines of *Facelina.*

Type species: *Adfacelina medinai* Millen & Hermosillo sp. nov.

Adfacelina medinai Millen & Hermosillo, sp. nov.

(Figures 1B, G, 4, 5)

Material: Holotype: CASIZ 176806, 14 mm, Islas Marietas, Bahía de Banderas, 20 December 2003, collected by A. Hermosillo. **Paratypes:** LACM 3043,

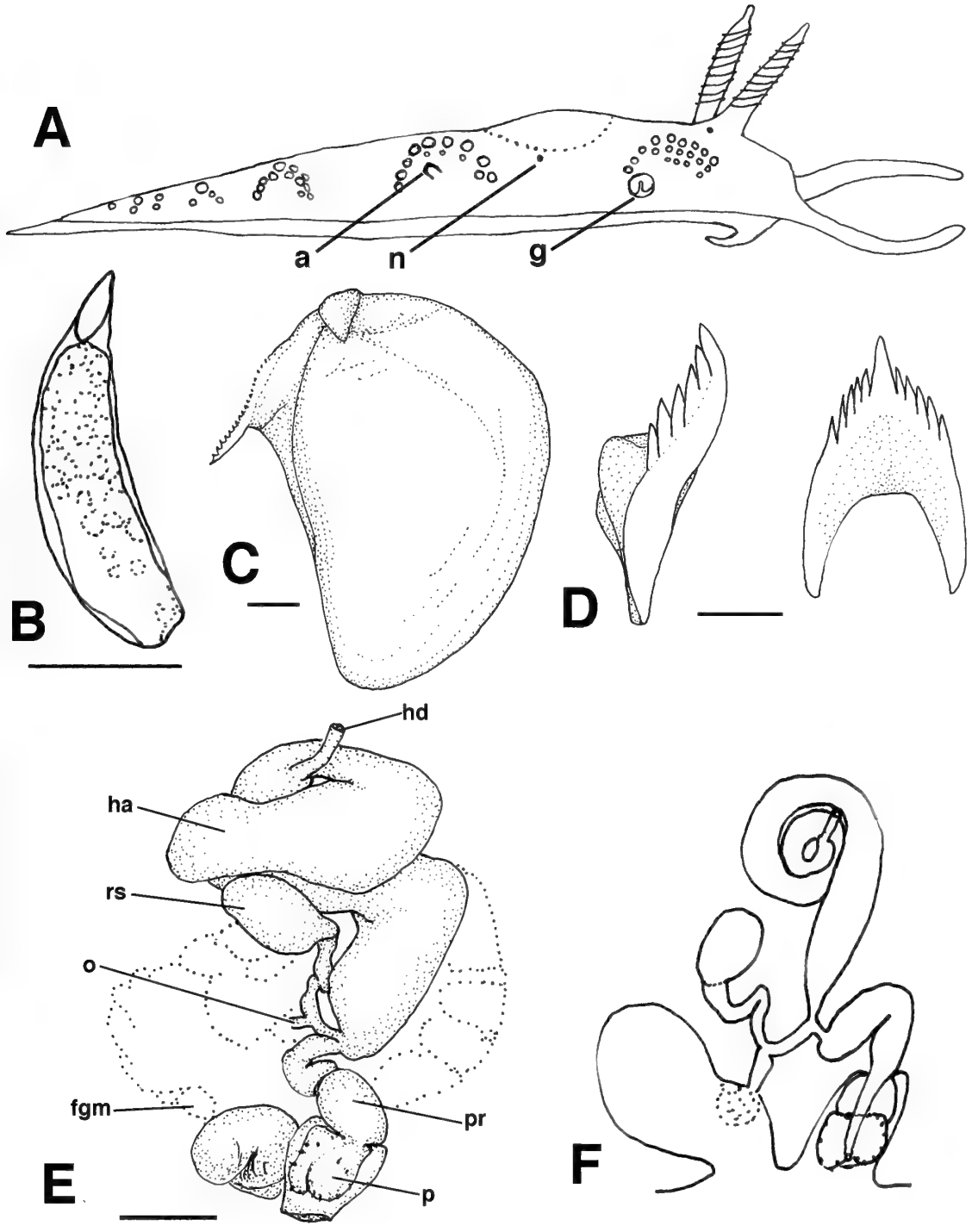

Figure 4. *Adfacelina medinai* sp. nov. from Bahía de Banderas, Mexico: **A**, Right lateral view showing position of ceratal insertions, stylized drawing; **B**, Ceras; **C**, One jaw; **D**, Radular tooth; **E**, Camera lucida drawing of the reproductive system; **F**, Stylized drawing of the reproductive system. Abbreviations: **a**, anus; **fgm**, female gland mass; **g**, genital apertures; **ha**, hermaphroditic ampulla; **hd**, hermaphroditic duct; **n**, nephroproctic opening; **o**, oviduct; **p**, penis; **pr**, prostate; **rs**, receptaculum seminis. Scale bars: B = 0.5 mm; C = 0.1 mm; D = 50 μm; E = 0.5 mm.

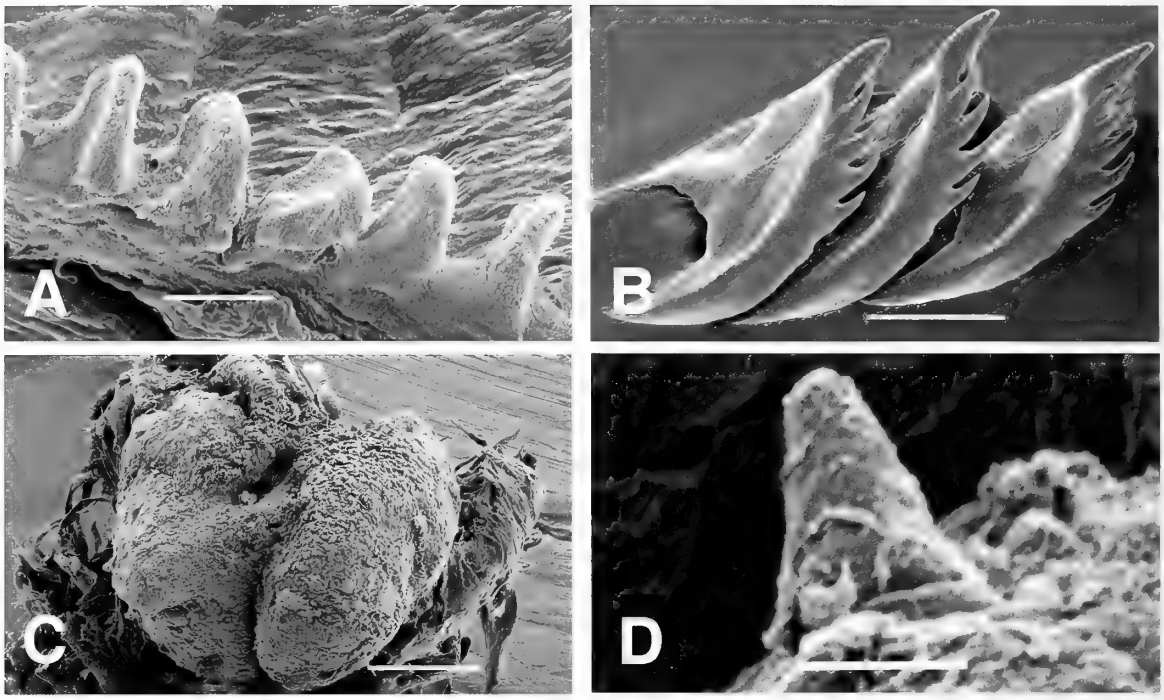

Figure 5. Scanning electron micrographs of *Adfacelina medinai* sp. nov. from Bahía de Banderas, Mexico: **A**, Denticles on masticatory flange of a jaw; **B**, Radular teeth; C, Penis showing its double structure and single row of papillae; **D**, Close-up of one penial papilla. Scale bars: A = 15 μm; B = 50 μm; C = 50 μm; D = 10 μm.

8 mm long, Islas Marietas, Bahía de Banderas, 29 May 2004 at 12 m depth, collected by A. Hermosillo. LACM 174197, 1 specimen, 5 mm, Île Clipperton, 18 April 2007, 93 m depth, collected by J. Bozanic. CASIZ 175779, 2 specimens, 11 mm long, 1 dissected, Islas Marietas, Bahía de Banderas, 12 April 2004. **Other material:** 1 specimen, 5 mm, 11 January 2003, Noche Iguana, Bahía de Banderas, dissected, collected by Alicia Hermosillo. 1 specimen, 9.5 mm, 10 June 2003, Islas Marietas, Bahía de Banderas, dissected, collected by Alicia Hermosillo.

Etymology: *Adfacelina medinai* is named in recognition of our friend Pedro Medina Rosas, who has been a dive and work partner of Alicia Hermosillo from day one. This species has been found in great depths (Île Clipperton) and inside sea caves (Bahía de Banderas), facts that are also a reminder of Pedro's experience as a technical diver.

External morphology: This aeolid reaches up to 14 mm in preserved length, 18 mm live length (Figure 1B). A 9.5-mm preserved specimen was 1.8 mm in width and 2 mm high. The rhinophores are 2 mm long, with a long, slender tip and up to 9–11 irregular perfoliations. The perfoliations have a small gap anteriorly and meet posteriorly. They are much wider on the sides and resemble annulations. The cerata are arranged in shallow arches on raised cushions (Figure 4A). The anterior-most, precardiac arch has a triple row anteriorly and a single or double row posteriorly. The first postcardiac arch has a double row anteriorly in the arch and a single or double row posteriorly. Subsequent arches usually have single rows of cerata. There are up to six postcardiac arches followed by a small posterior raised row and often a few cerata. The cerata are thick cylinders, up to 2 mm in length, with tiny pointed tips. The hepatic cores are wide and the cnidosacs are long and slender (Figure 4B). The broad head is a wide oval shape, the mouth a vertical slit. The head indents slightly anteriorly. The stout oral tentacles are 2.5 mm long, slightly longer than the rhinophores. They are flattened ventrally and are wider at the base. They originate at the oral surface and are held anterior-laterally. The foot is bilabiate and indented below the mouth. It is extended into stout, 1.2-mm-long, propodial tentacles. The foot is narrow at the middle attached portion with moderately wide lateral flanges, with a long, cylindrical, slender, 1-mm-long, trailing portion. The anus is cleioproct, located midway within the first posthepatic arch. The renal opening is slightly posterior to the middle of the interhepatic space.

Coloration: The coloration of the body is orange or reddish pink with irregular opaque yellow blotches

and spots covering it uniformly. The rhinophores are yellow with a medial dark pink band. There is a pinkish-orange area at the base of the rhinophores where the dark eyespots can be observed. The oral tentacles are long, with a dark pink medial band spotted with yellow and lighter towards the tip. The cerata are orange-red, covered with irregular opaque yellow blotches with a distal deep reddish-pink ring, just below the clear cnidosacs. The cephalic area is darker pink than the rest of the body, with the same yellow blotches.

Internal anatomy: The buccal mass has a short muscular oral tube with tiny labial glands attached. No compound oral glands were seen. There is a thin, round, chitinized lip disk in front of the jaws. The jaws (Figure 4C) are oval and pale yellow. They have a long masticatory margin with a single row of 18–22 well-developed denticles, which increase in size distally (Figure 5A).

The radular formula is 19–25 (1). The teeth are pale yellow and originate in a barely projecting radular sac. Each tooth has an elongate cusp, and 4–5 triangular denticles flanking the cusp (Figures 4D, 5B). The teeth are approximately 150 μm in length. The salivary glands are large irregular clusters located between the stomach and genital system. They have slender ducts that adhere to either side of the esophagus and insert on the buccal bulb. The esophagus is a wide, long cylindrical tube leading into a large, flattened, oval stomach. The posterior hepatic duct lies dorsal to the ovotestis. The intestine forms a long, shallow arch along the side of the ovotestis and ends at the anus, located high within the first posterior hepatic arch.

The central nervous system has large, oval, fused cerebropleural ganglia connected closely together by a narrow commissure. There are short nerves leading to round rhinophoral ganglia in the base of the rhinophores. The black eyes are almost sessile. Small statocysts lie directly behind each eye. The oval pedal ganglia are as long as the cerebropleural ganglia but only half as wide. They are connected by a short commissure to the cerebropleural ganglia and by a wide, longer commissure to each other beneath the esophagus. The smaller, round buccal ganglia lie beneath the esophagus and are connected to each other by a short commissure.

The ovotestis is composed of clusters with several tiny female acini peripheral to larger sac-like male acini, each with a small ductule leading to the hermaphroditic duct. The reproductive system is illustrated in Figure 4E, F. The hermaphroditic ampulla is swollen and folds back on itself and around, then down the length of the female gland mass. The ampulla then splits into the vas deferens and oviduct without a distinct postampullar duct. The oviduct is narrow and extends dorsally posterior to the base of the ampulla. It is joined by a duct from the semiserially arranged, oval, receptaculum seminis and then continues a short distance to enter the albumen (capsule) gland. There is no bursa copulatrix, nor a separate vagina. The female gland mass has a small albumen gland and complex, coiled membrane and mucous glands. The vas deferens immediately swells into a wide, short prostate, which enters the male atrium. The penis is wide and rounded at the tip. Two blunt lobes surround the vas deferens opening in the center, and each lobe bears one row of tiny papillae along the rim, although in one specimen the penis was even more inflated and the tip appeared as one slightly indented disk (Figure 5C, D). The penis appears to be glandular inside. The papillae are firm but fleshy with rounded bases embedded in the head of the penis, which stain differently than the penis itself. No accessory glands were seen. A small ridge separates the two genital openings. They are located below the posterior most limb of the first arch.

Natural history: This species is known only in Bahía de Banderas, Pacific coast of Mexico and Île Clipperton (Kaiser, 2007), where only one specimen was collected. The rest of the specimens have been found under rocks or inside a sea cave during the months of January, April, May, June, and December. The egg mass (Figure 1G) is pink, laid in irregularly folded strings upon an unidentified hydroid in the months of March and April.

Discussion: This animal belongs in the family Facelinidae with those species that have cerata arranged in arches both anteriorly and posteriorly and the arches are raised and consist of multiple (1–3) rows of cerata. Three genera in this family have tiny chitinous spines: Facelina, *Amanda* MacNae, 1954, and *Echinopsole* MacNae, 1954. *Amanda* is represented only by its type species, *A. armata* MacNae, 1954, and differs from this new species by its rounded foot corners, simple arches, and sparse, annulate cerata. The reproductive system has more prominent, chitinous hooks encircling the opening. The penis of *Facelina* is similar, but has a bulbous penial gland. *Echinopsole* is represented by two species, the type species, *E. fulvus* MacNae, 1954, and *E. breviceratae* Burn, 1962. This genus has multiple cerata in arches, but has many rows of chitinous spines on the penis, a small accessory gland, and annulate rhinophores. None of these genera appears to fit the new species, which has fleshy papillae. Fleshy papillae are found in *Caloria elegans*, which has its cerata in rows. This species differs from all of the current members of the family by its possession of cerata in multiple arches, penial armature, and its lack of an accessory penial gland; we have placed the new species in its own genus, *Adfacelina*.

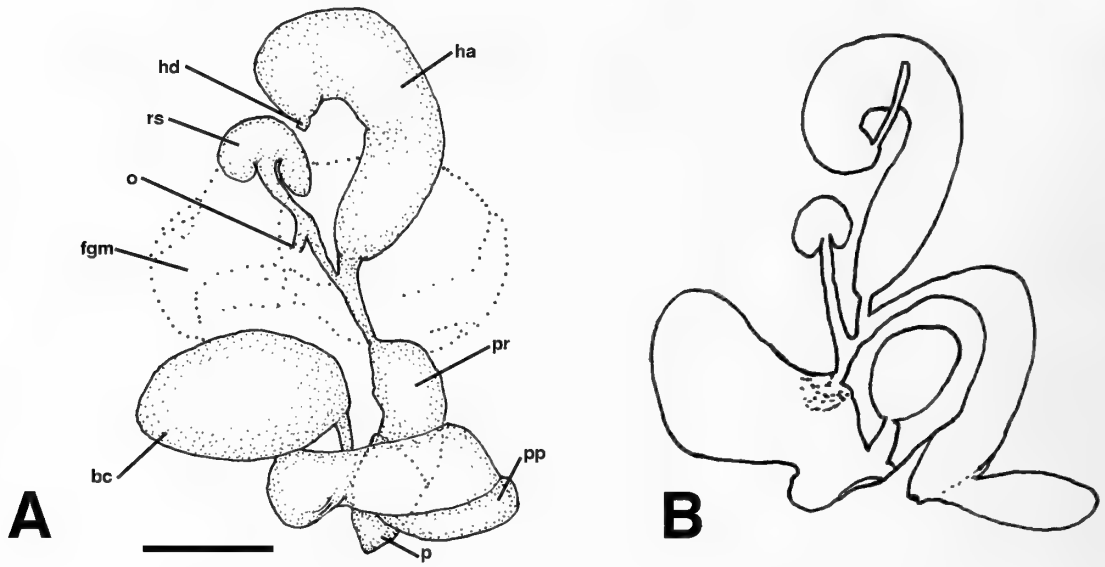

Figure 6. *Hermosita hakunamatata* (Ortea, Caballer, & Espinosa, 2003) comb. nov. from Bahía de Banderas, Mexico: **A**, Camera lucida drawing of the reproductive system; **B**, Stylized drawing of the reproductive system. Abbreviations: **bc**, bursa copulatrix; **fgm**, female gland mass; **ha**, hermaphroditic ampulla; **hd**, hermaphroditic duct; **o**, oviduct; **p**, penis; **pp**, penial papillae; **pr**, prostate; **rs**, receptaculum seminis. Scale bar: A = 0.5 mm.

Family FACELINIDAE Bergh, 1890

Genus *Hermosita* Gosliner & Behrens, 1986

Hermosita hakunamatata (Ortea, Caballer & Espinosa, 2003), comb. nov.

(Figures 1C, H, 6)

Phestilla hakunamatata Ortea, Caballer & Espinosa, 2003: 137–141, plate 1C, figures 3, 4C.

Material: Voucher specimens: LACM 173657, 1 specimen, 9 mm, Cerro Pelon, Isla Isabela, Bahía de Banderas, 14 December 2002, collected by Alicia Hermosillo. CASIZ 176805, 1 specimen, 9 mm, Cerro Pelón, Isla Isabela, Bahía de Banderas, 14 December 2002, with spawn, collected by Alicia Hermosillo. **Other material:** 7 specimens, Islas Marietas, Bahía de Banderas, 13 June 2003, collected by Alicia Hermosillo.

External morphology: This animal has been well photographed: Ajtai, in Rudman (2002) as *Flabellina* sp. 3; Hermosillo-González (2003) as *Flabellina* sp.; Ortea et al. (2003: plate 1C); Behrens & Hermosillo (2005: species #279, p. 122). The external description was based entirely on the type specimen, which is figured by Ortea et al. (2003) as figure 4C.

Internal anatomy: The radula and jaws of the type specimen were described and illustrated by Ortea et al. (2003: figures 3A, B, C). The remainder of the digestive tract, central nervous system, and reproductive systems were not examined and are described here for the first time.

The buccal opening is thick and muscular. Ventrally, ramified oral glands extend under the rounded buccal mass. The jaws are light yellow with smooth masticatory edges as illustrated by Ortea et al. (2003).

The radula formula is 12–15 (1) and the teeth are as illustrated by Ortea et al. (2003) with 5–14 long denticles per side. The salivary glands are small and round with a short, slender duct. They are located lateral to the buccal ganglia and are only slightly larger than each ganglion. The esophagus is a long, thin tube. The stomach is large and round or oval, the anterior hepatic ducts branching off the anterior portion. The intestine leaves the right side as a long, broad tube, looping down slightly before extending dorsally and narrowing just before the anus. The anus is in the cleioproct position on a small papilla within the first postcardiac arch and opposite the third ceras. The posterior hepatic duct runs ventrally with alternating branches beginning on the left. The hepatic branches run up the sides and between the clusters of acini to form horseshoe-shaped arches.

The central nervous system consists of fused, oval, cerebropleural ganglia connected by a short, wide commissure. The rhinophoral ganglia are large, lying at the bases of the rhinophores and are almost sessile. Large black eyes are on short optic nerves. Statocysts are directly behind the eyes at the junction of the pedal ganglia. The oval pedal ganglia are almost as large as the cerebropleurals and are connected to them by a short stalk. They are connected to each other by two longer, narrow cerebro-esophageal commissures. The small, round buccal ganglia lie close to each other beneath the esophagus.

The ovotestis forms a series of semicircular, somewhat flattened, clumps of acini. Each clump is joined by a short, narrow duct to the main collecting duct, which runs on top of the posterior hepatic duct, and to its right, anterior to the acini. This preampullar duct swells to form the hermaphroditic ampulla at the female gland mass (Figure 6). The long, sausage-shaped ampulla is curved. It splits into an oviduct and a vas deferens. The short oviduct is joined by the long duct of the receptaculum seminis, before inserting into the female gland mass. The receptaculum is usually only slightly swollen, but in one specimen was swollen into a small kidney-shaped sac. There is a separate, large, round bursa copulatrix with a short duct opening into the female gonopore. The oviduct enters the large, granular albumen gland. Eggs pass from the albumen gland to the highly convoluted membrane gland and thence to the larger, less convoluted mucous gland, which has anterior and posterior folds. The mucous gland exits at the female gonopore ventral to the duct of the bursa copulatrix. The vas deferens expands into a short, prostatic portion, which enters the penial sheath and slowly tapers to form a blunt, conical penis. There is no clear division between the prostatic portion of the vas deferens and the glandular penis. On the anterior side of the male gonopore is a disk-shaped, rounded, fleshy papilla, which can vary in its extension.

Natural history: *Hermosita hakunamatata* is found living and feeding on the hydroid *Solanderia* sp., which is dark purple with pink polyps. This hydroid lives in the undersides of overhangs on walls. In Bahía de Banderas, it has been found year-round in only a few sites. *Hermosita hakunamatata* is very cryptic in its habitat, particularly smaller specimens with darker coloration. The egg mass (Figure 1H) appears as rose-colored strings, which are laid in December on the distal part of the hydroid (see also Behrens & Hermosillo, 2005: species #279, p. 122).

Discussion: Ortea et al. (2003), having only one incompletely dissected specimen, believed the anus to be in an acleioproct position, posterior in the interhepatic space. Indeed, there is a prominent opening in this position, which upon dissection was revealed to be the nephroproct. The rather inconspicuous anal opening is in the cleioproct position, high within the first postcardiac arch. This error in anal position led Ortea et al. to place this species in the acleioproct family Tergipedidae Bergh, 1889, genus *Phestilla* Bergh, 1874. It is clear that this animal belongs in the family Facelinidae, as it has a cleioproct anus and uniseriate radula with cuspidate teeth. The ceratal groups are in simple arches and the presence of both a proximal, semiserial receptaculum seminis and a distal bursa copulatrix place it in the genus *Hermosita* Gosliner & Behrens, 1986. Other characteristics shared with *Hermosita* are the short prostate, which continues into the penis, an anterior penial flap, long denticles on the radular teeth, and perfoliate rhinophores. *Hermosita sangria* Gosliner & Behrens, 1986, is the only known species in the genus. It also occurs on the hydroid *Solanderia* sp. and is found just slightly north of this species' known distribution, on the outer coast of Baja California. Both species have reddish bodies, but can be distinguished as *Hermosita sangria* is larger (to 70 mm vs. 22 mm), has a violet cast to the body and lower half of the cerata, and a red band followed by yellow or white on the upper half of the cerata, foot corners, oral tentacles, and rhinophores. Internally it has a smooth masticatory margin to the jaw. *Hermosita hakunamatata* has no violet cast to the reddish body and has dark brown and golden spots on the foot, sides, dorsum, and lower half of the cerata. Brown spots are absent in two longitudinal strips between the cerata and are more prominent in smaller animals. The upper halves of the cerata are red, tipped with white cnidosacs. The rhinophores and oral tentacles, except for the most basal portion, lack brown and gold specks and are red with pale yellowish-white tips. The masticatory margin of the jaw bears one row of denticles.

Family UNIDENTIDAE Millen & Hermosillo, fam. nov.

Genus *Unidentia* Millen & Hermosillo, gen. nov.

Family diagnosis: Acleioproctic aeolids with smooth rhinophores, a raised anterior notal flange, and long propodial tentacles. Cerata in rows. Radula uniseriate. Oral glands present. Reproductive system with one proximal and no distal bursa. Penis armed with a long, curved, hollow chitinous stylet.

Generic diagnosis: With the characteristics of the family.

Etymology: The name of genus *Unidentia* Millen & Hermosillo gen. nov. is derived from the Latin *uni*, which means 'one', and *dentis*, which means 'tooth', calling attention to the fact that this flabellinid has a uniseriate radula combined with an acleioproctic anal position.

Type species: *Unidentia angelvaldesi* Millen & Hermosillo sp. nov.

Unidentia angelvaldesi Millen & Hermosillo, sp. nov.

(Figures 1D, E, I, 7, 8)

Material: Holotype: CASIZ 176809, 9 mm long, Los Arcos, El Bajo del Cristo, Bahía de Banderas, 12 June 2003, at 18 m depth, collected by A. Hermosillo.

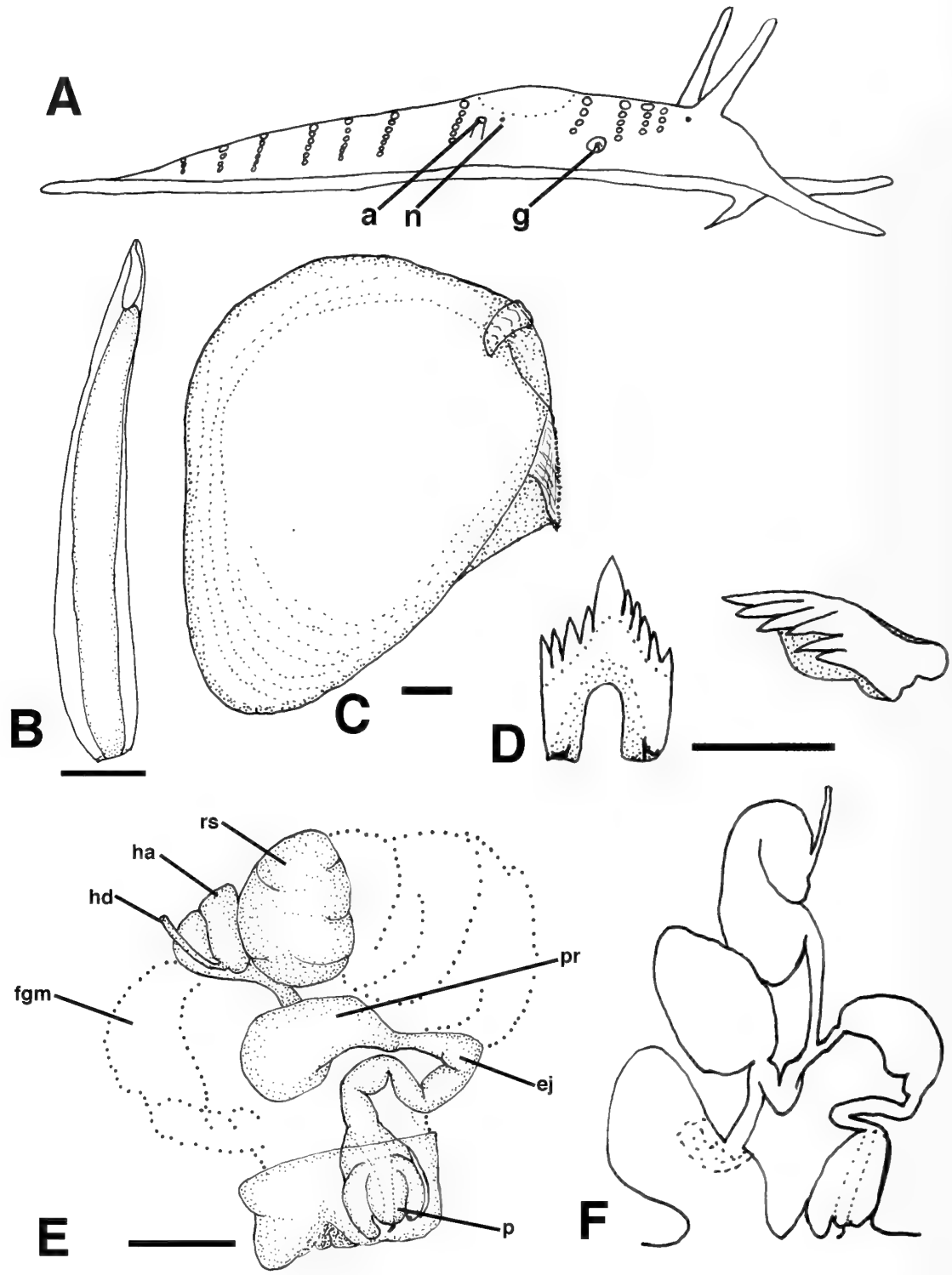

Figure 7. *Unidentia angelvaldesi* sp. nov. from Bahía de Banderas, Mexico: **A**, Right lateral view, showing position of ceratal insertions, stylized drawing; **B**, Ceras; **C**, One jaw; **D**, Radular tooth; **E**, Camera lucida drawing of the reproductive system; **F**, Stylized drawing of the reproductive system. Abbreviations: **a**, anus; **ej**, ejaculatory duct; **fgm**, female gland mass; **g**, genital apertures; **ha**, hermaphroditic ampulla; **hd**, hermaphroditic duct; **n**, nephroproctic opening; **p**, penis; **pr**, prostate; **rs**, receptaculum seminis. Scale bars: B = 0.5 mm; C = 0.1 mm; D = 50 μm; E = 0.5 mm.

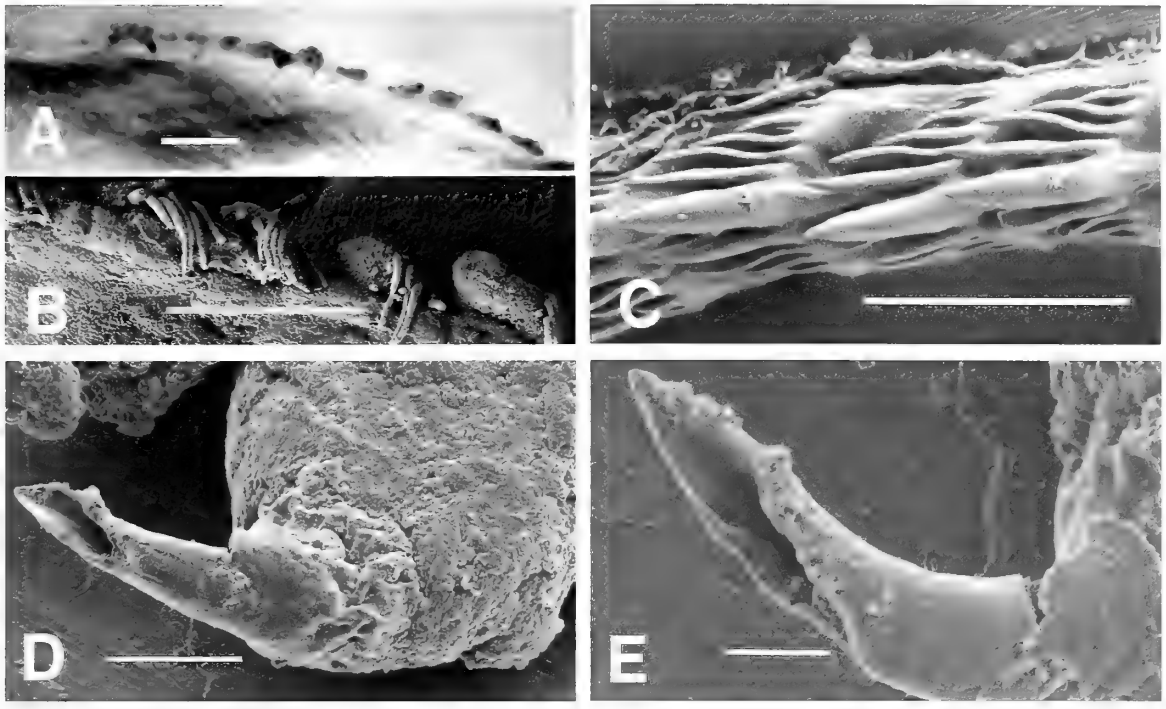

Figure 8. Scanning electron micrographs of *Unidentia angelvaldesi* sp. nov. from Bahía de Banderas, Mexico: **A**, Masticatory flange of a jaw; **B**, Denticles on masticatory margin of jaw; **C**, Radular teeth; **D**, Penis with penial spine; **E**, Close-up of the penial spine. Scale bars: A = 10 μm; B = 10 μm; C = 50 μm; D = 25 μm; E = 10 μm.

Paratypes: LACM 2890, 1 specimen, 6.5 mm long, Los Arcos, El Bajo del Cristo, Bahía de Banderas, 12 June 2003, at 15 m depth, collected by A. Hermosillo. CASIZ 085884, 4 specimens, Dakak, Northern Mindanao, Philippines, 100 m north of lighthouse, 1 April 1993, collected by T. Gosliner. CASIZ 89004, 1 specimen, 9.5 mm, dissected, Tengan Pier, Okinawa, Japan, 19 February 1993, photo 3150D, collected by B. Bolland. LACM 153355, 2 specimens, 3 and 10 mm long, Boca Grande estuary, Bahía Damas, east Isla de Coiba, Panamá, 18 May 2003. **Other material:** 6 specimens, 3 dissected, Los Arcos, La Quijada, Bahía de Banderas, 9 March 2003, 21 m depth, collected by A. Hermosillo. 3 specimens, 2 dissected, Los Arcos, El Bajo del Cristo, Bahía de Banderas, 12 June 2003, at 12 m depth, collected by A. Hermosillo and S. Millen. Futou, Suruga Bay, Japan, 13 October 2002, 3 m depth, photo by J. Imamoto. Bali and Komodo, Indonesia, October 2007, photo by A. Hermosillo.

Etymology: *Unidentia angelvaldesi* is named in honor of Dr. Angel Valdés and his invaluable contributions to the knowledge of the biology, ecology, and taxonomy of the opisthobranchs of the world.

External morphology: The body is long and slender with a preserved maximum size of 9.5 mm, a typical large specimen being 8 × 2 × 2 mm (l × w × h). The living length can be up to 20 mm (Figure 1D, E). The rhinophores are as long as the oral tentacles, up to 3.2 mm in preserved animals, and smooth.

The cerata are arranged in raised, single rows, which slope posteriorly (Figure 7A). The precardiac ceratal rows are on a slight lateral expansion of the body wall. There are 4–6 precardiac rows and 5–8 postcardiac rows. Each row bears up to 12 cerata, a typical formula being 4,4,5,4;7,8,7,6,6,4,3. The cerata are slender and cylindrical, up to 7 mm in length, with moderately long cnidosacs and a wide, irregular core (Figure 7B). The head is oval, wider than long, and equal to the foot width. The mouth is a small, vertical slit. The oral tentacles taper more than the rhinophores and are up to 3.2 mm long in preserved animals. They are slightly flattened on the ventral surface and originate dorsal to the oral surface. The foot is bilabiate but not notched and extended into 1.5-mm-long propodial tentacles. The attached portion of the foot is equal in width to the two moderate lateral flanges and together they are narrower than the body. The trailing portion of the foot is flat, 2.5 mm long, and pointed.

The genital openings have a large, protruding dorsal flap above the female opening. They are located below the third or fourth ceratal row. The anus is on a tall, slender papilla located posterior in the interhepatic space. The opening is anterior to the second to fifth ceras of the first posthepatic row, but the papilla begins

at the base of the row. The renal opening is directly anterior to the anal opening.

Coloration: Two distinct color forms have been observed, one presenting various shades of red and orange (Figure 1D); and a pale, almost white coloration (Figure 1E). In the darkly pigmented animals, the ground color is translucent with a faint red tint with orange or red ovotestis showing through. There are three purple lines running the entire length of the body. One is middorsal, the other two run just underneath the cerata, all three meeting behind the cerata to form a broad strip down the trailing portion of the foot. Opaque white can be found on the dorsal surface, particularly between the tops of the ceratal rows and on the sides of the cephalic area. The bases of the oral tentacles are the ground color followed by bands of opaque white, purple, and opaque white distally. The basal one-third of the rhinophores are the ground color, followed by a band of opaque white, a short band of ground color followed by a short band of purple, and ending in a distal band of ground color with some opaque white specks. The amount of opaque white varies. In some animals it is absent from the oral tentacles and replaced by purple. It often forms mottled rather than solid bands. In one specimen it was light yellow and on the rhinophores it became orange near the purple band. The propodial tentacles have opaque white specks and a purple stripe. The cerata are the same ground color, with cores of darker red, sometimes orange. Below the pale white cnidosacs is a thin band of purple. There is an occasional opaque white spot on the cerata. In the pale specimens, the color of the body and cerata vary from white to white with a purplish tint. It follows the same purple line regime on the body as does the darker variation. The oral tentacles are clear with the distal one-third colored purple. The rhinophores are clear proximally, with a ring of opaque white blotches followed by a purple ring and ending with a clear tip. The cerata are clear, with opaque white cores, a thin purple ring, and clear cnidosacs. A few specimens have pale pink ceratal cores.

Internal anatomy: There are two compact, ramified oral glands lying laterally behind the rhinophores and on either side of the stomach. Ducts enter on each side of the mouth opening. Posterior to the mouth, the anterior portion of the foot has large pedal glands. The buccal mass is oval, with a thin, muscular lip disk over a thin cuticle. The jaws are pale yellow and almost round in shape (Figure 7C). They have a small masticatory margin with one row of up to 22 blunt, jagged denticles (Figure 8A, B). The radular sac has a small projection. The radula has 28–35 median teeth with no lateral teeth. The teeth have a projecting cusp and 4–7 long denticles per side (Figures 7D, 8C). The teeth are approximately 75 μm in length. The posterior limbs articulate with the limbs of the following teeth. The salivary glands are short, wide and leaf-shaped. They have short, narrow ducts leading to the buccal mass. The esophagus is a short tube connected to a large, almost circular stomach. The hepatic ducts are wide leaving either side of the stomach. The posterior duct is dorsal to the ovotestis. The intestine is short, running posteriorly, curving abruptly up to a narrow anal papilla in the posterior interhepatic space. The renal syrinx is just anterior to the intestine, the renal opening is anterior to the anus.

The central nervous system consists of rounded, fused cerebropleural ganglia connected closely together by a wide commissure. The large, short-stalked rhinophoral ganglia lie at the bases of the rhinophores. The well-developed eyes are almost sessile. Small statocysts lie posterior to the eyes. The smaller, somewhat triangular pedal ganglia are ventral, joined to the cerebropleural ganglia by short commissures and to each other by a slightly longer circum-esophageal commissure. The oval buccal ganglia lie next to each other beneath the esophagus.

The reproductive system is illustrated in Figure 7E, F. The ovotestis form what appears to be one irregular mass from the stomach to the end of the body cavity. The female acini are distal to the male acini, which connect to small ducts, which join together. There is a short, narrow hermaphroditic duct that widens into an ampulla with a single tight bend. The long postampullar duct divides into the oviduct and vas deferens. The oviduct is wide, loops, and sometimes becomes swollen. It leads to a large, oval seminal receptacle. It then travels distally as a wide duct to join the female gland mass and continues as a common female duct. The female opening is under a dorsal, projecting flap just posterior to the male opening. There is no distal bursa. The female gland mass has folded mucous glands and an oval, central albumen gland. The vas deferens swells into a prostate after a short distance and forms a short, curved, tubular prostate, then narrows into a short ejaculatory duct, which enters an elongate penial sheath. The penis bears two unequal lobes, the posterior larger than the anterior. Between the lobes is a muscular penial papilla containing the vas deferens. At the opening of the vas deferens is a long, narrow, anteriorly directed, curved stylet (60 μm long) with a slanted opening (Figure 8D, E).

Natural history: This species is known from the tropical Indo- and eastern Pacific. In the Indopacific, from Futou, Suruga Bay, Japan (J. Imamoto, personal communication); Okinawa, Japan; Bali and Komodo, Indonesia; and the Philippines. In the eastern Pacific it has been found from Isla Isabel, Nayarit, Mexico, to Panama. The life cycle of this species has been observed for several yearly cycles in Bahía de Banderas (eastern

Pacific), where it lives on the widespread, orange gymnoblastic hydroid *Corydendrium parasiticum* (Linnaeus, 1767), on which it is very cryptic. The egg mass is 5–6 orange, slightly flattened coils laid in a slightly wavy string on the hydroid with a small capsule-free sheet. It is abundant during the summer months (May, June, and July) and found sporadically throughout the rest of the year. The white specimens from the Indopacific were found feeding on a white gymnoblastic hydroid also belonging to the genus *Corydendrium* Van Beneden, 1844. The difference in body coloration of these specimens indicates this different food source. Not much is known of the life cycle of Indopacific specimens that have been found in May and October.

Discussion: This species has probably long been confused with the similar-looking species *Flabellina rubrolineata* (O'Donoghue, 1929). The most obvious way to distinguish them externally is by the papillate rhinophores and pleuroproctic anus of *F. rubrolineata* opposed to the smooth rhinophores and acleioproctic anus of *Unidentia angelvaldesi.* Internally, the new species has one row of radular teeth as opposed to three found in the genus *Flabellina* Voight, 1834, and the penis is armed with a penial stylet.

The familial and generic placement of this species is problematic. It has the apomorphies of a uniseriate radula and the anus is acleioproctic in position. However, some of the advanced Flabellinidae Bergh, 1899 also have a high anal position close to the acleioproctic one. The reproductive system lacks the apomorphies of the acleioproctic family Tergipedidae, genus *Cuthona* Alder and Hancock, 1855, which has no proximal bursa, and possesses a distal bursa and a penial gland. *Cuthona* also has a shorter and less slender body shape and lacks tentacular propodial tentacles. However, a penial stylet is found in *Cuthona* and several other tergipedid genera.

Edmunds (1970) created the family Piseinotecidae, to separate the genus *Piseinotecus* Marcus, 1955, from the family Tergipedidae. Apomorphies of this genus are one row or tuft arising from the anterior hepatic duct, cerata on lateral projections, the uniseriate radula usually bearing fine denticles and long wings, and with one, proximal bursa. They retain the plesiomorphic feature of hermaphroditic follicles in the gonad. This new animal lacks the ceratal features but has one proximal bursa, a situation found in some Flabellinidae as well as most Facelinidae, all of which have a uniseriate radula but a cleioproctic anal position. Gosliner et al. (2007) produced a cladogram that suggests the genus Piseinotecidae is closest to the family Flabellinidae.

The newly described species possesses a hollow penial stylet at the end of the vas deferens, a situation found in the facelinid genera *Eumarcusia* Roller, 1972, *Noumeaella* Risbec, 1937, most *Herviella* Baba, 1949, *Anetarca* Gosliner, 1991, and *Favorinus* Gray, 1850 (one species). The anal placement in the family Facelinidae is in the apomorphic cleioproct position, between the postcardiac rows. In this new species, the anus is placed in the interhepatic space. The pleisomorphic condition of aeolids is pleuroproct (ventral to the cerata, interhepatic or slightly posterior). However, even in aeolids possessing a triseriate radula, there are several that have acleioproct anal positions (*Cumanotus* Odhner, 1907, some *Flabellina*), so this position appears to be easily derived from the pleuroproct one.

PHYLOGENETIC ANALYSIS

To elucidate the position of the two new genera described in this paper, and to compare the other two species with the types of their genera, a cladogram was generated, based on several previously published aeolid cladograms (Gosliner & Kuzirian, 1990; Wägele & Willan, 2000; Gosliner et al., 2007). The coding information for the 27 species used primarily came from descriptions of Schmekel & Portmann (1982), who provided descriptions of *Calmella cavolini* (Verany, 1846), *Spurilla neapolitana* (Delle Chiaje, 1841), *Berghia verrucicornis* (D. Costa, 1864), *Aeolidiella alderi* (as *sommeringi*) (Cocks, 1852), *Dichata odhneri* Schmekel, 1961, *Facelina auriculata* (O.F. Müller, 1776), *Cratena peregrina* (Gmelin, 1791), *Caloria elegans* (Alder & Hancock, 1845), *Favorinus branchialis* (J. Rathke, 1806), *Dondice* (as *Godiva*) *banyulensis* (Portmann & Sandmeier, 1960), and *Piseinotecus spaerifera* (Schmekel, 1965). Gosliner & Griffiths (1981) was used for *Flabellina capensis* (Thiele, 1925) and Gosliner & Behrens (1986) was used for *Hermosita sangria* Gosliner & Behrens, 1986. *Babakina festiva* (Roller, 1972) came from Roller (1972) and Gosliner et al. (2007), who also described *Babakina indopacifica* Gosliner, Gonzáles-Duarte & Cervera, 2007. *Pruvotfolia pselliotes* (Labbé, 1923) came from Tardy (1970) and *Notaeolidia gigas* Eliot, 1905, from Wägele (1990). Cervera et al. (1987) described *Piseinotecus gaditanus.* Coding information for specimens of *Cuthona punicea* Millen, 1986, *Flabellina verrucosa* (Johnson, 1832), *Dondice occidentalis* (Engel, 1925), *Eubranchus rupium* (Moller, 1842), and *Cumanotus beaumonti* (Eliot, 1906), as well as the four species in this paper, came from personal observation. A total of 27 species were used and 23 morphological characters, which are listed in Table 1 and discussed below. The complete character matrix for the species used is shown in Table 2.

All characters were treated as unordered except for no. 12, the number of lateral radular teeth, which was ordered following Gosliner et al. (2007). Characters were polarized using the primitive aeolid *Notaeolidia*

Table 1

Synopsis of the character states used in the present study.

1. **Notal brim:** 0 = present; 1 = interrupted; 2 = absent
2. **Propodial tentacles:** 0 = absent; 1 = angular; 2 = tentacular; 3 = hooked
3. **Body shape:** 0 = wide; 1 = narrow
4. **Cerata insert:** 0 = arise directly from the notum; 1 = arise from peduncles
5. **Ceratal number:** 0 = fewer than 100 cerata per side;1 = more than 100 per side
6. **First ceratal cluster** (precardiac): 0 = rows; 1 = single arch; 2 = compound arch
7. **Second ceratal cluster** (first postcardiac): 0 – rows; 1 = single arch; 2 = compound arch
8. **Ceratal shape:** 0 = cylindrical; 1 = inflated; 2 = flattened
9. **Anus:** 0 = pleuroproctic; 1 = cleioproctic; 2 = acleioproctic
10. **Rhinophoral base:** 0 = divided; 1 = united
11. **Rhinophoral ornamentation:** 0 = smooth or wrinkled; 1 = annulate; 2 = perfoliate; 3 = papillate; 4 = swollen
12. **Radula:** 0 = multiseriate; 1 = triseriate; 2 = uniseriate
13. **Rachidian tooth shape:** 0 = cuspidate; 1 = pectinate
14. **Rachidian tooth:** 0 = denticulate; 1 = smooth
15. **Rachidian radular teeth:** 0 = symmetrical; 1 = asymmetrical
16. **Jaw denticles:** 0 = multiple rows of denticles; 1 = a single row; 2 = smooth
17. **Reproductive bursae:** 0 = with a distal and a proximal bursa; 1 = with only a distal bursa (Dialauly 1); 2 = with only a proximal bursa (Dialauly II)
18. **Prostate:** 0 = with an enlarged prostate; 1 = without an enlarged prostate
19. **Ejaculatory duct:** 0 = with a muscular ejaculatory portion; 1 = with no distal, muscular narrowing
20. **Penis:** 0 = unarmed; 1 = with cuticular papillae or chitinous hooks; 2 = with a chitinous stylet
21. **Penis shape:** 0 = narrow; 1 = conical; 2 = bulbous
22. **Penial glands:** 0 = absent; 1 = present
23. **Food:** 0 = hydroids; 1 = sea anemones; 2 = opisthobranch eggs

gigas Eliot, 1905, from family Notaeolidiidae Eliot, 1910, as the outgroup species (Wägele and Willan, 2000). Phylogenetic analyses were performed using the program Phylogenetic Analysis Using Parsimony (PAUP), version 4.0b 10 (Swofford, 2002) using the heuristic algorithm (TBR branch swapping option), set at maximum parsimony. Morphological data were compiled using MacClade, version 4.05 (Maddison and Maddison, 2002). Synapomorphies were mapped using the character trace option for unambiguous changes, in MacClade using the single tree from the PAUP analysis (Figure 9). Bremer analyses were performed on this tree to estimate branch support and the numbers are placed on the tree (Bremer, 1994).

CHARACTERS

1. **Notal brim:** 0 = present; 1 = interrupted; 2 = absent. The presence of a notal brim, as is found in *Notaeolidia*, Eliot, 1910 has been considered primitive among the Aeolidacea (Odhner, 1939). A number of species have a discontinuous notal brim, which is thought to be a reduction of the brim; other species have no trace of the notal brim.
2. **Propodial tentacles:** 0 = absent, foot corners rounded; 1 = angular, with tentacles connected by a triangle of tissue; 2 = tentacular, with long extensions; 3 = hooked, with small tentacles. *Notaeolidia* has rounded foot corners. Hooked tentacles are shorter than long propodial tentacles, and angular tentacles have a veil-like connection from the foot to the tentacle. The direction used is that of Gosliner & Kuzirian (1990) and Wägele & Willan (2000).
3. **Body shape:** 0 = wide; 1 = narrow. The direction used is that of Gosliner & Kuzirian (1990) and Wägele & Willan (2000). Wide bodies are found in *Notaeolidia*, *Cumanotus*, and the Aeolidiinae.
4. **Cerata insert:** 0 = arise directly from the notum; 1 = arise from peduncles. Peduncles are found in *Calmella* Eliot, 1910 and *Piseinotecus*.
5. **Ceratal number:** 0 = usually fewer than 100 cerata per side of the body; 1 = numerous with many more than 100 per side. Large number of cerata are found on *Notaeolidia gigas* and the Aeolidiidae Odhner, 1907.
6. **First ceratal cluster** (precardiac): 0 = rows; 1 = single arch; 2 = compound arch consisting of more than one cerata per branch laterally or several rows preceding an arch, as in *Facelina auriculata*. Rows, as found in *Notaeolidia*, are considered plesiomorphic. Arches are common in the Facelinidae and Aeolidiidae.
7. **Second ceratal cluster** (first postcardiac): 0 = rows; 1 = single arch; 2 = compound arch consisting of more than one ceras per branch laterally, or several rows preceding an arch as in *Facelina auriculata*. The second cluster usually has fewer

Table 2

Morphological character states used in the phylogenetic analysis.

Taxon	1	2	3	4	5	6	7	8	9	10	11	12	13	14	15	16	17	18	19	20	21	22	23
Notaeolidia gigas	0	0	0	0	1	0	0	0	0	0	1	0	0	0	0	2	1	1	0	0	2	0	0
Flabellina capensis	1	2	1	0	0	0	0	0	0	0	0	1	0	0	0	0	0	0	0	0	2	0	0
Flabellina verrucosa	1	2	1	0	0	0	0	0	0	0	0	1	0	0	0	0	0	0	0	1	2	0	0
Calmella cavolini	1	3	1	1	0	0	0	0	0	0	0	1	0	0	0	0	2	0	1	0	0	0	0
Babakina festiva	0	2	1	0	0	0	0	0	0	1	2	2	0	0	1	0	0	1	1	0	0	0	0
Babakina indopacifica	0	2	1	0	0	0	0	0	0	1	2	2	0	0	1	0	0	1	1	0	0	0	0
Piseinotecus gaditanus	1	3	1	1	0	0	0	0	2	0	0	2	0	0	0	0	2	0	1	0	0	0	0
Piseinotecus spaerifera	1	3	1	1	0	0	0	0	2	0	0	2	0	0	0	1	2	0	1	0	1	0	0
Cuthona punicea	2	0	1	0	0	0	0	1	2	0	0	2	0	0	0	1	1	1	0	0	1	1	0
Eubranchus rupium	2	0	1	0	0	0	0	1	2	0	0	1	0	0	0	1	1	1	0	2	1	1	0
Cumanotus beaumonti	2	2	0	0	0	0	0	0	2	0	0	1	0	0	0	1	2	0	0	1	2	0	0
Unidentia angelvaldesi	1	2	1	0	0	0	0	0	2	0	0	2	0	0	0	1	2	0	0	2	2	0	0
Spurilla neopolitana	2	1	0	0	1	1	1	2	1	0	2	2	1	0	0	2	2	0	0	0	2	0	1
Berghia verrucicornis	2	1	0	0	1	2	1	0	1	0	3	2	1	0	0	2	2	0	0	0	1	0	1
Aeolidiella alderi	2	1	0	0	1	0	0	2	1	0	0	2	1	0	0	2	2	0	0	0	1	0	1
Dicata odhneri	2	2	1	0	0	1	1	0	1	0	0	2	0	0	0	2	0	0	0	0	0	0	0
Facelina auriculata	2	2	1	0	0	2	2	0	1	0	1	2	0	0	0	1	2	0	1	1	2	1	0
Cratena peregrina	2	2	1	0	0	1	0	0	1	0	0	2	0	0	0	1	2	0	1	0	2	0	0
Pruvotfolia pselliotes	2	2	1	0	0	0	0	0	1	0	1	2	0	0	0	1	2	0	1	1	2	0	0
Caloria elegans	2	2	1	0	0	0	0	0	1	0	0	2	0	0	0	1	2	0	1	1	2	0	0
Favorinus branchialis	2	2	1	0	0	1	1	0	1	0	4	2	0	1	0	0	2	1	0	0	0	0	2
Adfacelina medinai	2	2	1	0	0	2	2	0	1	0	2	2	0	0	0	1	2	0	1	1	2	0	0
Dondice banyulensis	2	2	1	0	0	2	2	0	1	0	1	2	0	0	0	1	2	1	1	0	1	0	0
Dondice galaxiana	2	2	1	0	0	2	2	0	1	0	1	2	0	0	0	1	2	0	1	0	2	1	0
Dondice occidentalis	2	2	1	0	0	2	2	0	1	0	1	2	0	0	0	1	2	1	1	0	2	1	0
Hermosita sangria	2	2	1	0	0	1	1	0	1	0	2	2	0	0	0	2	0	0	1	0	1	0	0
Hermosita hakunamatata	2	2	1	0	0	1	1	0	1	0	2	2	0	0	0	1	0	0	1	0	1	0	0

cerata than the first, and *Berghia verrucosa* on pg 159 changes from a double to a single arch, while *Cratena peregrina* changes from a single arch to rows.

8. **Ceratal shape:** 0 = cylindrical; 1 = inflated; 2 = flattened. Most aeolids have cylindrical cerata, but they are inflated in *Cuthona* and *Eubranchus* Forbes, 1838 and basally flattened in *Aeolidiella* Bergh, 1867 and *Spurilla* Bergh, 1864.
9. **Anus:** 0 = pleuroproctic; 1 = cleioproctic; 2 = acleioproctic. *Notaeolidia* is pleuroproctic, as are *Flabellina* species, *Calmella*, and *Babakina* Roller, 1973. *Cuthona*, *Eubranchus*, *Cumanotus*, *Piseinotecus*, and *Unidentia* are acleioproctic, whereas the rest of the aeolids are cleioproctic.
10. **Rhinophoral base:** 0 = divided; 1 = united. The united base is an apomorphy of the genus *Babakina*.
11. **Rhinophoral ornamentation:** 0 = smooth or wrinkled; 1 = annulate, with a series of rings; 2 = perfoliate with sloping lamellae; 3 = papillate, with papillae; 4 = swollen, with one or more swellings along the length. *Notaeolidia gigas* has annulate rhinophores, but the absence of increased surface area on smooth rhinophores is considered plesiomorphic.
12. **Radula:** 0 = multiseriate with several rows of lateral teeth; 1 = triseriate with a lateral tooth on each side of the rachidian tooth; 2 = uniseriate, with only a rachidian row. See Wägele & Willan (2000) and Gosliner et al. (2007). This character has been treated as ordered as in Gosliner et al. (2007).
13. **Rachidian tooth shape:** 0 = cuspidate, with a series of denticles flanking a triangular cusp; 1 = pectinate, with larger comb-like denticles flanking a small central cusp. The latter is found in the Aeolidiidae.
14. **Rachidian tooth:** 0 = denticulate; 1 = smooth. This is an apomorphy for *Favorinus*.
15. **Rachidian radular teeth:** 0 = symmetrical, with the same number of denticles on either side of the cusp; 1 = asymmetrical, with different numbers of denticles on either side of the cusp. The latter is an apomorphy for some species of *Babakina* (Gosliner et al. 2007).
16. **Jaw denticles:** 0 = with multiple rows of denticles on the masticatory margin; 1 = with a single row of denticles; 2 = smooth, without denticles. Although *Notaeolidia gigas* has a smooth masticatory margin, multiple rows of denticles as found

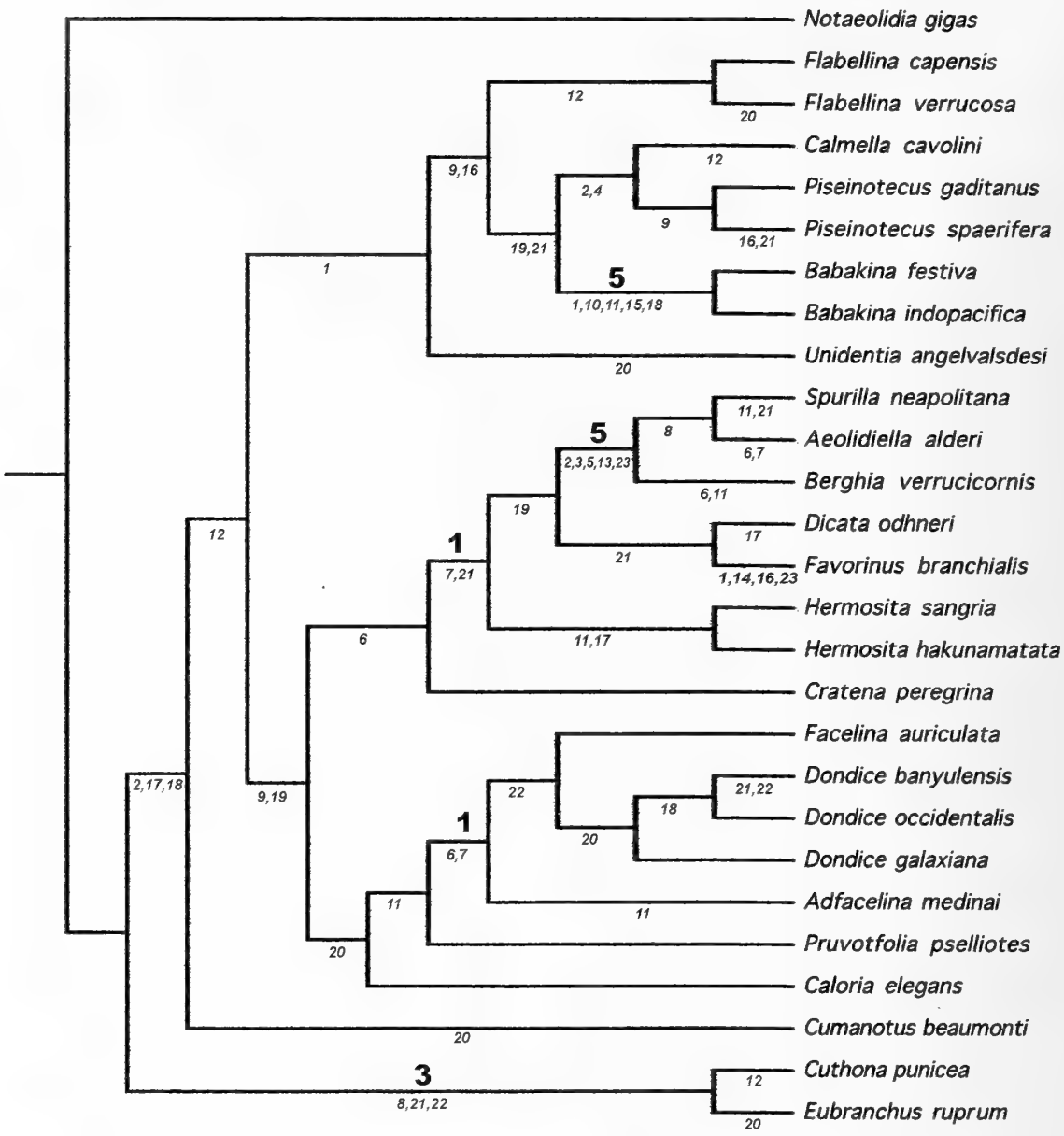

Figure 9. Single tree obtained from the analysis of the characters listed in Table 1 and the matrix in Table 2. Character numbers are plotted below the line in lowercase italics; larger numbers above the line represent Bremer support values.

in *Flabellina*, *Calmella*, and *Babakina* are considered plesiomorphic.

17. **Reproductive bursae:** 0 = with a distal and a proximal bursa; 1 = with only a distal bursa (Dialauly 1); 2 = with only a proximal bursa (Dialauly II). As pointed out by Wägele & Willan (2000), the functions of the distal bursa may differ. The proximal bursa, when present, is always a receptaculum seminis. The presence of both a proximal and a distal bursa is considered plesiomorphic by Wägele & Willan (2000).
18. **Prostate:** 0 = with a widening of the vas deferens into an enlarged prostate; 1 = without a widening of the vas deferens into an enlarged prostate. The presence of a widened prostatic portion of the vas deferens is considered plesiomorphic by Gosliner et al. (2007).
19. **Ejaculatory duct:** 0 = with a distal narrowing between the prostate and penis to form a muscular ejaculatory portion of the vas deferens: 1 = with no distal, muscular narrowing between the prostate and the penis.

20. **Penis:** 0 = unarmed and smooth; 1 = armed with cuticular papillae or chitinous hooks; 2 = armed with a chitinous stylet. Most species have an unarmed penis, but it is not clear at present whether hooks and papillae which may or may not be chitinous are homologous. A stylet of chitin is found in some *Eubranchus* species and *Unidentia*.
21. **Penis shape:** 0 = narrow, not tapering; 1 = conical, wider proximally, with a narrow tip; 2 = bulbous, wide, with a wide tip. The directionality is as in Gosliner et al. (2007).
22. **Penial glands:** 0 = absent; 1 = present as a secondary structure to the penis. Glands found in *Eubranchus*, *Cuthona*, and *Dondice* may replace prostatic portions of the vas deferens. The function of the gland entering the penial sheath in *Facelina* may not be homologous.
23. **Food:** 0 = hydroids; 1 = sea anemones; 2 = opisthobranch eggs. Most aeolids feed on hydroids, but the Aeolidiidae feed on sea anemones. *Favorinus* feeds on opisthobranch eggs.

The single tree derived from the analysis is shown in Figure 9. It has a length of 78 steps and a consistency index of 0.50, a retention index of 0.7068, and a homoplasy index of 0.50. Bremer values are generally weak, most nodes are unsupported, but a few are strong (5). These values are plotted onto Figure 9.

PHYLOGENETIC DISCUSSION

Two other cladograms have been published that encompass a large number of aeolid genera, with *Notaeolidia* as the basal genus. Wägele & Willan (2000) have a large tree with a subset of seven aeolid genera, four of which are included here. The basic tree pattern is similar in that both phylogenies indicate that a clade, containing sister families (Bremer support value 3), Eubranchidae Odhner, 1934, and Tergipedidae Bergh, 1889, diverged from the rest of the aeolids. In their tree, the first branch is the clade of family Flabellinidae Bergh, 1899. A sister clade to the *Cuthona*, *Tergipes* Cuivier, 1805, *Eubranchus* clade is a clade that contains members of two large families, the Facelinidae Bergh, 1890, and the family Aeolidiidae Grey, 1827. Gosliner et al. (2007) present a consensus tree based entirely on aeolids, with 15 of the genera in common with our analysis to which we have added six others. Their analysis did not contain the genera *Cuthona* and *Eubranchus* or the family Cumanotidae Odhner, 1907. In our analysis, all three genera branched off early from the rest of the aeolids. Their first branch is that of the Flabellinidae, which agrees with this analysis in that it is in the same clade and basal to the genera *Calmella* and *Piseinotecus*. They found *Babakina* formed a separate clade. In our analysis, *Babakina* is well separated (Bremer support 5) but appears to be intermediate between *Flabellina* and the *Calmella–Piseinotecus* genera. This clade is joined basally by a new sister genus *Unidentia* in the newly created family Unidentidae.

The majority of aeolids in this analysis belong to the family Facelinidae. This analysis, consistent with that of Gosliner et al. (2007), does not support the Facelinidae as a clade. Instead, the Facelinidae are found in two weakly separated sister clades and the family Aeolidiidae is nested within one of these clades, with strong Bremer support values (5) for the Aeolidiidae. This combined clade, containing family Aeolidiidae, is supported by character 6, precardiac cerata in single arches, and with the exception of *Cratena peregrina*, character 7, postcardiac cerata in simple arches. It also contains the newly reassigned species *Hermosita hakunamatata*, which is a sister species to *Hermosita sangria*. The second facelinid clade is separated by character 20, an armed penis. Most species in this clade have a compound pre- and postcardiac arch, characters 6 and 7 (Bremer support value 1). Within this clade, the new species *Dondice galaxiana* is basal to *Dondice banyulensis* and *Dondice occidentalis*, and is thus correctly placed in this genus. The new genus and species *Adfacalina medinai* is basal to *Facelina* and the genus *Dondice*, and appears to be allied to these two genera.

Acknowledgments. We would like to thank Roberto Chávez Arce, Pedro Medina, Buceo Vallartech, ITMAR No. 6, and Centro Universitario de la Costa for assistance with field work. Terry Gosliner and Bob Bolland, through the California Academy of Sciences, provided a specimen and photo of *Unidentia angelvaldesi* from the Philippines. We would also like to thank the Department of Zoology and the BioImaging Facility of the University of British Columbia.

LITERATURE CITED

Angulo-Campillo, O. & A. Valdés. 2003. A new species of *Cuthona* Alder & Hancock, 1855, from the Gulf of California, Mexico (Opisthobranchia: Nudibranchia: Tergipedidae). The Veliger 46:179–182.

Behrens, D. W. & A. Hermosillo. 2005. Eastern Pacific Nudibranchs: A Guide to the Opisthobranchs from Alaska to Central America. Sea Challengers: Monterey, California. 137 pp.

Bremer, K. 1994. Branch support and tree stability. Cladistics. 10:295–300.

Camacho-Garcia, Y., T. M. Gosliner & A. Valdés. 2005. Field Guide to the Sea Slugs of the Tropical Eastern Pacific. California Academy of Sciences: San Francisco, California.

Cervera, J. L., J. C. García & F. J. García. 1987. Una especie de *Piseinotecus* Marcus, 1955 (Gastropoda:Nudibranchia) del Litoral Iberico. Bollotano Malacologico Milano 22:9–12.

Dayrat, B. 2005. Advantages of naming species under the Phylocode: an example of how a species of Discodorididae (Mollusca, Gastropoda, Euthyneura, Nudibranchia, Doridina) may be named. Marine Biology Research 1:216–232.

EDMUNDS, M. 1970. Opisthobranchiate Mollusca from Tanzania. II. Eolidacea (Cuthonidae, Piseinotecidae and Facelinidae). Proceedings of the Malacological Society of London 39:15–57.

GOSLINER, T. M. & D. W. BEHRENS. 1986. Two new species and genera of aeolid nudibranchs from the tropical eastern Pacific. The Veliger 29:101–113.

GOSLINER, T. M. & H. BERTSCH. 2004. Systematics of *Okenia* from the Pacific Coast of North America (Nudibranchia: Goniodorididae) with descriptions of three new species. Proceedings of the California Academy of Sciences 55: 414–430.

GOSLINER, T. M., M. M. GONZÁLEZ-DUARTE & J. L. CERVERA. 2007. Revision of the systematics of *Babakina* Roller, 1973 (Mollusca: Opisthobranchia) with the description of a new species and a phylogenetic analysis. Zoological Journal of the Linnean Society 151:671–689.

GOSLINER, T. M. & R. J. GRIFFITHS. 1981. Description and revision of some South African aeolidacean Nudibranchia (Mollusca, Gastropoda). Annals of the South African Museum 84:105–150.

GOSLINER, T. M. & A. M. KUZIRIAN. 1990. Two new species of Flabellinidae (Opisthobranchia: Aeolidacea) from Baja California. Proceedings of the California Academy of Sciences 47:1–15.

HERMOSILLO, A. 2004. Opisthobranch mollusks of Parque Nacional de Coiba, Panamá (Tropical Eastern Pacific). The Festivus 36:105–117.

HERMOSILLO, A. & D. W. BEHRENS. 2005. The opisthobranch fauna of the Mexican states of Colima, Michoacán and Guerrero: filling in the faunal gap. Vita Malacologica 3: 11–22.

HERMOSILLO, A., D. W. BEHRENS & E. RÍOS-JARA. 2006. Opistobranquios de México. Guía de Babosas Marinas del Pacífico, Golfo de California y las Islas Oceánicas. CONABIO, Dirección de Artes Escénicas y Literatura, Universidad de Guadalajara: Guadalajara, México.

HERMOSILLO, A. & Y. CAMACHO-GARCIA. 2006. A note on the opisthobranchs of Parque Nacional de Coiba, Panama (tropical eastern Pacific). The Festivus 38:95–98.

HERMOSILLO, A. & A. VALDÉS. 2004. Two new Dorids (Mollusca: Opisthobranchia) of Bahía de Banderas and La Paz, México. Proceedings of the California Academy of Sciences 55(28):550–560.

HERMOSILLO, A. & A. VALDÉS. 2007a. Five new species of Aeolid nudibranchs (Mollusca, Opisthobranchia) from the Tropical Eastern Pacific. American Malacological Bulletin 22:119–137.

HERMOSILLO, A. & A. VALDÉS. 2007b. A new *Polycera* (Opisthobranchia: Mollusca) from Bahía de Banderas, México. Proceedings of the California Academy of Sciences 58(23):477–484.

HERMOSILLO-GONZÁLEZ, A. 2003. New distributional records (Mollusca: Opisthobranchia) for Bahía de Banderas, Mexico (Eastern Pacific). The Festivus 35:21–28.

HERMOSILLO-GONZÁLEZ, A. 2006. Ecología de los opistobranquios (Mollusca) de Bahía de Banderas, Jalisco-Nayarit, México. Doctoral Dissertation, Universidad de Guadalajara, Guadalajara, Jalisco, Mexico.

KAISER, K. L. 2007. The recent molluscan fauna of Île Clipperton (Tropical Eastern Pacific). The Festivus 39(Suppl.):1–162.

MADDISON, D. R. & W. P. MADDISON. 2002. MacClade ver. 4.05. Sinauer Associates Inc.: Sunderland, Massachusetts.

MILLEN, S. & J. C. HAMANN. 1992. A new genus and species of Facelinidae (Opisthobranchia, Aeolidacea) from the Caribbean Sea. The Veliger 35:205–214.

MILLEN, S. & A. HERMOSILLO. 2007. The genus *Flabellina* Voight, 1834 (Mollusca: Opisthobranchia) from Bahía de Banderas (Pacific Coast of Mexico) with ecological observations, the description of a new species and the redescription of *Flabellina cynara.* Proceedings of the California Academy of Sciences 58(26):543–559.

ODHNER, N. H. 1939. Opisthobranchiate Mollusca from the western and northern coasts of Norway. Det Kongelige Norske Videnskabernes Selskabs Skrifter 1:1–93.

ORTEA, J., M. CABALLER & J. ESPINOSA. 2003. Nuevos aeolidaceos (Mollusca:Gastropoda) de Costa Rica. Avicennia 16:129–142.

ROLLER, R. A. 1972. Three new species of eolid nudibranchs from the west coast of North America. The Veliger 14: 416–423.

RUDMAN, W. B. 2002. Comment on *Flabellina* from Costa Rica by Peter Ajtai. (Message in) Sea Slug Forum. http://www.seaslugforum.net/find.cfm?id = 6825. Accessed May 12, 2002.

SCHMEKEL, L. & A. PORTMANN. 1982. Opisthobranchia des Mittelmeeres: Nudibranchia und Sacoglossa. Springer-Verlag: New York. 410 pp.

SWOFFORD, D. I. 2002. PAUP*. Phylogenetic Analysis Using Parsimony (*and other methods) Ver. 4.0b10. Sinauer Associates Inc.: Sunderland, Massachusetts.

TARDY, J. 1970. Un nouveau genre de nudibranche méconnu des côtes Atlantique et de La Manche: *Pruvotfolia* (nov. g.) *pselliotes*, (Labbé). 1923. Vie et Mileu (A) 20:327–346.

WÄGELE, H. 1990. Revision of the Antarctic genus *Notaeolidia* (Gastropoda, Opisthobranchia, Nudibranchia). Zoologica Scripta 19:309–330.

WÄGELE, H. & R. C. WILLAN. 2000. Phylogeny of Nudibranchia. Zoological Journal of the Linnean Society 130: 83–181.

The Veliger 51(3):165–176 (November 16, 2012)

THE VELIGER

Phylogeny and Biogeography of *Paradoris* (Nudibranchia, Discodorididae), with the Description of a New Species from the Caribbean Sea

VINICIUS PADULA*

Zoologische Staatssammlung München, Mollusca Sektion, Münchhausenstr. 21, 81247, München, Germany
(e-mail: viniciuspadula@yahoo.com)

AND

ÁNGEL VALDÉS

Department of Biological Sciences, California State Polytechnic University, 3801 West Temple Avenue, Pomona, California 91768-4032, USA
(e-mail: aavaldes@csupomona.edu)

Abstract. *Paradoris adamsae* sp. nov. is described based on three specimens collected in Bocas del Toro, on the Caribbean coast of Panama. The new species is clearly a member of *Paradoris* because of the presence of a jaw with three plates, a narrow radula, a grooved outer edge of the lateral tooth hook, and grooved oral tentacles. It differs from other members of the genus by having a relative large body size, brownish body color, small rhinophores, and high rounded tubercles on the mantle. This is the second record of the genus *Paradoris* in the western Atlantic, where *Paradoris mulciber* has been reported from Brazil, Costa Rica, and the Caribbean Sea. A phylogenetic analysis including 25 taxa shows that *Paradoris* is monophyletic and divided into two main clades, one containing all tropical eastern Pacific, tropical Atlantic, and Mediterranean species, which is sister to a clade composed of tropical and temperate Indo-Pacific species. In the Indo-Pacific clade, three taxa from the southern temperate seas are sisters to the rest of the Indo-Pacific species. According to the present phylogenetic hypothesis, *P. adamsae* sp. nov. is more close related to *Paradoris lopezi* Hermosillo & Valdés, 2004, from the tropical eastern Pacific than to *P. mulciber*, from the western Atlantic. The present phylogeny is similar in several regards to hypotheses proposed for other groups of opisthobranchs and other marine organisms and suggests that the same major vicariant events had affected the biogeography of these groups. As a result of the present study at least 16 distinct species can be recognized in *Paradoris*, more than the double the number of valid species cited in the last revision of the genus.

INTRODUCTION

The genus *Paradoris* is currently considered a member of the Discodorididae nudibranch clade (Valdés, 2002). *Paradoris* is characterized by having a jaw composed of a pair of lateral jaw plates with a third ventral plate, a narrow radula, grooved oral tentacles, and the radular tooth hook with a grooved outer edge. Accessory glands at the distal portion of the reproductive system, which are often associated with stylets, tubercles, and large holes on the mantle, are generally present in this group (Dayrat, 2006). Before a recent worldwide revision, 12 species names were considered as valid. Dayrat (2006) reexamined all available type material and examined newly collected specimens of described species. Furthermore, this author transferred three additional species to *Paradoris* (*Discodoris erythraeensis* Vayssière, 1912; *Discodoris lora* Marcus, 1965; and *Discodoris cavernae* Starmühlner, 1955), proposed new synonyms and identified three new morphotypes, which were called *Paradoris* sp. A, *Paradoris* sp. B, and *Paradoris* sp. C. The conclusion of Dayrat's revision is that *Paradoris* is composed by only eight valid species names and three unnamed taxa (see Dayrat, 2006:128,229). More recently Camacho-García & Gosliner (2007) described an additional species from South Africa. Furthermore, these authors noted that some specimens that Dayrat had suggested as conspecific, such as *Paradoris erythraaensis*, probably represent distinct species.

Paradoris is distributed throughout tropical and temperate oceanic areas, but most of the described

*Corresponding author.

species occur in shallow waters of the Indo-Pacific region. Two species are know from deep waters of the south Pacific, *Paradoris araneosa* Valdés, 2001, and *Paradoris imperfecta* Valdés, 2001. The present paper includes the description of a new species from the Caribbean Sea, which is the second record of the genus from the western Atlantic. The single species previously reported from this region was *Paradoris mulciber* (Ev. Marcus, 1970), described as *Percunas mulciber* based on specimens collected in northern Brazil.

In the present study we propose a new phylogenetic hypothesis for *Paradoris*. Two previous phylogenetic studies dealt with species of *Paradoris*. Dayrat & Gosliner (2005) included five species of *Paradoris* in a general phylogenetic analysis of the family Discodorididae and Dayrat (2006) conducted a phylogenetic analysis of *Paradoris* including 13 taxa, but he did not include all species, excluding for example *Paradoris lopezi* Hermosillo & Valdés, 2004. These two previous studies show the relations of *Paradoris* with other Discodorididae taxa but the phylogenetic relationships within *Paradoris* remained unresolved. The present study aims to provide a more comprehensive phylogenetic hypothesis for *Paradoris* species, including examination of patterns of biogeography.

MATERIAL AND METHODS

Taxonomy

Three specimens of a new species of *Paradoris* were collected in Bocas del Toro, on the Caribbean coast of Panama. All specimens were photographed alive to document color information. All material of the new species is deposited at the Natural History Museum of Los Angeles County (LACM). Two specimens were dissected through a dorsal incision. The internal features were examined and drawn using a stereomicroscope with *camera lucida*. Special attention was paid to the morphology of the reproductive system, including observations on the presence of accessory glands and stylet sacs. The buccal mass was removed and dissolved in 10% sodium hydroxide until the armed labial cuticle and the radula were isolated from the surrounding tissue. Then they were rinsed in water, dried, and mounted for scanning electron microscope (SEM) observation. Dorsal portions of the center and margin of the mantle were critical-point dried and mounted for SEM study. Other specimens from the California Academy of Sciences, San Francisco (CASIZ), and the South African Museum, Cape Town (SAM), are mentioned in the paper but have not been directly examined.

Phylogeny

The data were obtained from dissected specimens and from the literature (Table 1). In order to calculate the most parsimonious phylogenetic tree, data were analyzed by means of Phylogenetic Analysis Using Parsimony (PAUP) (version 4.0b4a, Sinauer Associates, Sunderland, Massachusetts) using the branch-and-bound algorithm. All characters were treated as unordered and unweighted. A Bremer support analysis (Bremer, 1994) was carried out to estimate branch support. In the cases in which the number of possible trees exceeded computer memory, the strict consensus was calculated using the first 10,000 trees obtained. Synapomorphies were obtained using the trace option in MacClade 4.08 (Sinauer Associates, Sunderland, Massachusetts) using the single most parsimonious tree from the PAUP analysis.

SYSTEMATICS

Family DISCODORIDIDAE Bergh, 1891

Genus *Paradoris* Bergh, 1884

***Paradoris adamsae* sp. nov.**

(Figures 1–3)

Paradoris mulciber Ev. Marcus, 1970: Collin et al. 2005:692.

Paradoris sp. Valdés et al., 2006:180–181.

Type material

Holotype: Crawl Key, Bocas del Toro, Panama, 20 February 2004, 6 m depth, 1 specimen 45 mm preserved length (LACM 3094). **Paratypes:** Crawl Key, Bocas del Toro, Panama, 20 February 2004, 6 m depth, 2 specimens 45–50 mm preserved length, dissected (LACM 3095). SEM stubs with radula and labial cuticle deposited together the specimens. All specimens collected by A. Valdés.

Etymology: Dedicated to Peggy Adams and the Adams Foundation in gratitude for the internship in Biological Sciences at the Natural History Museum of Los Angeles County given to the senior author.

Geographic distribution: *Paradoris adamsae* sp. nov. is only known from the type locality, Bocas del Toro, along the Caribbean coast of Panama.

External morphology: Body oval and elevated. Dorsum covered with large, conical, irregular tubercles, some of them clearly larger than the rest. Larger and higher tubercles often situated on the dorsal hump. Small tubercles found on the mantle margin. Entire dorsum covered with small holes of different diameters (up to 100 μm). Short, perfoliate rhinophores composed of about 16 lamellae. Gill composed of six tripinnate

Table 1

Species included in the analysis, with the sources of information.

Taxa	Source of information
Peltodoris atromaculata Bergh, 1880	Valdés, 2002
Peltodoris nobilis (MacFarland, 1905)	Valdés, 2002
Geitodoris planata (Alder & Hancock, 1846)	Valdés, 2002
Paradoris adamsae sp. nov.	LACM 3094, LACM 3095
Paradoris araneosa Valdés, 2001	Valdés, 2001
Paradoris caerulea Camacho-García & Gosliner, 2007	Camacho-García & Gosliner, 2007
Paradoris ceneris Ortea, 1995	Ortea, 1995
Paradoris dubia (Bergh, 1904)	Bergh, 1904; Dayrat, 2006*
Paradoris erythraeensis	Dayrat, 2006*
Paradoris imperfecta Valdés, 2001	Valdés, 2001
Paradoris indecora (Bergh, 1881)	Bergh, 1881; Valdés, 2002
Paradoris inversa Ortea, 1995	Ortea, 1995
Paradoris leuca Miller, 1995	Miller, 1995; Dayrat, 2006*
Paradoris liturata (Bergh, 1905)	Dayrat, 2006
Paradoris lopezi Hermosillo & Valdés, 2004	Hermosillo & Valdés, 2004
Paradoris lora (Marcus, 1965)	Marcus, 1965
Paradoris mollis Ortea, 1995	Ortea, 1995
Paradoris mulciber (Marcus, 1970)	Marcus, 1970; Marcus, 1976; LACM 173261
Paradoris tsurugensis Baba, 1986	Baba, 1986; Dayrat, 2006
Paradoris sp. 1	Dayrat, 2006 (CASIZ 157029)
Paradoris sp. 2	Gosliner, 1987; Dayrat, 2006 (SAM A32370, SAM A35586)
Paradoris sp. 3	Dayrat, 2006 (CASIZ 099390)
Paradoris sp. 4	Dayrat, 2006 (CASIZ 089053, CASIZ 099080, CASIZ 105261, CASIZ 115827)
Paradoris sp. 5	Dayrat, 2006 (CASIZ 167456, CASIZ 110387)
Paradoris sp. 6	Dayrat, 2006 (CASIZ 072185)

* In these cases we only considered the remarks on the holotype and paratype (or paratypes).

branchial leaves, with four leaves pointing anteriorly and two leaves that border the anus pointing posteriorly. Ventrally, oral tentacles short, conical and grooved longitudinally. Anterior border of the foot grooved and notched. Dorsal color of living animal brown, with many small white cream spots and some dark dots covering the notum. Pale brown rhinophores with dark spots.

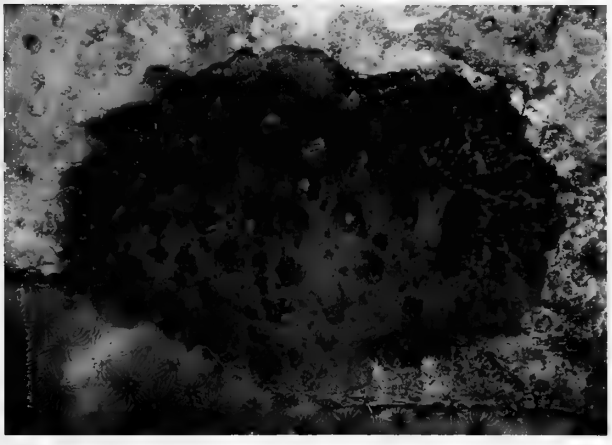

Figure 1. Dorsal view of the living holotype of *Paradoris adamsae* sp. nov. from Bocas del Toro, Panama (LACM 3094).

Grayish-brown branchial leaves scattered with dark spots. Tips of the branchial leaves orange/cream. Ventral color pale cream with few small brown dots.

Radula and jaw: Radular formula 65 × 24.0.24 in the 50 mm-long paratype and 68 × 24.0.24 in the 45 mm-long paratype (LACM 3095). Rachidian teeth absent. Lateral teeth hook-shaped with a grooved outer edge. Lateral teeth devoid of denticles. Innermost lateral teeth with a wide, large base and a thin, long cusp (Figure 2A). After the first three or four lateral teeth the shape changes to teeth with a stronger cusp, small spur, and short base (Figure 2C). Teeth increase in size from the innermost end to two-thirds of the half-row, where they began to decrease in size. Short outermost teeth; different in shape from all others; they can be a simple plate or have two irregular short cusps (Figure 2B). Labial cuticle armed with two lateral plates and one ventral plate. Each plate possesses numerous single, thin, and unicuspid rodlets with noncurved tips (Figure 2D).

Reproductive system: Reproductive system triaulic. Ampulla long; simple or with a single loop; it branches into a short oviduct and the prostate (Figure 3A). The oviduct enters the female glands mass in a depression near its

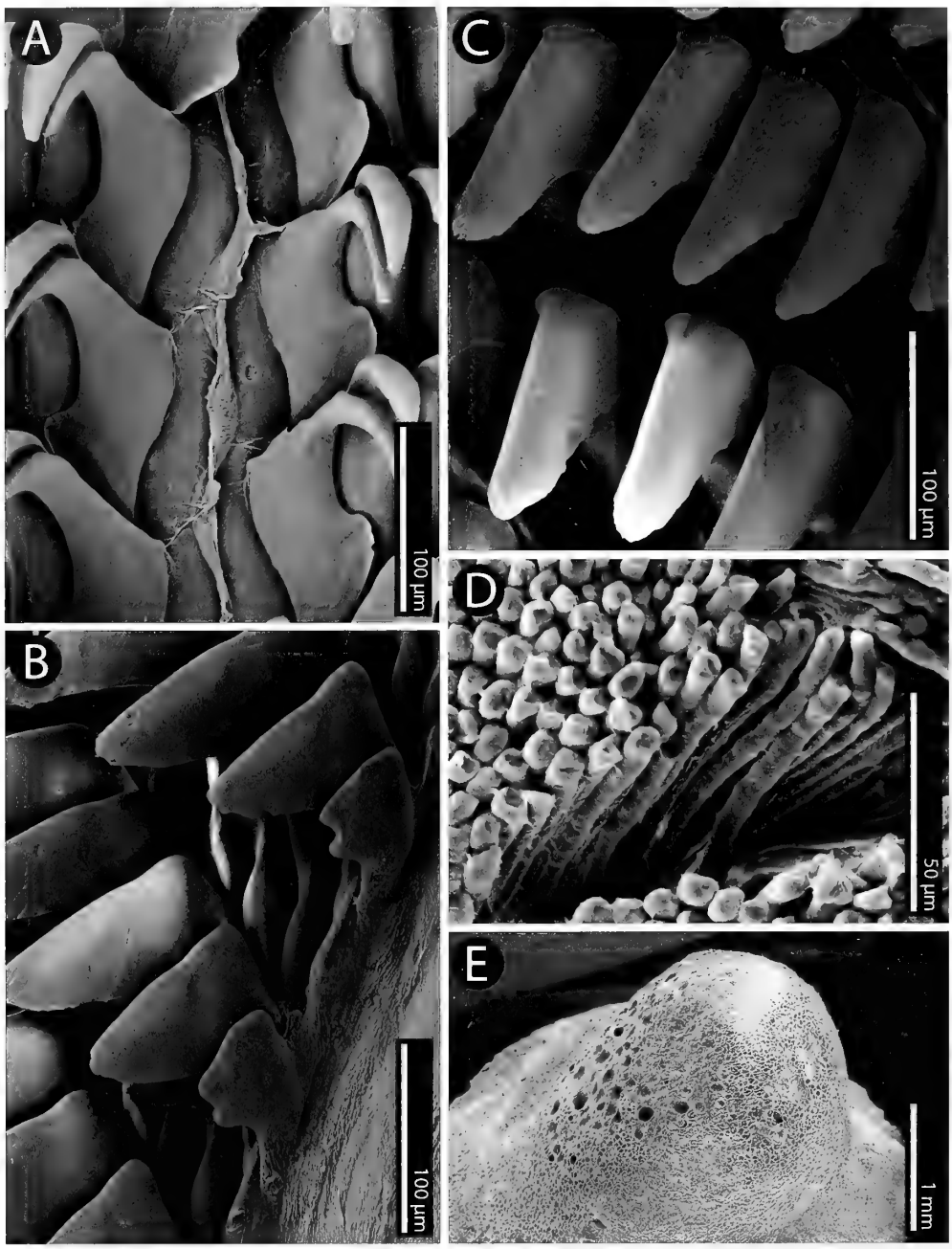

Figure 2. SEMs of a paratype of *P. adamsae* sp. nov. (LACM 3095). **A.** Innermost lateral radular teeth. **B.** Outermost lateral teeth. **C.** Midlateral radular teeth. **D.** Jaw rodlets. **E.** Dorsal tubercle showing the dorsal holes.

center. Prostate long and granular, divided into two portions clearly distinguishable by their different texture and color. Deferent duct with few, about three, loops; it opens into a common atrium with the vagina. Penis unarmed. The two paratypes dissected (LACM 3095) each have two accessory glands connected to the atrium (Figure 3B). Stylets sacs and stylets absent. Vagina long and thin, connects to a large, smooth and oval bursa copulatrix. From the bursa copulatrix leads another duct that connects to an oval and muscular seminal receptacle and to a thin uterine duct. Bursa copulatrix about four times larger than the seminal receptacle.

Remarks: *Paradoris adamsae* sp. nov. is here regarded as a member of *Paradoris* because of the presence of grooved oral tentacles, an armed labial cuticle with a pair of lateral plates with a third ventral jaw plate, a

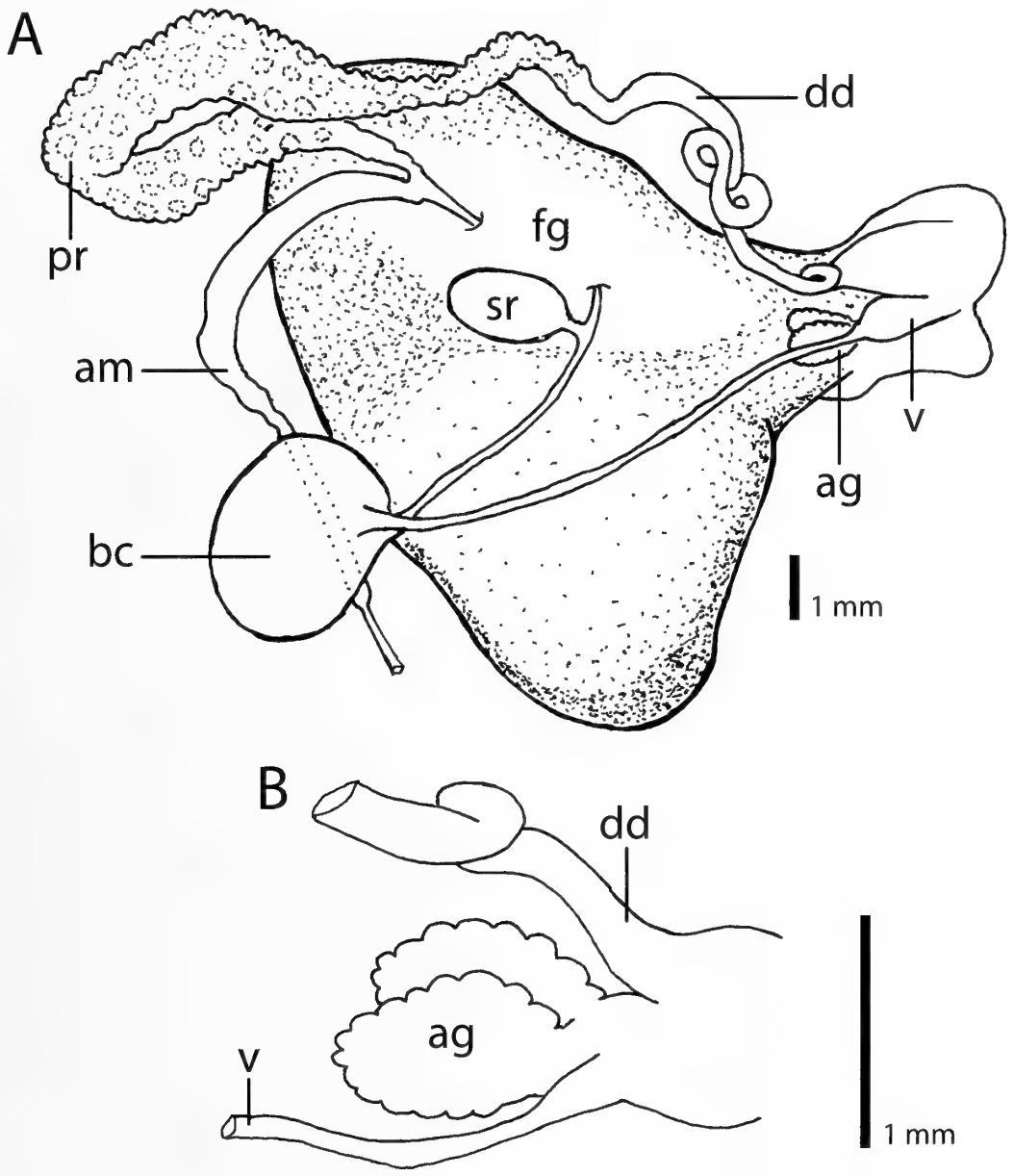

Figure 3. Reproductive system of a paratype of *P. adamsae* sp. nov. (LACM 3095). **A**. General view of the reproductive organs. **B.** Detail of the genital atrium showing the accessory glands. Abbreviations: **ag,** accessory gland; **am:** ampulla; **bc,** bursa copulatrix; **dd,** deferent duct; **fg,** female glands mass; **pr,** prostate; **sr,** seminal receptacle; **v,** vagina.

narrow radula, and a grooved outer edge of the lateral hook-shaped teeth, all characteristics of *Paradoris* (Dayrat, 2006).

Paradoris adamsae sp. nov. is different from other species of *Paradoris* described to date. *Paradoris lopezi* is similar to *Paradoris adamsae* sp. nov. because of the presence of large and conical tubercles on the dorsum, but these two species are easily distinguishable by their external coloration; *P. lopezi* is a pale grey species with orange tubercle tips, whereas *P. adamsae* sp. nov. is dark brown with the tubercles having the same color as the rest of the dorsum. Anatomically, *P. lopezi* has stylet sacs with stylets, which are absent in *P. adamsae* sp. nov. The only other species described from the western Atlantic, *P. mulciber*, has been recently redescribed by Camacho-García & Gosliner (2007) and it is also distinguishable from *P. adamsae* sp. nov. in several regards. Externally, the tubercles of *P.*

mulciber are more rounded, less conical and more spaced than those of *P. adamsae* sp. nov., and the color of *P. mulciber* is paler than that of *P. adamsae* sp. nov. In the reproductive system, the main difference between these two species is the presence of stylet sacs with stylets in *P. mulciber*, which are absent in *P. adamsae* sp. nov.

PHYLOGENETIC ANALYSIS

Taxa

For the phylogenetic analysis, 25 taxa have been considered. All nominal species of *Paradoris*, including species recently synonymized by Dayrat (2006) were included, in addition to *Paradoris adamsae* sp. nov. Representatives of other Discodorididae taxa have been included in the analysis for outgroup comparative purposes, these include *Peltodoris atromaculata* Bergh, 1880, *Peltodoris nobilis* (MacFarland, 1905), and *Geitodoris planata* (Alder & Hancock; 1846). Data on species were obtained from various sources (Table 1).

As Camacho-García & Gosliner (2007) observed, the specimens referred as *P. erythraeensis* by Dayrat (2006) constitute a group of species easily distinguishable by internal and external characteristics. For the present analysis, the data for *P. erythraeensis* were obtained from the description of the type material of this species. From the group of specimens considered as *P. erythraeensis* by Dayrat (2006), three different species were identified and are here called *Paradoris* sp.1 (CASIZ 157029), *Paradoris* sp. 2 (SAM A32370, SAM A35586), and *Paradoris* sp. 3 (CASIZ 099390). Dayrat's (2006) species *Paradoris* sp. B and *Paradoris* sp. C are here referred as *Paradoris* sp. 4 and *Paradoris* sp. 5, respectively. Specimen CASIZ 089053 was excluded from other specimens that belong to *Paradoris* sp. 4. This specimen differs from other members of Dayrat's *Paradoris* sp. B by having tubercles on the dorsal hump and may constitute a different species. It is not included in the present phylogenetic analysis because it is an immature specimen and no reproductive system was found (Dayrat, 2006).

Dayrat's *Paradoris* sp. A is also not included at the analysis. The description of *Paradoris* sp. A was made based on 11 specimens collected in four different localities and, as in the case of *P. erythraeensis*, these specimens present a wide range of morphological and anatomical differences and appears to correspond to a group of species. Because there were no morphological data available of most of these specimens, we prefer to not include *Paradoris* sp. A in the present phylogenetic analysis. The specimen CASIZ 072185 studied by Dayrat (2006) is included in the analysis and herein called *Paradoris* sp. 6.

Characters

The characters used to resolve the phylogeny of *Paradoris* are detailed below. They reflect a range of morphological and anatomical features of the taxa involved. The original list of characters was in part based on the characters selected by Dayrat (2006) and subsequently modified to include additional characters that appear to be more informative. Eleven characters are coded as binary and five characters as multistate. Character states are indicated with numbers: 0, plesiomorphic condition; 1–4, apomorphic conditions. The polarities discussed below have been obtained as the result of outgroup comparison. A data matrix of character states is found in Table 2.

1. **Dorsal brownish-black patches:** Present in *Peltodoris atromaculata*, *Peltodoris nobilis*, and 10 species of *Paradoris* (1). Absent in all other taxa studied (0). In species with dark background color this character is treated as not applicable.
2. **Dorsal brownish-black patches pattern:** Four states are recognized for this character. Some species including *Paradoris leuca* Miller, 1995 and *Paradoris* sp. 1 have irregular dark dots (0). *Paradoris* sp. 4 and *Paradoris* sp. 5 have short stripes (1). In *P. liturata* the stripes are long, making a network at the dorsum (2). *Peltodoris atromaculata* has large and ovoid patches (3) and *Paradoris caerulea* Camacho-García & Gosliner, 2007 has two circular patches at the dorsal hump (4). In species with dark background color or species without dorsal dark patches this character is treated as not applicable.
3. **Gill apex color:** In *P. araneosa* and *P. lora* (Marcus, 1965) the gill apex color is the same as the rest of the gill (0). In *Paradoris indecora* (Bergh, 1881) and *P. lopezi* the gill apices have a distinct color (1). The character state could not be determined for *Paradoris mollis* Ortea, 1995 and *Paradoris* sp. 1.
4. **Oral tentacles:** They are grooved in all *Paradoris* species (1). In the outgroup taxa this condition is absent (0) and it is considered the plesiomorphic state.
5. **Mantle:** Most species of Discodorididae have dorsal structures such as tubercles and/or granules (0). The mantle is smooth in *Paradoris* sp. 4 and *Paradoris* sp. 5, which is considered the apomorphic state (1). Specimens of *Paradoris dubia* (Bergh, 1904) may present dorsal tubercles or not.
6. **Dorsal tubercle size and arrangement:** *Peltodoris atromaculata*, *Paradoris mulciber*, *P. lopezi* and *P. adamsae* sp. nov. have large tubercles on the central part of dorsum (0). *Paradoris indecora* and *Paradoris ceneris* Ortea, 1995 have large tubercles on the margin of the dorsum (1). Similar-sized or

Table 2

Data matrix of character states used in the phylogenetic analysis. The character states are indicated with numbers: 0, plesiomorphic condition; 1–4: apomorphic conditions. Question marks indicate unknown data. Dashes indicate nonapplicable characters.

Species	Character state																		
	1	2	3	4	5	6	7	8	9	10	11	12	13	14	15	16	17	18	19
P. atromaculata	1	3	0	0	0	0	0	0	0	0	0	0	1	0	0	0	1	0	0
P. nobilis	1	0	1	0	0	0	0	0	0	0	0	0	0	0	0	0	0	0	0
G. planata	0	–	1	0	0	2	0	0	1	0	0	0	0	0	0	0	0	1	0
P. adamsae sp. nov.	0	–	1	1	0	0	1	1	2	1	0	1	0	0	0	0	0	1	0
P. araneosa	0	–	0	1	0	2	0	0	2	1	0	1	0	0	0	0	0	1	1
P. caerulea	1	4	0	1	0	2	1	0	2	1	0	1	0	1	0	0	0	1	1
P. ceneris	0	–	1	1	0	1	1	0	2	1	0	1	1	0	0	1	0	0	0
P. dubia	1	0	0	1	0/1	2	0/1	0	2	1	0	1	0/1	0	1	0	0	0	0
P. erythraeensis	1	0	?	1	0	?	0	0	2	1	0	1	1	?	0	0	0	1	1
P. imperfecta	0	–	0	1	0	2	0	0	2	1	0	1	0	1	0	0	1	0	1
P. indecora	0	–	1	1	0	1	1	0	2	1	0	1	1	0	0	0	0	1	1
P. inversa	0	–	1	1	0	1	1	0	2	1	0	1	1	0	0	0	0	1	1
P. leuca	1	0	0	1	0	2	0	0	2	1	0	1	1	0	1	1	0	0	0
P. liturata	1	2	0	1	0	2	0	0	2	1	1	1	1	0	0	0	0	1	1
P. lopezi	0	–	1	1	0	0	1	1	2	1	0	1	1	0	0	0	0	1	1
P. lora	0	–	0	1	0	2	0	0	2	1	0	1	0	1	0	0	0	?	?
P. mollis	0	–	?	1	0	1	1	0	2	1	0	1	1	1	0	0	0	1	1
P. mulciber	0	–	1	1	0	0	1	0	2	1	0	1	1	0	0	0	0	1	1
P. tsurugensis	1	0	0	1	0	2	1	0	2	1	0	1	0	0	?	0	0	1	1
Paradoris sp. 1	1	0	0	1	0	2	0	0	2	1	0	1	1	0	0	1	0	1	1
Paradoris sp. 2	1	0	0	1	0	2	0	0	2	1	0	1	?	0	0	0	0	0	0
Paradoris sp. 3	0	–	0	1	0	2	0	0	2	1	1	1	0	0	0	1	0	1	1
Paradoris sp. 4	1	1	1	1	1	–	0	0	2	1	1	1	0	0	0	0	0	0/1	0/1
Paradoris sp. 5	1	1	1	1	1	–	0	0	2	1	0	1	?	0	0	?	?	1	1
Paradoris sp. 6	0	–	0	1	0	2	0	0	2	1	1	1	0/1	0	?	?	0	1	1

large tubercles distributed all over the dorsum, which occur in *P. lora* and *P. imperfecta*, represent another apomorphic state (2). The character state could not be determined for *Paradoris* sp. 1.

7. **Dorsal large granular tubercles:** In *P. lopezi* and *P. mulciber* there are some large granular tubercles on the dorsum (1). *Paradoris liturata* Bergh, 1905 has large tubercles but they are not granular and *P. erythraeensis* has no large tubercles (0).
8. **Dorsal high granular tubercles:** *Paradoris adamsae* sp. nov. and *P. lopezi* have high granular tubercles at the dorsum (1). In *P. liturata* there are some high tubercles but they are not granulated and all other *Paradoris* taxa lack highly elevated tubercles (0).
9. **Jaw:** *Peltodoris nobilis* has a smooth labial cuticle with no rodlets (0), *Geitodoris planata* has a labial cuticle armed with a pair of lateral jaw plates (1). All *Paradoris* species have the labial cuticle armed with a pair of lateral jaw plates and a ventral plate (2).
10. **Radula width:** All *Paradoris* species have a narrow radula relative to length (1). The absence of this condition is considered the plesiomorphic state and it is present in all members of the outgroup (0).
11. **Radula symmetry:** Some *Paradoris* species have an asymmetrical radula with a higher number of teeth on the left side than the right side (1). All other known Discodorididae have symmetrical radulae (0).
12. **Outer edge of lateral teeth hook:** All *Paradoris* species have a grooved outer edge of the lateral tooth hook (1). The absence of a groove in the outer edge of the tooth hook is considered plesiomorphic (0).
13. **Outermost tooth size:** In *P. lopezi* and *P. mulciber* the outermost teeth are very reduced compared to the lateral teeth (1), in *P. araneosa* and *P. imperfecta* the outermost tooth are of similar size to the adjacent lateral teeth (0). The asymmetrical radula of *Paradoris* sp. 6 has outermost teeth with different sizes on each side of the radula (0/1). The character state could not be determined for *Paradoris* sp. 2 and *Paradoris* sp. 5.
14. **Ampulla length:** *Paradoris imperfecta*, *P. mollis*, and *P. lora* all have a short ampulla (1). All other species have a long ampulla (0). The character state could not be determined for *Paradoris* sp. 1.
15. **Prostate shape:** The majority of Discodorididae

have a flattened prostate (0). Some *Paradoris* species have a tubular prostate (1).

16. **Relative size of bursa copulatrix/seminal receptacle:** A larger bursa copulatrix is considered the plesiomorphic state (0). *Paradoris leuca* and *P. ceneris* have a bursa copulatrix with similar size to that of the seminal receptacle (1).
17. **Seminal receptacle surface:** In *Peltodoris atromaculata* and *Paradoris imperfecta* the seminal receptacle surface is irregular (1). All other species studied have smooth seminal receptacle surface (0).
18. **Accessory glands:** Some Discodorididae have accessory glands at the distal portion of the reproductive system. The presence of these glands is considered the apomorphic state of this character (1). The majority of *Paradoris* species have accessory glands but *P. dubia* and *P. ceneris* lack these structures (0). According to Dayrat (2006), specimens of *Paradoris* sp. 4 may or may not present accessory glands. The character state could not be determined for *P. lora*.
19. **Stylet sacs and stylets:** Some Discodorididae have stylet sacs with stylets at the distal portion of the reproductive system. The majority of *Paradoris* species have these structures and this is the apomorphic state of the character (1). *Peltodoris atromaculata*, *P. nobilis*, and *Paradoris dubia* lack these structures (0). According to Dayrat (2006) specimens of *Paradoris* sp. 4 may present or not stylet sacs. The character state could not be determined for *P. lora*.

PHYLOGENETIC RESULTS

Phylogenetic analysis of the data matrix resulted in a single most parsimonious tree, with a length of 46 steps, a consistency index of 0.522 and a retention index of 0.722. The tree is shown in Figure 4, including character numbers to trace character evolution. Bold and italic numbers indicate reversals and larger numbers on the lower side of the branches indicate Bremer support analysis results.

The single tree shows that *Paradoris* is a monophyletic group supported by five synapomorphies: gill apex color (3), grooved oral tentacles (4), presence of an armed labial cuticle with a pair of lateral plates and a third ventral jaw plate (9), narrow radula (10), and lateral teeth hook with a grooved outer edge (12). Within *Paradoris*, there are two major clades. One contains all known tropical and subtropical eastern Pacific, Atlantic, and Mediterranean species. *Paradoris ceneris* is the most basal member of this clade. There is a polytomy including *P. indecora*, *P. mollis*, and *P. inversa* Ortea, 1995 (eastern Atlantic taxa), which are sister taxa to a clade containing western Atlantic and eastern Pacific species. *Paradoris adamsae* sp. nov. from the Caribbean of Panama appears to be more closely related to *P. lopezi* (from the eastern Pacific) than to *P. mulciber* (from Brazil and the Caribbean Sea).

The second main clade includes a monophyletic assemblage of temperate and tropical Indo-Pacific species distributed in two sister groups. One is composed of three temperate taxa: *P. dubia*, *P. leuca*, and *Paradoris* sp. 2, from southern temperate waters of Australia, New Zealand, and South Africa, respectively. The other clade constituted by the remaining Indo-Pacific species, including other two temperate species, *P. caerulea* from South Africa and *Paradoris tsurugensis* Baba, 1986 from Japan that are sister, but derived species. In this second main clade there seems to be a pattern of monophyly related to geographic range, with species clades or species pairs arranged in latitudinal and longitudinal layers around the central Pacific and Indian oceans, providing a biogeographic pattern, possibly related to vicariant events at the edge of the central Pacific Ocean (Figure 5).

DISCUSSION

Tree Resolution and Characters

The present phylogenetic tree is highly resolved in comparison to previous phylogenetic hypothesis proposed by Dayrat (2006). The removal of continuous/noninformative characters used by Dayrat (2006), as relative to the jaw rodlets and the angle of the radular rows; the selection of additional informative characters; and the inclusion of many morpho-species that Dayrat (2006) synonymized into the same taxa probably account for the different results.

Phylogeny and Biogeography

The topology of the phylogenetic tree of *Paradoris* here presented, in which tropical eastern Pacific and Atlantic species constitute a monophyletic group, is similar to hypotheses proposed for other groups of nudibranchs (Gosliner & Johnson, 1999; Garovoy et al., 2001; Dorgan et al., 2002; Alejandrino & Valdés, 2006), other marine invertebrates such as sea urchins (Lessios et al., 1999; McCartney et al., 2000), shrimps (Baldwin et al., 1998), and also vertebrates such as reef fishes (Rocha, 2003). In most of these cases there is a repeated pattern in which the monophyletic group composed by tropical eastern Pacific and Atlantic species is sister to another monophyletic group containing tropical Indo-Pacific species. It has been proposed that the origin of this biogeographic pattern is related to two consecutive vicariant events: (1) the closure of the Tethys Sea approximately 20 million years ago (Mya), which communicated the Indo-Pacific region with the Atlantic and eastern Pacific and (2) the rise of the Panama isthmus approximately 3.1 Mya (see

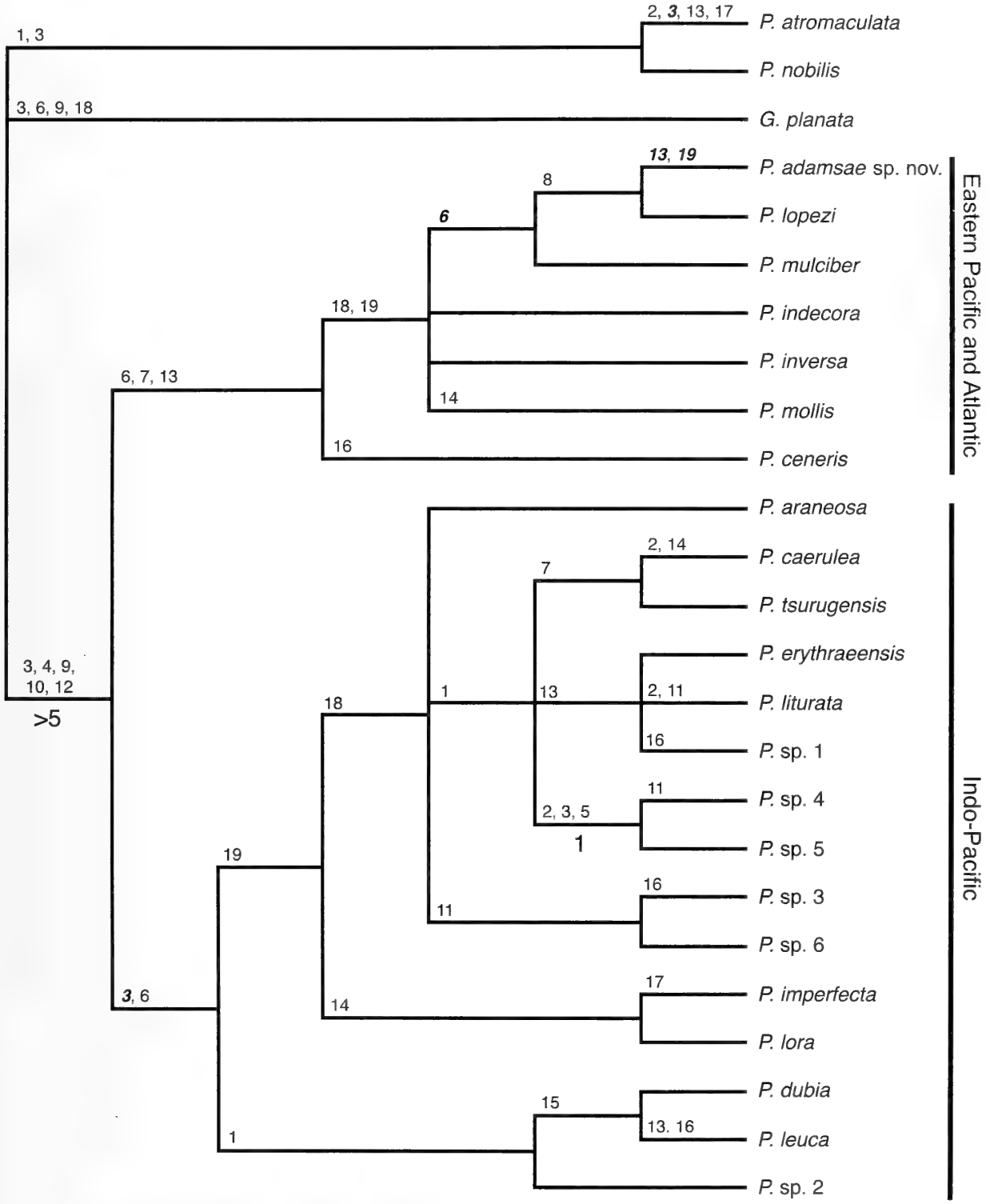

Figure 4. Phylogenetic hypothesis of *Paradoris*. Numbers above the branches show character evolution. Numbers in bold italics show cases of reversal and parallel evolution. Larger numbers below the branches show the results of the Bremer support analysis.

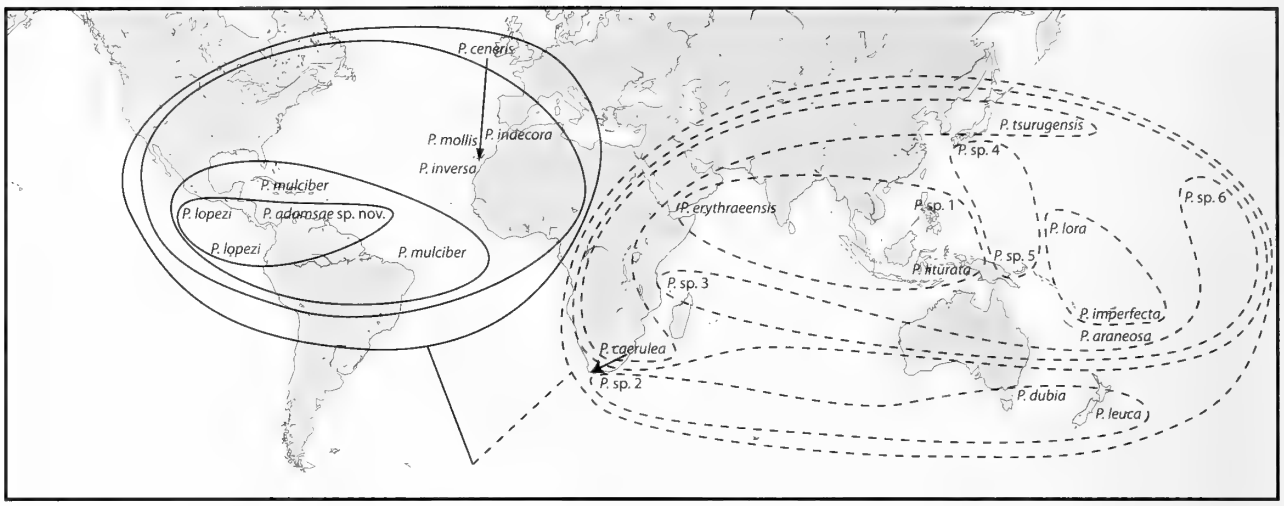

Figure 5. Map showing the biogeographic signal provided by the phylogenetic hypothesis. Species names are situated on the map in the approximate areas where the species occurs; due to space limitations, an arrow points to the actual geographic range of *P. caerulea*. Taxa and clades with sister relationships in the phylogenetic hypothesis are encircled together. Line patterns indicate to which of the main two clades of *Paradoris* each taxon or clade belongs; for a description of the main two clades see the Results section.

Coates & Obando, 1996; Badlwin et al., 1998; Lessios, 1999; McCartney et al., 2000; Valdés, 2004). It seems that these events, and the fact the eastern Pacific is isolated from the western Pacific by the East Pacific Barrier, would produce effective isolation that allowed allopatric speciation.

In the present phylogenetic hypothesis three southern temperate species (*Paradoris dubia*, *P. leuca*, and *Paradoris* sp. 2) are grouped in a sister clade to the remaining Indo-Pacific *Paradoris* (Figures 4, 5), which are mostly tropical species. A similar pattern can be observed in other dorid nudibranchs such as *Rostanga* (Garovoy et al., 2001) and *Acanthodoris* (Fahey & Valdés, 2005). In the phylogenetic hypothesis of *Rostanga*, a small clade containing South African and subarctic species is sister to a clade with all other species (Garovoy et al., 2002). The phylogenetic hypothesis proposed for *Acanthodoris* shows that the basal species of this group are found in temperate southern waters of South America, South Africa, and Australia (Fahey & Valdés, 2005). This recurrent pattern suggests either a southern temperate origin of these groups or an early divergence of southern temperate and tropical taxa. In the case of *Paradoris*, other temperate species such as *P. tsurugensis* (from Japan) and *P. caerulea* (from South Africa) are derived members of the Indo-Pacific clade, which seem to suggest that these species derived from tropical Indo-Pacific ancestors.

Taxonomic Remarks

Dayrat (2006) recognized only eight valid species names in *Paradoris*: *P. araneosa*, *P. dubia*, *P. erythraeensis*, *P. indecora*, *P. liturata*, *P. lopezi* and *P. tsurugensis*. He also proposed six new synonyms for *Paradoris* species. Camacho-García & Gosliner (2007) criticized the taxonomy proposed by Dayrat (2006) on the basis that in some cases Dayrat defined species based on the presence of a shared characteristic between several specimens, rather than on the correlation of characters, which appears to produce better estimations of species boundaries and diagnostic characters. In light of Camacho-García & Gosliner's (2007) paper, it becomes clear that the synonymies proposed by Dayrat (2006) require a careful reevaluation.

Dayrat (2006) may be correct about the synonym of *P. dubia* and *P. leuca*, species described from southern Australia and New Zealand, respectively. We were unable to detect any consistent anatomical difference between these two species with the exception of the presence of a bursa copulatrix with similar size to that of the seminal receptacle in *P. leuca*. However, some differences in the dorsal color appears to separate these species (Rudman, 2007).

The synonymy proposed by Dayrat (2006) for *P. inversa* and *P. mollis*, species described from the Canary Islands by Ortea (1995), with *P. indecora*—known from the Canary Islands, Morocco, the Atlantic coast of Portugal, and the Mediterranean—also seems to be based on a correct interpretation of data; however, the lack of mention of accessory glands and stylet sacs in the original description of the single dissected specimen of *P. ceneris*, also synonymized with *P. indecora*, may indicate that this is indeed a distinct species from *P. indecora*. Finally, we disagree with Dayrat's (2006) proposal to synonymize *P. araneosa*

and *P. imperfecta*, two species from deep waters off south New Caledonia. Differences between these two species include the size of the ampulla, the morphology of the seminal receptacle surface, and the outermost tooth size. They are clearly two different species that according to the phylogenetic hypothesis here proposed do not share an immediate common ancestor. Furthermore, the documented external morphology and coloration of living animals of these two species is dramatically different (see Valdés, 2001).

The specimen here referred as *Paradoris* sp. 1 (CASIZ 157029) may belong to *P. erythraeensis* but the absence of data in the description of this specimen and differences found by Dayrat (2006) and here observed in the relative size of the bursa copulatrix and the seminal receptacle do not allow a definitive conclusion. As a result of the present study we recognize at least 16 distinct *Paradoris* species: *P. adamsae* sp. nov., *P. araneosa*, *P. caerulea*, *P. dubia*, *P. erythraeensis*, *P. imperfecta*, *P. indecora*, *P. liturata*, *P. lopezi*, *P. mulciber*, *P. tsurugensis*, *Paradoris* sp. 2, *Paradoris* sp. 3, *Paradoris* sp. 4, *Paradoris* sp. 5, and *Paradoris* sp. 6. This is more than the double of valid species cited in the last revision of the genus (Dayrat, 2006).

Acknowledgments. This research project was possible thanks to the financial support of the Adams Foundation to the senior author to complete an internship for international students at the Natural History Museum of Los Angeles County (2006). We thank Terrence Gosliner (California Academy of Sciences) for the constructive comments on the manuscript. The senior author also thanks the Conselho Nacional de Desenvolvimento Científico e Tecnológico (CNPq-Brasil) and the Deutscher Akademischer Austausch Dienst (DAAD-Germany) for their support. Research materials were supported by the NSF PEET grants DEB-9978155 and DEB-0329054 to Terrence M. Gosliner and the junior author. The fieldwork in Panama was supported by a travel research grant of the Smithsonian Institution Tropical Research Institute to the junior author. The scanning electron microscope work was conducted at LACM in the facility supported by NSF DBI-0424911 and with the assistance of Giar-Ann Kung. Lindsey Groves (LACM) assisted with the curation of the material examined.

LITERATURE CITED

ALEJANDRINO, A. & A. VALDÉS. 2006. Phylogeny and biogeography of the Atlantic and eastern Pacific *Hypselodoris* Stympson, 1855 (Nudibranchia, Chromodorididae) with the description of a new species from the Caribbean Sea. Journal of Molluscan Studies 72:189–198.

BABA, K. 1986. Description of a new species of nudibranchiate Mollusca, *Paradoris tsurugensis*, Doridídae, from Japan. Boletim de Zoologia, Universidade de São Paulo 10:1–8.

BALDWIN, J. D., A. L. BASS, B. W. BOWEN & W. H. CLARK, JR. 1998. Molecular phylogeny and biogeography of the marine shrimp *Penaeus*. Molecular Phylogenetics and Evolution 10:399–407.

BERGH, L. S. R. 1881. Malacologische Untersuchungen. Pp. 79–128 in Reisen im Archipel der Philippinen von Dr. Carl Gottfried Semper. Zweiter Theil. Wissenschaftliche Resultate. Band 2, Theil 4, Heft 2.

BERGH, L. S. R. 1904. Malacologische Untersuchungen. Pp. 1–56 in Reisen im Archipel der Philippinen von Dr. Carl Gottfried Semper. Zweiter Theil. Wissenschaftliche Resultate. Band 9, Theil 6, Lief. 1.

BREMER, K. 1994. Branch support and tree stability. Cladistics 10:295–304.

CAMACHO-GARCÍA, Y. & T. M. GOSLINER. 2007. The genus *Paradoris* Bergh, 1884 (Nudibranchia: Discodorididae) in the tropical Americas, and South Africa with the description of a new species. Veliger 49:105–119.

COATES, A. G. & J. A. OBANDO. 1996. The geologic evolution of the Central American isthmus. Pp. 21–56 in J. B. C. Jackson, A. F. Budd & A. G. Coates (eds.), Evolution and Environment in Tropical America. University of Chicago Press: Chicago.

COLLIN, R., M. C. DÍAZ, J. NORENBURG, R. M. ROCHA, J. A. SÁNCHEZ, A. SHULZE, M. SCHWARTZ & A. VALDÉS. 2005. Photographic identification guide to some common marine invertebrates of Bocas del Toro, Panama. Caribbean Journal of Science 41:638–707.

DAYRAT, B. 2006. A taxonomic revision of *Paradoris* sea slugs (Mollusca, Gastropoda, Nudibranchia, Doridina). Zoological Journal of the Linnean Society 147:125–238.

DAYRAT, B. & T. M. GOSLINER. 2005. Species names and metaphyly: a case study in Discodorididae (Mollusca, Gastropoda, Euthyneura, Nudibranchia, Doridina). Zoologica Scripta 34(2):199–224.

DORGAN, K. M., A. VALDÉS & T. M. GOSLINER. 2002. Phylogenetic systematics of the genus *Platydoris* (Mollusca, Nudibranchia, Doridoidea) with descriptions of six new species. Zoological Scripta 31:271–319.

FAHEY, S. J. & A. VALDÉS. 2005. Review of *Acanthodoris* Gray, 1850 with a phylogenetic analysis of Onchidorididae Alder and Hancock, 1845 (Mollusca, Nudibranchia). Proceedings of the California Academy of Sciences 56(20): 213–272.

GAROVOY, J. M., A. VALDÉS & T. M. GOSLINER. 2001. Phylogeny of the genus *Rostanga* (Mollusca, Nudibranchia), with descriptions of three new species from South Africa. Journal of Molluscan Studies 67:131–144.

GOSLINER, T. M. 1987. Nudibranchs of Southern Africa, a Guide to Opisthobranch Molluscs of Southern Africa. Sea Challengers: Monterey. 136 pp.

GOSLINER, T. M. & R. F. JOHNSON. 1999. Phylogeny of *Hypselodoris* (Nudibranchia: Chromodorididae) with a review of the monophyletic clade of Indo-Pacific species, including descriptions of twelve new species. Zoological Journal of the Linnean Society 125:1–114.

HERMOSILLO, A. & A. VALDÉS. 2004. Two new species of dorid nudibranchs (Mollusca, Opisthobranchia) from Bahía de Banderas and La Paz, Mexico. Proceedings of the California Academy of Sciences 55:550–560.

LESSIOS, H. A., B. D. KESSING, D. R. ROBERTSON & G. PAULAY. 1999. Phylogeography of the pantropical sea urchin *Eucidaris* in relation to land barriers and ocean currents. Evolution 53:806–817.

MARCUS, ER. 1965. Some Opisthobranchia from Micronesia. Malacologia 3:263–286.

MARCUS, EV. 1970. Opisthobranchs from Northern Brazil. Bulletin of Marine Science 20:922–951.

MARCUS, EV. 1976. Marine euthyneuran gastropods from Brazil (3). Studies on the Neotropical Fauna & Environment 11:5–23.

McCartney, M. A., G. Keller & H. A. Lessios. 2000. Dispersal barriers in tropical oceans and speciation in Atlantic and eastern Pacific sea urchins of the genus *Echinometra*. Molecular Ecology 9:1391–1400.

Miller, M. C. 1995. New species of the dorid nudibranch genus *Paradoris* Bergh, 1884 (Gastropoda: Opisthobranchia) from New Zealand. Journal of Natural History 29: 901–908.

Ortea, J. A. 1995. Estudio de las especies atlánticas de *Paradoris* Bergh, 1884 (Mollusca: Nudibranchia: Discodorididae) recolectadas en las Islas Canarias. Avicennia, Revista de Oceanología, Ecología y Biodiversidad Tropical 3:5–27.

Rocha, L. A. 2003. Patterns of distribution and processes of speciation in Brazilian reef fishes. Journal of Biogeography 30:1161–1171.

Rudman, W. B. 2007. Paradoris dubia and P. leuca. Sea slug forum. http://www.seaslugforum.net/display.cfm?id=19195. Accessed January 11, 2007.

Valdés, A. 2001. Deep-sea cryptobranch dorid nudibranchs (Mollusca, Opisthobranchia) from the tropical West Pacific, with descriptions of two new genera and eighteen new species. Malacologia 43:237–311.

Valdés, A. 2002. A phylogenetic analysis and systematic revision of the cryptobranch dorids (Mollusca, Nudibranchia, Anthobranchia). Zoological Journal of the Linnean Society 136(4):535–636.

Valdés, A. 2004. Phylogeography and phyloecology of dorid nudibranchs (Mollusca,Gastropoda). Biological Journal of the Linnean Society 83:551–559.

Valdés, A., J. Hamann, D. Behrens & A. Dupont. 2006. Caribbean Sea Slugs. A Field Guide to the Opisthobranch Mollusks from the Tropical Northwestern Atlantic. Sea Challengers, Gig Harbor. Washington.

Instructions to Authors

The Veliger publishes original papers on any aspect of malacology. All authors bear full responsibility for the accuracy and originality of their papers.

Presentation

Papers should include an Abstract (approximately 5% of the length of the manuscript), Introduction, Materials and Methods, Results, and Discussion. Short Notes should include a one-sentence Abstract. In taxonomic papers, all names of taxa must be accompanied by author and date of publication, and by a full citation in the bibliography. In papers on other subjects and in the non-taxonomic portions of taxonomic papers, author and date of names need not be accompanied by a full citation. All genus and species names should be in italics. All references to new molecular sequences must be linked to GenBank.

Literature Cited

References in the text should be given by the name of the author(s) followed by the date of publication: for one author (Phillips, 1981), for two authors (Phillips & Smith, 1982), and for more than two (Phillips et al., 1983).

The Literature Cited section should include all (and only) references cited in the text, listed in alphabetical order by author. Each citation must be complete, with all journal titles unabbreviated, and in the following forms:

(a) Journal articles:

Hickman, C. S. 1992. Reproduction and development of trochacean gastropods. The Veliger 35:245–272.

(b) Books:

Bequaert, J. C. & W. B. Miller. 1973. The Mollusks of the Arid Southwest. University of Arizona Press: Tucson. 271 pp.

(c) Composite works:

Feder, H. M. 1980. Asteroidea: the sea stars. Pp. 117–135 in R. H. Morris, D. P. Abbott & E. C. Haderlie (eds.), Intertidal Invertebrates of California. Stanford University Press: Stanford, Calif.

Tables

Number tables and prepare on separate pages. Each table should be headed by a brief legend. Avoid vertical lines.

Figures and Plates

Each image should have a concise legend, listed on a page following the Literature Cited. Text figures should be in black ink and completely lettered. Keep in mind page format and column size when designing figures. Images for halftone reproduction must be of good quality. Where appropriate, a scale bar may be used in the image; otherwise, the specimen size should be given in the figure legend.

Use one consecutive set of Arabic numbers for all illustrations (that is, Figures 1, 2, 3 . . . , *not* Figures 1a, 1b, 1c . . . , *nor* Plate 1, fig. 1 . . .).

Submitting manuscripts

All manuscripts should be submitted as Word files, by e-mail or on disc, double spaced, plus one optional double-spaced paper copy. For convenience of review, figures are best submitted initially in a form and size suitable for electronic mail. Figures for publication may be submitted on disc. Halftones should be at least 300 ppi; graphics in TIFF or EPS format.

Send manuscripts, proofs, books for review, and correspondence on editorial matters to:

David R. Lindberg
Editor, *The Veliger*
Museum of Paleontology
1101 VLSB MC# 4780
University of California
Berkeley, CA 94720-4780, USA

Veliger@Berkeley.edu
T 510.642.3926
F 510.642.1822

In the cover letter, authors should briefly state the point of the paper, and provide full and electronic addresses of at least three reviewers who have not previously seen the manuscript. If authors feel strongly that certain reviewers would be inappropriate, they should indicate reasons for their views.